MODELLING OF CORRODED REINFORCED CONCRETE BEAMS

BY

HAMDI AHMED AL-SAKKAF

A Thesis Presented to the
DEANSHIP OF GRADUATE STUDIES

KING FAHD UNIVERSITY OF PETROLEUM & MINERALS

DHAHRAN, SAUDI ARABIA

In Partial Fulfillment of the
Requirements for the Degree of

MASTER OF SCIENCE

In

CIVIL ENGINEERING

MAY 2016

KING FAHD UNIVERSITY OF PETROLEUM & MINERALS

DHAHRAN- 31261, SAUDI ARABIA

DEANSHIP OF GRADUATE STUDIES

This thesis, written by **HAMDI AHMED AL-SAKKAF** under the direction of his thesis advisor and approved by his thesis committee, has been presented and accepted by the Dean of Graduate Studies, in partial fulfillment of the requirements for the degree of **MASTER OF SCIENCE IN CIVIL ENGINEERING.**

Prof. Alfarabi Mohammad Sharif
(Advisor)

Dr. Salah U. Al-Dulaijan
Department Chairman

Dr. Mohammed A. Al-Osta
(Co-Advisor)

Prof. Shamshad Ahmad
(Member)

Dr. Salam A. Zummo
Dean of Graduate Studies

Dr. Muhammad K. Rahman
(Member)

15/6/16
Date

Dr. Ali H. Al-Gadhib
(Member)

بسم الله الرحمن الرحيم

DEDICATED TO

MY BELOVED FATHER, MOTHER, WIFE, BROTHER, AND SISTERS

ACKNOWLEDGEMENTS

First and foremost, Alhamdulillah. Indeed, all praise and thanks are due to Allah for giving me the knowledge, health, and everything to complete this research successfully.

Acknowledgement is due to the King Fahd University of Petroleum & Minerals for the support given to this research and for giving me the opportunity to pursue my graduate studies with financial support.

I would like to express my deep appreciation to my advisor Prof. Alfarabi M. Sharif and my co-advisor Dr. Mohammed Al-Osta who guided me with their knowledge, dedicated attention, continuous support, and encouragement throughout this research. Their invaluable suggestions made this work interesting and a great learning experience for me. Thereafter, I am grateful to my Committee Members, Prof. Shamshad Ahmad, Dr. Muhammad K. Rahman, and Dr. Ali H. Al-Gadhib, for their cooperation, encouragement, and important comments. Furthermore, I acknowledge, with deep appreciation, Prof. Muhammed Baluch who gave me solid and invaluable knowledge during the three courses I took with him in addition to his help in this research.

I would like to express my sincere thanks to my beloved father, Prof. Ahmed M. Al-Sakkaf, who always support me with his love, encouragement, and advice regarding the research and life in general. Moreover, my heartfelt gratitude is given to my mother, the one who can never ever be thanked enough, for her patience, love, encouragement, and constant prayers for me. Special thanks are due to my beloved wife for her continuous love, understanding, and overwhelming care during all stages of my study. I would like to express my grateful thanks to my brother, sisters, and all my relatives for their emotional and moral support throughout my life.

Finally, thanks are due to my colleagues in the Civil Engineering Department, for their help and support. Thanks are also due to all my friends for their support and encouragement.

TABLE OF CONTENTS

LIST OF TABLES

LIST OF FIGURES

ABSTRACT

Full Name : HAMDI AHMED AL-SAKKAF

Thesis Title : MODELLING OF CORRODED REINFORCED CONCRETE BEAMS

Major Field : CIVIL ENGINEERING

Date of Degree : MAY 2016

Corrosion of reinforcement steel in reinforced concrete (RC) structure is the most common durability problem especially in coastal regions. Corroded RC beam experiences different deterioration problems that affect its load carrying capacity such as loss of bond between reinforcement bars (rebars) and the surrounding concrete, cracking or spalling of concrete cover, and loss in area and strength of the rebar. This study has developed a three-dimensional (3D) model using finite element (FE) analysis in ABAQUS to simulate corroded beams considering all corrosion-induced damages (bond loss, cracking of concrete, and reduction in steel area and strength).

Prior to modeling the corroded beam, several FE models in ABAQUS constructed first for a selected un-corroded short beam to investigate different approaches for modeling the bond as 3D surface interaction without inserting additional interface elements. Comparison between FE and the experimental results of the selected beam showed that using *surface-based cohesive behavior*, which is a mechanical model based on traction-separation behavior, is found to be accurate for modeling the bond in 3D model of RC beams.

Then, the proposed finite element model was conducted to include all damage parameters due to corrosion in the model and use the appropriate reduction empirical models available in the literature for corrosion-induced damages. Validation of the model was conducted with experimental simply supported beams, tested by other researchers, having different failure modes (flexural, shear, bond). Good matching between FE and experimental load

deflection curves was observed and the difference in the ultimate load capacities was less than 5% for all cases.

Finally, a parametric study was conducted to investigate the effects of different types of corrosion damages, corrosion degree, and location of the corrosion, in the behavior response and capacity of the corroded beam. Results illustrated that the most critical corrosion-induced damage is the complete loss of bond between reinforcement and the concrete as it causes sudden failure and the beam behaves as un-reinforced beam. Moreover, this failure can happen in situations where the corrosion is only at extreme quarters of the beam span, where bond is most critical at these locations. It was also noted that variation of corrosion level in the lateral direction caused lateral deflection due to the developed un-symmetry of the cross section.

ملخص الرسالة

الاسم الكامل: حمدي أحمد محمد السقاف

عنوان الرسالة: نمذجة الكمرات الخرسانية المسلحة المعرضة للتآكل

التخصص: الهندسة المدنية

تاريخ الدرجة العلمية: مايو 2016 م

يعتبر تآكل حديد التسليح من أكثر المشاكل خطورة وشيوعاً التي تتعرض لها المنشآت الخرسانية المسلحة خصوصاً في المناطق الساحلية. حيث تتعرض الكمرات التي تحتوي على حديد تسليح متآكل لأضرار مختلفة تؤثر على سلوكها وقوة تحملها ، هذه الأضرار تشمل نقصان التماسك بين حديد التسليح والخرسانة المحيطة به ، تشقق الغطاء الخرساني وانفصاله ، و نقصان مساحة مقطع الحديد المتآكل وصفاته الميكانيكية. هذا البحث يقدم نمذجة ثلاثية الأبعاد بإستخدام طريقة العناصر المحدودة (FEM) في برنامج ABAQUS لمحاكاة كل الأضرار المذكورة الناتجة عن التآكل.

قبل البدء بنمذجة الكمرات المعرضة للتآكل، تم إنشاء عدة نماذج لكمرة معينة بدون تآكل لغرض إختبار عدة طرق لنمذجة التماسك بين حديد التسليح والخرسانة وذلك بإستخدام التفاعل بين الأسطح الثلاثية الأبعاد لعناصر الحديد والخرسانة . أظهرت المقارنة مع النتائج التجريبية أن طريقة الترابط التماسكي (Cohesive Behavior) في برنامج ABAQUS هي الأدق في محاكاة الترابط بين الخرسانة وحديد التسليح.

بعد ذلك تم تطوير النموذج وذلك بإضافة تأثير التآكل بإستخدام المعادلات التجريبية المناسبة التي تصف أضرار التآكل من الدراسات السابقة في هذا المجال . تم التحقق من النموذج عبر المقارنة مع نتائج تجريبية من عدة أبحاث سابقة لكمرات ذات حديد تسليح متآكل ذات أنواع إنهيار مختلفة (إنهيار نتيجة عزوم الإنعطاف أو قوة القص أو إنهيار نتيجة فقدان التماسك بين الحديد والخرسانة). وقد أظهرت المقارنة بين نتائج التى تم الحصول عليها من النمذجة والنتائج التجريبية لمنحنى الحمل مقابل الازاحة تشابه جيد وكانت الفروقات كا قيمة أعلى للحمل أقل من 5% لكل الحالات .

في الأخير تم إجراء دراسة عوامل التأثير لإختبار تأثير أنواع أضرار التأكل ، درجة التآكل ، و أثر تغيير المنطقة المعرضة للتآكل في سلوك وقدرة تحمل الكمرات . وقد وجد أن أخطر آثار التآكل هو الفقدان الكامل للتماسك بين حديد التسيح والخرسانة لأنه يودي إلى إنهيار مفاجئ للكمرة وكأنها لاتحتوي على أي حديد تسليح بالإضافة إلى أن هذا الانهيار قد يحدث في حالات يكون التآكل فقط في منطقتي الربع الطرفي من بحور الكمرات البسيطة لأن هذه المناطق حرجة بالنسبة للتماسك . لوحظ ايضا من خلال نتائج الدراسة أن الإختلاف في درجة التآكل في الاتجاه العرضي للكمرة يسبب إزاحة جانبية عند التحميل بسبب مقطع الكمرة الغير متماثل .

CHAPTER 1

INTRODUCTION

1.1 Background

Corrosion is the most serious problem among the durability issues of reinforced concrete (RC) structures. As stated by the World Corrosion Organization (WCO), corrosion costs over 3% of the world's Gross Domestic Product (GDP) every year (Bossio et al. 2015).

Degradation of RC structures because of the reinforcement corrosion is a major problem faced by the construction industry in worldwide and especially in the Arabian Gulf as repairing of corrosion-deteriorated infrastructure requires billions of dollars. Researchers in KSA and in the Middle East pointed out that the buildings in Arabian Gulf have only 10 to 15 years of service life (Imam 2012).

Availability of inexpensive coating material that provides protection against corrosion is not yet developed. Even with epoxy-coated rebar, the corrosion will start once the coating is damaged and the rate of corrosion becomes much faster at these localized locations.

When reinforcing steel is corroded in the concrete structure, several damages types occur: (1) reduction in the cross sectional area of the reinforcing steel, (2) cracking and spalling of the concrete cover, which is resulted from pressure exerted by corrosion by-products (Figure 1-1), (3) decrease in the bond strength between steel and surrounding concrete. These problems will eventually affect the integrity and load-carrying capacity of the structure.

The corrosion process is usually not uniform and therefore corrosion-damages can vary along the steel bar. In fact, corrosion in particular local zones (pitting corrosion) can occur by localized ingress of chlorides, water, and oxygen in Honeycombs or zones of structural cracks. This causes corrosion effects at these locations, while the remainder of the rebar

may be left un-corroded. Figure 1-2 illustrates the effect of corrosion-induced deteriorating on the capacity of concrete element and shows the interaction between these damages.

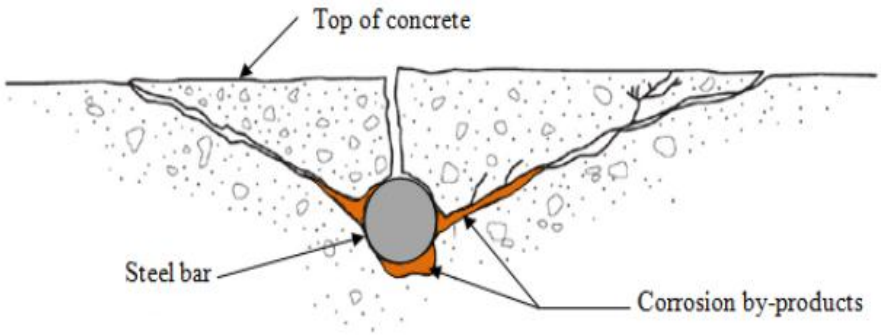

Figure 1-1 : Cracking and spalling of concrete cover induced by corrosion (Elbusaefi 2014)

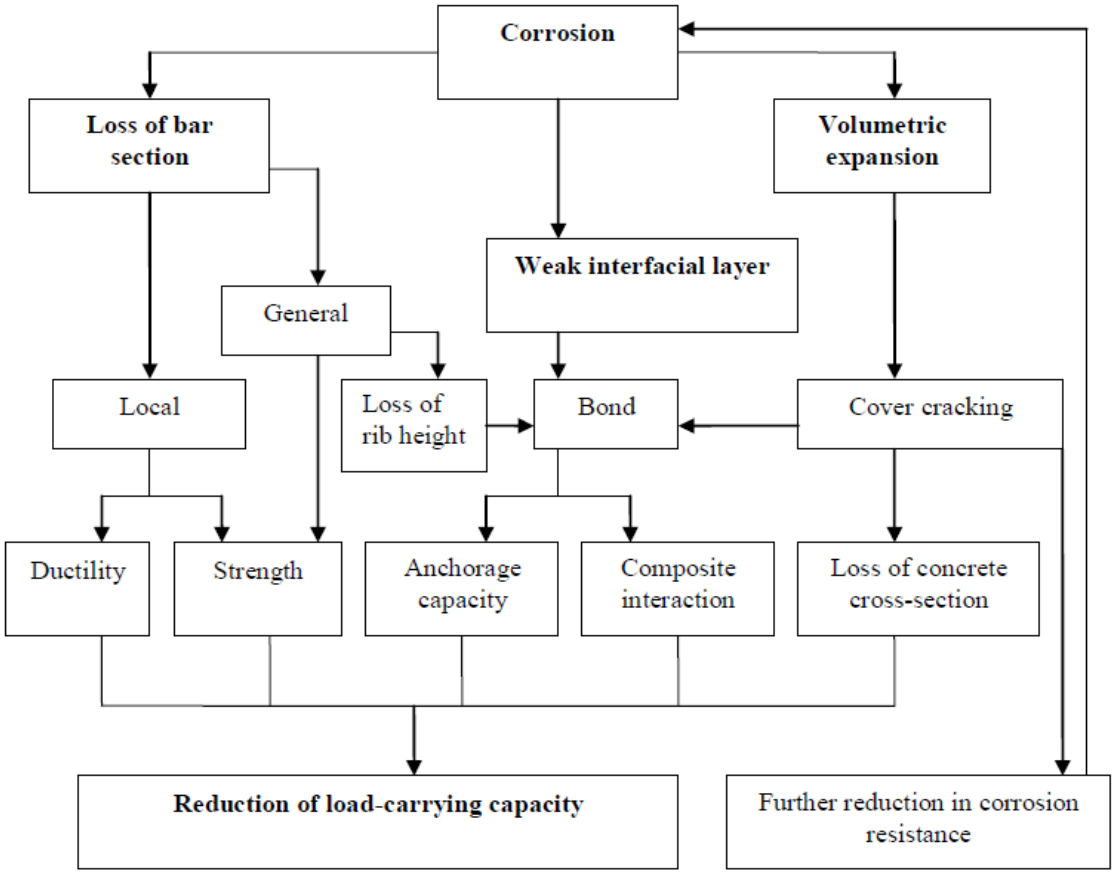

Figure 1-2: The consequence of reinforcement corrosion on RC Structures (Ayop & Cairns 2013)

1.2 Objectives and Scope

The main objective of this study is to develop a three-dimensional (3D) finite element (FE) model that can predicts, with reasonable accuracy, the behavior and load carrying capacity of corroded RC beams. This FE model should simulate the effect of various corrosion-induced degradations such as: (1) bond loss between corroded steel bars and the surrounding concrete, (2) decrease in bar's cross-section area, (3) cracking of concrete cover, and (4) degradation in the mechanical properties of corroded steel bars (strength and ductility).

In order to achieve this objective, the following tasks conducted:

1- Extensive literature review in various topics related to modeling of corroded RC beams with more emphasis in both modeling of concrete-steel interaction and effect of corrosion in the mechanical properties of corroded steel bars.

2- A 3D FE model in ABAQUS software constructed first for un-corroded beam to investigate different methods for modeling the bond between steel bars and concrete.

3- The proposed FE model validated with experimental results done by other researchers for beams failed in flexural as well as beams failed in shear.

4- A parametric study conducted to investigate the effect of changing the corrosion degree and the corrosion location within beam's longitudinal and transverse directions.

1.3 Significance of the Study

Review of the literature implies that many researchers have been working in this direction to model the corroded beam using the finite element analysis. However, most of them focused on two-dimensional (2D) modeling. Thus far, three-dimensional modeling of RC beam with 3D element type especially for the steel bars has received limited attention. Therefore, in this study, RC beams model were developed in ABAQUS by using 3D elements for both concrete and steel bars.

Three-dimensional FE modelling of corroded RC beams enables the researchers to study the behaviour of these beams in a more general way including beam's behaviour in the transverse direction. In fact, in some practical cases, corrosion might happens only on the exterior face of the beam or at one of its corners, and the 3D modelling can simulates these situations.

The modelling of bond loss in most of the previous research works involves adding new interface element to represent bond stress vs. slip behaviour between steel bar and concrete. However, this method consumes more time and effort and therefore impractical for modelling large 3D structures. This study used direct surface interaction between the 3D surfaces of steel bar and concrete, which is simpler using ABAQUS and works for both corroded and un-corroded cases.

Almost all of the available analytical or FE models in literature developed for either flexural-critical or shear-critical corroded beams. In this study, the developed FE model has the ability to model beams with different failure modes (shear, flexural, and bond failure).

CHAPTER 2

LITERATURE REVIEW

This chapter provides extensive literature review in various topics related to modeling of corroded RC beams with more emphasis in modeling of concrete-steel interaction (bond) and effect of corrosion in the mechanical properties of corroded steel bars.

A review of literature was carried out under the following subheadings:

- Mechanical properties of corroded reinforcement bars
- Bond between concrete and reinforcement steel bars
- Experimental works on corroded beams
- Modeling of corroded beams

2.1 Mechanical Properties of Corroded Reinforcement Bars

Almusallam (2001) tested corroded rebars (6 and 12 mm in diameter) in tension with different degrees of corrosion. Results showed that the tensile strength calculated based on actual residual area remained the same as the un-corroded strength. Brittle failure was observed in bars having more than 12% corrosion degree.

Cairns et al. (2005) studied corrosion effects on reinforcement's mechanical properties by conducting physical tests on reinforcing bars (rebars) with simulated (machined defects), real corrosion deterioration, and using numerical model. It was concluded that accelerated corrosion produces more uniform section loss than corrosion in natural and the major change in mechanical characteristics of corroded steel is in its ductility.

Du et al. (2005) studied the remaining capacity of corroded steel rebars by performing simulated and accelerated corrosion on reinforcing bars and in rebars embedded in concrete (total of 108 reinforcement specimens were tested). It is found that the remaining capacity of the corroded reinforcing bars and embedded reinforcing rebars is the same and the effects of diameter and type of reinforcing bars are insignificant and can be ignored in

practical engineering. In addition, the results showed that the force-deflection curve for corroded bar still has a substantial yield plateau and it is not substantially altered by corrosion up to 16%.

Apostolopoulos et al. (2006) examined the mechanical behavior of corroded steel bars by an experimental study using laboratory salt spray corrosion. Results showed that increasing duration of exposure results in mass loss increasing. It was noted that corrosion causes a moderate reduction in tensile strength, but they are lying below the standard limits for using steel bars in RC members, and significant reduction of the tensile ductility.

Moreno Fernández et al. (2007) addressed the decline in ductility of rebars embedded in concrete when exposed to accelerated corrosion. Results showed that damage in strain capacity was much higher than in yield strength as some corroded bars had elongation at maximum load equal to half of the control un-corroded bars. Their results served as a foundation for a discussion of the most appropriate methodology for structural analysis.

Lee & Cho (2009) investigated experimentally the connection between the mechanical properties of corroded steel bars and corrosion degree. The experiment work was conducted with the tensile test of the steel bars of different degree of corrosion. The results showed that the pitting corrosion is developed by chloride-induced corrosion, whereas uniform corrosion is developed by the electrical current. It was concluded that elastic modulus and the yield strength decreased with increasing the level of corrosion.

The influence of chloride-induced corrosion on the pit depth and mechanical characteristics of steel bars (type B500c) embedded in concrete was evaluated by Apostolopoulos et al. (2013). Their results indicated that much degradation, in yield strength, ductility, and depth of pitting, accrued in embedded steel samples than in bare samples for same mass loss.

François et al. (2013) investigated the effect of corrosion on the mechanical characteristics of steel embedded in concrete that had been vulnerable to natural corrosion for 27-year-old. The tensile test was conducted on the corroded and control steel bars. Results demonstrated that the degree of corrosion affected the ultimate stress and strain. It was

noted that the true yield stress of all corroded bars unchanged. However, the ultimate stress increased and ultimate elongation decreased.

Al-Osta (2013) used direct tension test for reinforcing bars, 18 mm and 20 mm in diameter, extracted from corroded specimens to obtain stress-strain plots. The results demonstrated that the total elongation and the ductility of corroded bar decreased as degree of corrosion (X_p) increased, and the corroded bars had well-define yield point. It was observed that the ultimate tensile load for the corroded rebars decreased with increasing the degree of corrosion.

Tang et al. (2014) examined the influence of corrosion's non-uniformity on the mechanical property of rebars. Three-dimensional laser scanner was used to calculate the average and critical cross sectional areas of corroded rebars. Results showed that increasing the degree of corrosion resulted in linear decrease in the yield and ultimate loads. However, the elongation and ductility decreased exponentially. In addition, change of failure mode from mixed ductile/brittle to brittle was observed because of corrosion.

Zhu & François (2014) conducted experiment tests on corroded rebars taken from beams subjected to chloride environment for 26 and 28 years. It was found that corrosion results in change in the ultimate elongation of steel bars. In addition, the remaining cross-section shape is the most parameter affecting the ductility of the bars.

Taha & Morsy (2015) studied the residual strength and mechanical attributes of corroded reinforcing bare bars. The study compared between two methods of repairing the corroded steel bar, the first one which is painting half surface area of corroded bar; and the other one by coating the full surface area of corroded bar. The experimental results indicated that, the corrosion process alters the external surface of steel bar due to pitting. The residual cross section of the corroded bar is not round anymore and considerable variation is noted along its length and circumference so the residual diameter is better defined by loss of weight.

2.2 Bond between Concrete and Reinforcement Steel Bars

2.2.1 Experimental work in bond strength

In the past century, Al-Sulaimani et al. (1990) studied the effect of corrosion on bond behavior of RC members by conducting pullout and simply supported beam tests. The beam specimens were of 150×150×1000 mm size, reinforced with 2-10 mm diameter top bars, 1-12 mm diameter corroded bottom bar and stirrups 6 mm diameter at 50 mm spacing. The bond failure in beams was studied by using two development lengths of bottom bar: one having embedded length of 144 mm and the other with 300 mm embedded length. The bond was investigated at different phases of reinforced bar corrosion: un-corroded, pre-cracking, cracking, and post-cracking levels. It was noted that the bond strength increases with increasing corrosion up to a definite quantity, however, with progressive increasing in corrosion degree, the bond strength declines rapidly for pullout tests.

Almusallam et al. (1996) conducted a study on the bond strength for corroded bars using pullout test. First, an increase on bond strength was observed in the pre-cracking stage (0–4% mass loss), then a rapid decrease up to a certain degree of corrosion (6% mass loss). After that, for 6% to 80% mass loss, the rate of ultimate bond strength decrease was much slower. It was seen that the first corrosion crack appears at 5% degree of corrosion. Likewise, Auyeung et al. (2000) noted that the bond was not completely destroyed even when there was extensive corrosion with considerable cracking of concrete.

Mangat and Elgarf (1999) used beam specimens recommended by Committee of RILEM/CEB/FIP. The beams were subjected to corrosion by applying current of 0.8 and 2.4 mA/cm2 at different degree of loss: 0, 0.3, 0.4, 0.5, 1, 2 and 5 percent. The curves of load vs. free end slip were obtained. The results indicated that the bond strength at small amounts of corrosion increases with increasing the degree of corrosion. The maximum increase was found to be more than 25 % at 0.4% corrosion (by rebar diameter loss). However, at high degree of corrosion, the bond strength drops sharply with increasing corrosion level.

Chan (2012) investigated the influence of rib patterns and relative rib area (Rr) of deformed bar with different grades on bond strength between concrete and steel. It was observed that the specimens with steel bars that have higher Rr exhibited higher bond stress.

Choi et al. (2014) conducted experimental work to investigate the differences of bond characteristics in RC members corroded by artificial rapid and natural corrosion methods. The artificial corrosion was done before concrete placement (method A) and after concrete placement (method B), whereas chlorides were directly mixed in fresh concrete to induce the natural corrosion in (method C) which was performed within a period of two years. Using non-destructive test (NDT), a formula of corrosion area prediction was proposed.

2.2.2 **Modelling the bond without corrosion**

The bond stress vs. relative displacement (bond-slip) for both cyclic and monotonic loading was studied in detailed by (Gan 2000). Two types of bond interaction elements with their bond stiffness matrices (contact elements and linkage elements) were developed. Four bond-slip models were presented in this study based on the outcomes of previous experimental studies.

Planner 2D FE analysis was conducted by Ogura et al. (2008) in order to study the effect of transverse reinforcement, the location of the main rebars, and concrete compressive strength on the bond splitting failure. FE analyses results for specimens of pullout and lap splice, tested in a former experimental program, indicated that the experimental bond splitting capacities are approximately proportional to the FE values of maximum average radial stress. Furthermore, it was found that in cases of a large amount of lateral reinforcement, concrete compressive strength could control the bond strength. However, the influence of the concrete remaining tensile strength in the splice region cannot be ignored.

Wenkenbach (2011) studied the tension stiffening in RC members containing large diameter rebars under sustained loading. Testing was done for four tension specimens with one embedded steel bar (25, 32, 40, 50 mm diameter). Evaluating of various steel-concrete bond models that have different bond evolution models was completed using a finite element model in ABAQUS.

Wu and Zhao (2013) developed a model for bond–slip using a continuous single equation that is appropriate for numerical simulations. The model equation does not differentiate between confined and plain concrete or pullout and splitting failure. Results showed that the model outperformed the existing models in the precision of its predictions.

As a part of benchmark examples, using ABAQUS, dealing with different components of composite beam to RC wall joints, Henriques et al. (2013) simulated the bond by using contact with cohesive behavior (the bond slip curve was approximated by the uncoupled traction–separation equation). Solid 3D element type, C3D8R, was used for both rebars and concrete. Good validation results were obtained using two tests, the first was pull-out tests of hooked rebars embedded in concrete blocks, and the second was a simply supported RC beam loaded with point load at the mid-span.

Dehestani and Mousavi (2015) presented a simple embedded steel bar element considering bond-slip behavior by an addition of equivalent strain. As a result, effective stiffness of the rebar decreased in the model. Model validation with the experimental data, which was done using the nonlinear FE software ABAQUS, showed its capability to reflect the effect of bond with using embedded elements in the analysis of RC structures. Modification factors for the effect of parameters: bar diameter, steel, and concrete properties, confinement conditions, and reinforcement ratio was obtained by comprehensive parametric study.

New FE bond element incorporating bond–slip relationship was introduced by (Santos & Henriques 2015) including steel strain effect. The proposed element consists of an orthotropic 4-node plane stress element with modified constitutive material laws. Validation results showed that the use of this element is needed to obtain good results. It was also noted that the bond element and the proposed reduction function are important in the following problems: tension stiffening, crack spacing, rotation capacity, minimum reinforcement, ductility, and deflection of cracked RC structures.

Murcia-Delso and Shing (2015) presented a new interface model simulating the bond-slip performance of reinforcement bars. A semi-empirical law was adopted which accounts for the steel yield strength, the bond loss produced by cyclic slip reversals, and the splitting of concrete. The results revealed that the model could be used accurately to estimate the bond-

slip performance of bars embedded in well-confined concrete and simulate splitting bond failures.

2.2.3 **Modelling the bond with corrosion**

Lee et al. (2002) conducted experimental and FE modeling for pullout tests for specimens with accelerated corrosion. It was noted that the bond strength and bond rigidity decrease as the degree of corrosion increase. The study presented empirical equations for calculating the strength and rigidity of the bond as a function of corrosion percentage.

Amleh and Ghosh (2006) modeled the bond and bond loss by using contact interaction approach in a 3D ABAQUS model for pullout test. The pressure perpendicular to contact surfaces of bar and concrete and the friction between them were reduced in case of concrete cracking. This reduction in pressure and friction was assessed using different corrosion levels in pullout tests. The result was based on the relationship that defines the loss in friction bond and contact pressure in terms of corrosion mass loss.

By taking into account many published experimental works, the authors of papers (Bhargava et al. 2006; Bhargava et al. 2007; Bhargava et al. 2008) added good contribution to research on corrosion-induced bond degradation. Bhargava et al. (2008) presented a simple empirical model to calculate the bond loss as a function of corrosion. Required time to cause concrete cracking and weight loss was studied by (Bhargava et al. 2006). It was noted that the required time to cause concrete cracking is greatly affected by tensile capacity of concrete cover, modulus of elasticity of steel, annual mean corrosion rate plus corrosion products combined. Bhargava et al. (2007) introduced analytical model for calculating the residual bond strength that accounts for various parameters such as expansive pressure due to rust formation, friction and adhesion between the cracked concrete and the corroded bar, and modeling of tensile behavior of cracked concrete.

In the study of Berto et al. (2008), two method of bond modeling was introduced: “damage type” and "frictional type". In the friction type, bond loss was represented by changing maximum bond strength (τ_{max}) and the slope of initial linear part of the bond-slip curve, whereas in the damage type, the whole shape of the curve could be modified according to

corrosion level. At the end, experimental tests of corroded beams were numerically simulated.

Lundgren et al. (2009) proposed one-dimensional analytical model for bond stress vs. slip behavior of corroded reinforcing bars. Shifting of the curve of CEB-FIP Model Code 1990 bond stress-slip model, with factors accounting for change of failure modes, was presented in this study to represent bond loss. In addition, the study presented calculation of the needed anchorage length using 1-D bond stress-slip differential equation.

Richard et al. (2010) presented a constitutive law for modeling concrete-steel interaction including corrosion effects. The study proposed 3D formulation based on continuum damage mechanics. Corroded and un-corroded pullout tests were simulated to show efficiency of the model. The study included a qualitative comparison between the experimental crack path due to corrosion and the damage pattern.

Shang et al. (2011) investigated the crack spacing and serviceability that can be adversely affected by rebars corrosion. Axial nonlinearity associated with corrosion in RC member under tension was examined to study that effect. The results showed that as rebars corrosion going on, less transverse cracks with larger spacing occur.

Recently, a study was done by Elbusaefi (2014) to examine the effect of corrosion on the bond capacity of concrete made using different cement replacement materials. The cement replacement binders included blended cements of fly ash (PFA), CEM II, metakaolin (MK), ground granulated blast-furnace slag (GGBS), and silica fume (SF). The influence of the corrosion rate was predicted by concrete permeability. Evaluation of bond strength was done using pullout test. Numerical modeling of these tested specimens was done using the ABAQUS program by employing a cohesive zone element for concrete-steel interface. Good agreement was noted between the experimental and numerical results for all specimens except for the PFA concrete in which the numerical results of bond strength was overestimated to the experimental ones.

Jnaid and Aboutaha (2014) studied the bond loss of corrosion by investigating the remaining flexural ultimate capacity of beams with un-bonded rebars. The approach used to calculate

ultimate stress in prestressed concrete, "neutral axis depth" approach, was modified. Using ANSYS software, a FEA model was created and verified with many experimental data (109 beams) that include many variables such as a/d ratio, length of un-bonded region, and type of loading. Analytical model for calculating the remaining flexural capacity was presented by using the experimental data and the FEA model. The results showed that major effects on the residual flexural capacity of un-bonded reinforcement beams are the reinforcement ratio and the un-bonded length, while other variables have limited impact.

Bossio et al. (2015) performed a preliminary FEM analysis using a cylindrical specimen reinforced by a single bar to simulate general or pitting corrosion. Furthermore, to evaluate the stresses in the concrete surrounding the rebars, a mechanical analytical model was proposed. In addition, crack propagation and non-linear development of stresses inside concrete when rebar start to corrode were evaluated through a sophisticated model. The results provided the relationships between the decrease of the steel area and the cracking development. Finally, satisfactory agreement was found between numerical findings and the experimental results available in the literature.

Chen and Nepal (2015) presented a new analytical model to estimate the remaining bond strength as well as predicting the cracking development of concrete cover. Thick-walled cylinder model was adopted for concrete cover considering residual tensile capacity, reduced tensile stiffness, and anisotropic behavior. The radial bursting pressure in the bond interface and the crack width development in the concrete cover were evaluated using a developed governing equation that takes into account, as a function of corrosion degree, the contributions of confinement, adhesion, and corrosion pressure. The suggested analytical model was validated successfully with the available experimental data.

2.3 Experimental Works on Corroded Beams

2.3.1 Flexural capacity of corroded beams

Cabrera and Ghoddoussi (1992) conducted experimental tests on corroded beams with dimensions of 160×125×1000 mm. A potentiostatic procedure was used to corrode the bottom bars by applying a current density for 40 days. The results indicated that a reduction of 9% of the cross-section area of bottom bar due to corrosion could result in a reduction

of 20% of the ultimate flexural capacity of the beams, and 40% increase in deflection value at mid-span at the service load.

An international experimental project, Brite/Euram project BE-4062 started in 1992, was conducted to investigate the service life of deteriorated concrete structures. Some outcomes from this project were presented on (Rodriguez et al. 1996; 1997). Most of the FE models accomplished by other researchers on corroded beams were validated with experimental data of this project. (Rodriguez et al. 1996) summarized some relevant aspects related to the assessment of structure conditions in corroded concrete structures. Comments on both steel section reduction and bond deterioration are also included together with their application to the study of corroded beams. Rodriguez et al. (1997) used beams with dimensions of 150 × 200 × 2300 mm having different reinforcement ratios. The ultimate flexural capacity of the control beams was found 37 kN-m. The capacity of corroded beam after 100 days and 200 days was reduced to 26 kN-m and 20 KN-m, respectively. It is found that a good agreement between the experimental ultimate flexural capacities of beam with only corroded bottom bars and the calculated value by using the residual area of the bottom bars. It was concluded that using RC conventional models taking into account the residual sectional area of both concrete and steel could be used to obtain conservative estimation of the ultimate bending moment and shear capacity value for high corrosion degree.

Mangat and Elgarf (1999) examined corrosion effects on the flexural capacity of RC beams by examining 111 simply supported beams. The beams were exposed to an accelerated corrosion technique in the laboratory and then tested using four-point loading. It was observed that the residual strength of corroded sample with 10% of corrosion was 75% of un-corroded sample.

Castel et al. (2000) (a&b) studied mechanical performance of RC beams with reinforcement corrosion. It was illustrated that the concrete cracking created by corrosion of compressive reinforcements does not significantly influence the mechanical characteristics of the RC beams in service. It was stated that the residual capacity of a

corroded beam could be predicted in most cases by taking into consideration only the reduction in tension steel area and ignoring the loss of bond.

Du et al. (2007) studied the ductility behavior and failure modes of corroded beams by conducting experimental study using electrochemically accelerated corrosion. The results showed that corroded beams were affected by corrosion in their ductile behavior and failure mode substantially in addition to their flexural strength. It was also noted that corrosion increases the ductility for beam in which the response is dominated by the reduction of its tension bars area and/or cracking of its compression concrete. However, corrosion decreases beam ductility for beam with behavior controlled by the reduction of its steel ductility and/or loss of its bond strength. The study raised a warning for the expected sudden failure in the mostly used under-reinforced RC beams if the corrosion percent is beyond approximately 10% because the considerably reduced ultimate strain of corroded rebars results in sudden rupture of those bars.

Based on extensive laboratory generated test data, Azad et al. (2007) suggested a two-step analytical approach for prediction of the residual flexural capacity. In this proposed method, first the strength was calculated using conventional theory using only the reduced tension steel area, and ignoring adverse implication of bond strength. In the next step, this value was corrected to yield the theoretical prediction by multiplying it with a reduction factor developed by means of a multi-level regression analysis of test data.

Malumbela et al. (2010) presented results of the difference of mass loss of the corroded RC beams under a sustained load by using an impressed current and constant wetting cycles (two different drying cycles). It was indicated that the highest degree of corrosion could be obtained with longer drying cycles. The results showed that the level of sustained load did not significantly influence the rate of corrosion of RC beam.

Azad et al. (2010) revised the analytical prediction presented in their previous study (Azad et al. 2007) of residual flexural strength of corroded beams in the context of relatively larger size beams reinforced with larger diameter tension bars to exclude the size-effect of beams in the proposed modeling and to improve further the accuracy of the analytical method. A new correction factor that replaced the previous one by correctly taking into

account the size-effect of the tension bars has been accomplished for a more compliant prediction approach. The results showed that the proposed method produced values that were in good matching with the test data of current and other experiments.

A long-term experimental project for corroded beams, started in 1984, was presented in references including (Dang & François 2014; Dang & François 2013; Castel et al. 2000a; Zhu & François 2014; François et al. 2013; Zhu et al. 2013). Total of 36 RC beams in two different common dimensions were stored in a chloride environment under sustained loading. Other batches of 36 beams with same properties were kept under laboratory environments as control beams. Dang and François (2013) investigated the structural performance of the 27-years-old corroded beam. Load-carrying capacity, the area loss, and force–deflection were measured. It was noted that both ultimate load and ductility were reduced after 27 years of heavy corrosion and this reduction in ductility was related to the reduction in mechanical properties of corroded rebars comparing with non-corroded rebars. Mechanical properties reduction for the same reinforcement bars used in the project was studied in (François et al. 2013) by making comparison between nominal and true stress for corroded and control steel bar specimens. Dang and François (2014) focused on studying the ductility reduction. Based on the ratio between ultimate deflection of corroded and non-corroded beams, they proposed a new ductility factor. Furthermore, the relation between cross-section loss of steel bars and ductility factor of corroded beams was investigated.

2.3.2 **Shear capacity of corroded beams**

Few researchers have studied corrosion effects in longitudinal steel bars and stirrups on shear strength. Xu et al. (2003) investigated experimentally the shear performance of corroded RC beams. It was seen that shear capacity reduction depends on span to depth ratio (a/d), for example in specimens that has 20% corrosion, the reduction was 10% when a/d = 1 and 20% when a/d = 2.

Toongoenthong and Maekawa (2004) investigated pre-induced damage effect on the shear strength of RC beams that has no stirrups. It was seen that RC beams with local corrosion

damage has lower reduction than the ones with extreme simulated corrosion conditions. The latter was 20% to 60% according to damage extension to anchorage zone.

Higgins and Farrow III (2006) studied experimentally shear capacity of corroded beams with accelerated corrosion. Three different corrosion damage levels were used for the embedded stirrups of large-size beam specimens. Results displayed that there was reduction in both shear strength and overall deflection at failure.

Val (2007) studied the effect of pitting and general corrosion on the shear and flexural behavior of RC beams by conducting reliability analysis. The results exposed that shear failure becomes the prevailing type of failure at higher corrosion rates in case of pitting corrosion. This says that, under pitting corrosion, shear strength reduction is higher than flexural strength reduction.

Research done by Suffern (2008) focused on studying the shear transfer mechanism nearby beam ends beside point loads, knowing as disturbed regions. The strength reduction, which occurs in disturbed regions, in beams with corroded stirrups was investigated through an experimental program and analytical strut and tie modeling. Furthermore, the feasibility of strengthening the corroded beams with dry lay-up CFRP was studied. It was noted from the experimental tests that a strength reduction was clear in most corroded specimens and the stiffness was also reduced in the those specimens. Moreover, the reduction on strength depended on corrosion level, i.e. 41% reduction in high corrosion level, 18-53% reduction in medium corrosion level, and 26% reduction with low corrosion level. The main contribution of this study is allowing the designers to analyze the disturbed regions and determine the strength reduction in beams with corroded stirrups.

Imam (2012) studied experimentally the shear behavior of corroded RC beams with different corrosion duration and two different beam cross-sections (140x220x1150mm and 150x240x1150mm) and developed a prediction model that estimate the residual shear strength of corroded beam. The beam specimens were corroded by impressed current technique before tested in four-point loading system. The reinforcing steel was extracted from tested beams to calculate gravimetric weight loss after the loading test. It was noted that the product of corrosion current density and corrosion period $I_{corr}T$ significantly affects

the shear capacity of a corroded beam. Furthermore, based on the developed strength prediction model, Monte Carlo simulation was conducted to estimate the probability of failure.

Short-span corroded beam specimens, part of the French project started on 1984, were tested on (Zhu et al. 2013) by three-point loading in order to investigate corrosion effects on shear strength. The configuration and the widths of the cracks were depicted prior to the flexural test. Load-deflection curves and slip of tension rebars were recorded. It was observed that the loss in bond strength and cross-sectional area of rebars resulting from chloride-induced corrosion have a substantial effect on the bending capacity of short-span beams.

Lachemi et al. (2014) evaluated the corrosion effects on shear behavior for beams made of self-consolidating concrete (SCC). Control beams specimens were made by normal concrete that has equal compressive strength as the (SCC) ones. The experimental program was consist of 20 RC beams (10 SCC and 10 NC) with 150mm x 220mm x 1400mm dimensions and shear span to depth ratio a/d = 2.5 subjected to four levels of corrosion (at 5%, 10%, 15%, and 20% of mass loss) using accelerated corrosion. It was noted that the obvious changes in structural capacity and failure mode are associated with increased corrosion levels regardless of concrete type.

2.4 Modeling of Corroded Beams

2.4.1 Analytical models for flexural capacity of corroded beams

Maaddawy et al. (2005) presented an analytical model that predicts the behavior of corroded and un-corroded beams. In the model, the deflection of the RC beam was calculated based on the elongation of the reinforcement steel between flexural cracks rather than on curvature of the beam. A new bond-slip model was proposed based on published data to calculate the loss of bond strength due to corrosion. The accuracy of the model was validated by conducting new experimental study and the results showed that the model is accurate in prediction the load-deflection curves of both corroded and un-corroded beams.

Wang and Liu (2008) calculated the flexural strength of corroded RC beam considering the loss of bond strength between concrete and corroded steel. An analytical model for the estimation of flexural capacity of the corroded RC beam was proposed based on compatibility of deformations and equilibrium of forces for the whole beam. Results from this perdition model were validated with published experimental data and this showed the practicality of the proposed method.

Wang & Liu (2010) proposed a simplified methodology to estimates of the residual life of corroded beams. The results showed that the flexural capacity of these beams did not significantly affected by bond or corroded length if tensile reinforcements of these beams can reach their yield strength.

Hanjari et al. (2011) conducted both FE and analytical modeling to study the behavior and residual capacity of corroded RC structures. Modeling was done by changing in properties and geometry of corroded reinforcement steel and concrete such as reduction of rebar's area and ductility, modification of bond-slip properties, and adjustment of concrete response caused by corrosion cracks. Suggestion was made to show pitting corrosion effect on the capacity of corroded RC beams.

Han et al. (2014) introduced a model for assessment of the flexural capacity in corroded RC members. The model was based on extension of models of concrete-steel bond that depends on thick-walled cylinder theory. It was proposed by incorporating the concept of average expansion pressure to the non-linear flexural analysis model and to the bond strength model. Validation of the proposed model was done using 59 corroded RC flexural members taken from four different references. This proved that the model gives very good prediction of the flexural capacity degradations.

2.4.2 **FE models for flexural capacity of corroded beams**

Coronelli and Gambarova (2004) studied the influence of corrosion on the performance of beams by developing 2D nonlinear FE modeling. Many damage parameters was considered in existing structure such as cracking and crushing, bar yielding, bond failure, and the assessment of the actual safety level. The effect of corrosion in nonlinear finite element analysis was modeled by changing the properties of elements such as rebar's area and by

applying the appropriate material's constitutive laws and the bond between reinforcement steel and the surrounding concrete. Cracking and spalling in the compressed concrete are described by reducing the strength of the concrete elements belonging to the cover. It was claimed that the use of a specific model for bond deterioration seemed to be of paramount importance to evaluate the residual ductility of a structural elements.

Kallias and Rafiq (2010) studied the structural behavior of corroded beams using nonlinear FEM using DIANA software in two-dimensions. Validation of the FE models was done, with good agreement in terms of load deflection characteristics, with experimental tests from (Rodriguez et al. 1996; Du et al. 2007). Corrosion effects were introduced in the FE analysis by modifying the constitutive material relationships for reinforcing steel, concrete, and bond properties in addition to reducing the geometry of both steel and concrete. They investigated the effects on both serviceability and ultimate limit states. It was concluded from the results that increasing bond loss results in increasing crack spacing and widths but does not affect the ultimate capacity if the tensile rebars are well anchored at their ends. It was also observed that ignoring cover concrete damage in the compressive zone leads to over-estimation of structural behavior at the both the serviceability and ultimate limit states.

Sánchez et al. (2010) presented a FE model to simulate corroded RC members. The developed model has capability to simulate the various corrosion effects on the predictions of the load carrying capacity. An elasto-plastic constitutive relation and "Continuum Strong Discontinuity Approach" (CSDA) are used to model the reinforcement bars and concrete, respectively. The concrete-steel interface was modeled by using contact-friction elements with the friction loss as a function of the level of corrosion. Validation of the proposed model was based on previous numerical and experimental results.

Wurst (2013) carried out a FE modeling using ABAQUS software to study the effect of corrosion in the bridge deck on load redistribution between girders and system capacity of bridges. First, to find the material input values required to simulate corrosion, FEA model of beam (corroded and un-corroded) was done using the available material modeling techniques such as Brittle Cracking (BC), Smeared Crack (SC), and Concrete Damage

plasticity (CDP) models for concrete. Both 2D and 3D element types were used for both concrete and rebars. After the FE input values were calibrated using the experimental results, they were applied to three full-scale bridge models to investigate how corrosion in the deck affects the system capacity of the bridges. Results from one bridge model showed that stress distribution in the corroded deck, and therefore in the girders, is more uniformed than with the un-corroded deck. Other bridge models had divergence problems.

Ou and Nguyen (2014) investigated the corrosion effects on the length of plastic hinge (Lp) in RC beams by developing nonlinear FEA model. Verification of the FE model was done using experimental data from two different references: (Rodriguez et al. 1997) and (Du et al. 2007). A parametric study was carried out then to study the effects of shear span, corrosion level, the longitudinal tension reinforcement ratio, and concrete compressive strength on the plastic hinge length of reinforced concrete. Results of the parametric study stated that no strong correlation exists between the Lp and concrete strength or ratio of longitudinal reinforcement but Lp has a positive correlation with shear span for both corroded and un-corroded beams. In addition, it was noted that as the corrosion increases, the plastic hinge length decreases.

Biondini and Vergani (2014) presented a nonlinear 3D FEM beam element for analysis of corroded RC beams, which accounts for both geometrical and material nonlinearity. The FE model considered the pitting and uniform corrosion and included the area loss of rebars, the weakening of concrete due to splitting cracks, and delamination and spalling of the cover concrete, but bond loss was not included in this study. A very good validation results were noticed for the corroded beam FE models with experimental beam specimens of (Rodriguez et al. 1997). Two 3D FE analyses for a statically indeterminate RC beam and arch bridge under different deterioration situations and corrosion levels were done as an application of the proposed formulation.

German and Pamin (2015) started their nonlinear FEM modeling in ABAQUS by carrying out a 2D FE model for corroded beam section with corrosion product (rust) modeled as interface element (COH2D4 element type in ABAQUS). The aim of the 2D model was to simulate reinforcement corrosion influence on the concrete cover. Explicit and implicit

algorithms of nonlinear computations were used and compared in the cross section analysis. At the end, a 3D FEM modeling of a beam subject to static loading and corrosion was analyzed. The sequence of application of displacement load and corrosion load was changed. It was noted that the ending destruction of concrete was the same regardless of what the loading order was.

Almassri et al. (2015) investigated corroded RC beams, exposed to natural corrosion for 25 years, repaired with near surface mounted reinforcement (NSM) CFRP rods, and studied the mode of failure of the repaired beam according to experimental and numerical modeling results. Experimental results and numerical modeling results of a 2D finite element (FE) model using the FEMIX computer code were obtained. The FE numerical modeling results from FEMIX were compatible with the experimental ones except for the repaired corroded beam, for which a three-dimensional model using the commercial software ABAQUS was required. It was noted that the NSM technique increased the overall capacity (ultimate load capacity and yielding capacity) of control and corroded beams despite a non-classical mode of failure with separation of the concrete cover occurring in the corroded beam due to damage induced by corrosion. Three-dimensional FEM analysis using ABAQUS was able to predict both load-bearing capacity and ultimate deflection reduction due to corrosion if the crack plane induced by corrosion was taken into account in the model.

2.4.3 **Modeling the shear-critical corroded beams**

Potisuk et al. (2011) conducted a study on the shear-dominated behavior beams. Finite element was developed to study the contributions of corrosion damage parameters such as spalling of concrete cover, uniform and pitting corrosion of stirrup, and loss of bond between stirrups and concrete on structural behavior of corroded beams. Both individual and combined damages were performed by FE analyses. Good agreement was observed between the FE and experimental results in estimating the residual capacity of corroded beams.

Bernard (2013) investigated the capacity and the behavior of shear critical RC beams with corrosion in shear reinforcement only. FE modeling approach was used with different degree of corrosion (10%, 30%, and 50%). The study included a parametric study of some

shear design parameters such as stirrup spacing, shear span-to-depth ratio, and beam width. The results concluded that with increasing level of corrosion, a softening of the load-deformation curves came with the reduction in load carrying capacity.

Review of the literature implies that many researchers have been working in this direction to model the corroded beam using the finite element analysis. However, most of them focused on two-dimensional (2D) modeling, furthermore, the available analytical or FE models were for either flexural-critical or shear-critical corroded beams. Therefore, in this study, RC beam FE models were developed in ABAQUS by using 3D elements for both concrete and steel bars and the model is capable of modelling both types of beams with different failure modes (shear, flexural, and bond failure).

CHAPTER 3

FINITE ELEMENT MODEL

3.1 Introduction

The modeling of the corroded member is quite difficult as cracking in concrete cover due to corrosion is random and corrosion degree can vary considerably along the beam. This chapter provides detailed descriptions for the proposed finite element model including the required concrete and steel material models and discusses some bond modeling approaches.

In the FE analysis, the material properties for un-corroded beam were modified to reflect the corrosion damage by taking into account the following corrosion-induced phenomena:

- Reduction of bond-slip properties.
- Reduction of steel area.
- Degradation in mechanical properties of steel (yield and ultimate strengths, strain values, and modulus of elasticity).
- Cracking of concrete cover.

The following tasks have been done in this study in order to construct and validate the proposed FE model in ABAQUS:

1. Select concrete behavior model.
2. Select steel behavior model.
3. Construct FE model for one actual control beam (un-corroded beam) with perfect bond between reinforcement bars and the surrounding concrete.
4. Validate the results of the FE model with experimental results.

5. To select bond-modeling method, use the same FE model of the un-corroded beam but now with different bond modeling methods

6. Choose the method that give load-deflection close to perfect bond case (because the beam is un-corroded)

7. To consider corroded beam case, apply the appropriate modification for steel, concrete, bond strength according to corrosion degree.

8. Validate with experimental results for corroded beams.

Tasks 1 to 7 discussed in details in this chapter, the last task regarding validation with experimental results presented in chapter 4. Firstly, section 3.2 presents the first three tasks for developing FE model of un-corroded beam with perfect bond. Secondly, sections 3.3 and 3.4 discuss the selection of bond modeling method (tasks 4, 5, and 6) after trying different approaches. Finally, details of applying corrosion effect in the model presented in section 3.5.

3.2 FE modelling of control (un-corroded) beam

The numerical finite element method (FEM) tool used in this research is the nonlinear finite element package ABAQUS. It is one of the most widely used and available software packages for FEM. Its ability can be applied in a many situations to develop a general reinforced concrete model. The FE model of RC beams can be used to estimate the capacity of beams and therefore to reduce the time and cost of expensive experimental tests.

The type of analysis used was "Dynamic Explicit" which has a conditionally stable solution technique using explicit integration. This type was chosen based on the fact that this method is a very powerful in solving problems that are static such as Quasi-static process modelling problems including complex contact (Simulia 2013). From many previous researchers, analysis using this method rarely encountered any problems of convergence. However, for static problems using dynamic analysis, inertial effects should be minimized by using slow loading rates or increasing the mass density so that the oscillation of the results is limited (Mercan 2011). In this study, it has been found that using loading time of one second with increasing the mass density gives good results.

3.2.1 **Mesh and boundary conditions**

In this study, the developed numerical FE models involve three-dimensional (3D) solid elements (C3D8R: An 8-noded linear brick element type) for both concrete and longitudinal reinforcement bars and two-node elements (T3D2: A 2-noded linear 3-D truss element type) for the stirrups. The brick elements after the meshing was having face dimension of 20mm. the model of the beams were simply supported using pin and roller, it was noted from initial modelling that using of pin support, restraining in horizontal direction, provides better results because it represent the friction resistant in the experimental test. These boundary conditions were applied to middle bottom line of the supporting steel plates. Loading was applied as uniform pressure to the top surface of steel loading plates to avoid stress concentration problems. Example of many beams modelled in this study is shown in Figure 3-1.

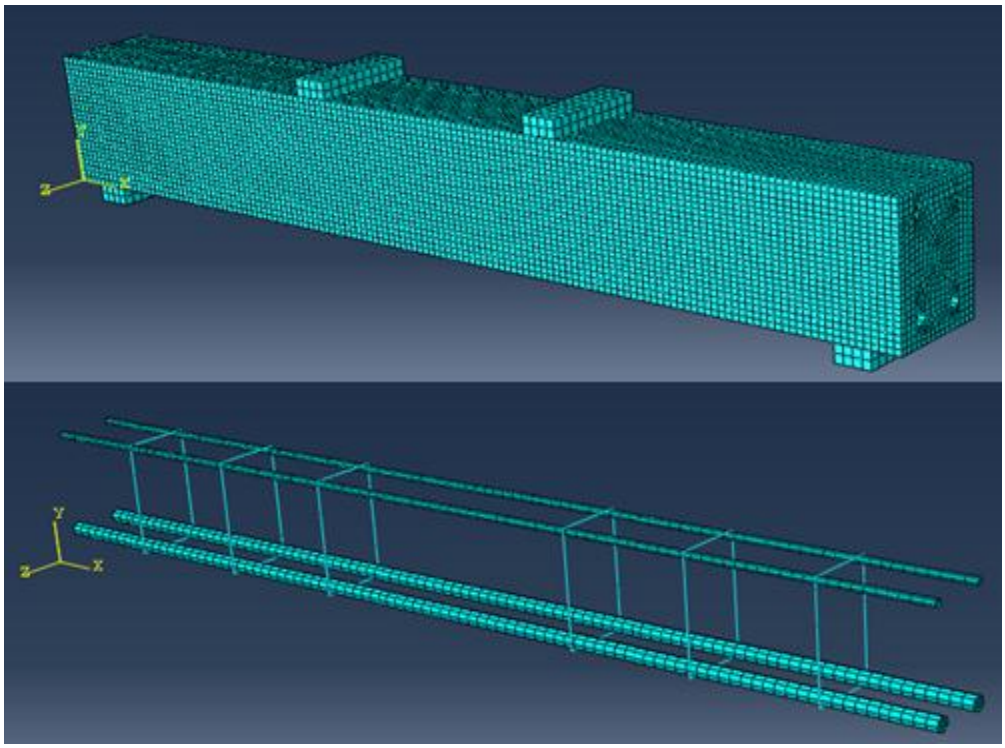

Figure 3-1: Example of the 3D FE model for beams in ABAQUS

3.2.2 **Concrete behavior model**

Three different techniques for modeling nonlinear behavior of concrete are available in ABAQUS: the Smeared cracking model (SC), the Concrete Damaged Plasticity model (CDP), and the Brittle Cracking model. The CDP model, developed by Lubliner et al. (1989) and extended by Lee and Fenves (1998), uses concepts of isotropic damaged elasticity in combination with isotropic tensile and compressive plasticity to represent the inelastic behavior of concrete. It assumes that the main two failure mechanisms are tensile cracking and compressive crushing of the concrete material (Simulia 2013). This concrete model was used in this study because it is more stable for the numeric calculation.

3.2.2.1 **CDP parameters**

To define the CDP model in ABAQUS, several parameters need to be input including: Poisson's ratio, which was assumed = 0.2 for concrete, elastic modulus, compressive and tensile behavior (presented in the next sections), and five plastic damage parameters. They are (ψ – dilatation angle; ε – flow potential eccentricity; f_{b0}/f_{c0} – ratio of initial equibiaxial compressive yield stress to initial compressive yield stress; K_c – ratio of second stress invariant on the tensile meridian; μ –viscosity parameter). Dilatation angle used was 36^o that is common value of concrete. For the remaining parameters, default values were used as suggested by ABAQUS (Table 3-1).

Table 3-1: Plastic damage parameters used for concrete modeling

ψ	ε	f_{b0}/f_{c0}	K_c	μ
36	0.1	1.16	0.67	0

3.2.2.2 **Concrete behavior in compression**

The CDP model requires as input the stress vs. inelastic strain of concrete for both compression and tension, which obtained from uniaxial compression and tension tests. In this study, the hardening and softening behavior in compression of the concrete are implemented in the FE code based on CEB-FIP model code (2010) (FIB 2010) as shown in Figure 3-2 and expressed on equations (1) to (3) and the linear part of compression curve was assumed to be up to $0.4\, f_c'$.

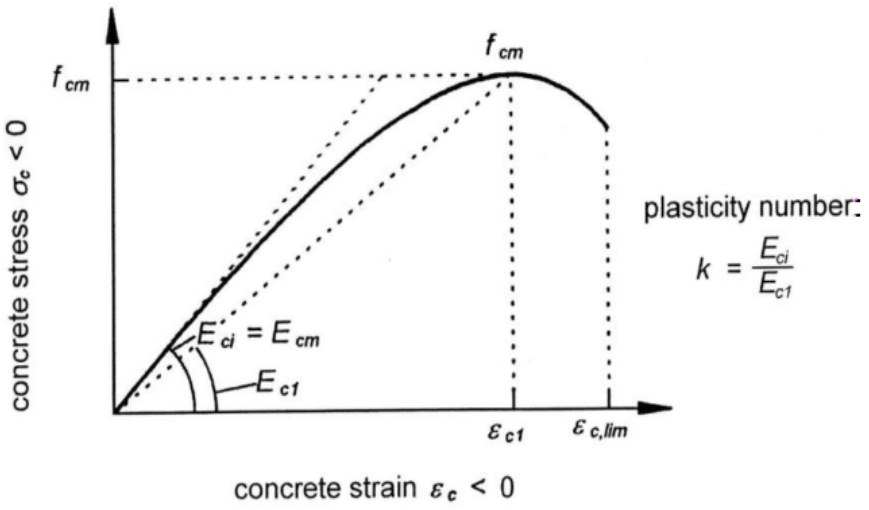

Figure 3-2: Schematic representation of the stress-strain relation for uniaxial compression (FIB 2010)

$$\frac{\sigma_c}{f_{\mathrm{cm}}} = \frac{\mathrm{k}\eta - \eta^2}{1 + \eta(k-2)} \tag{1}$$

Where σ_c is the compressive stress, f_{cm} is the mean concrete cylinder compressive strength, k and η are two factors calculated using equations (2) and (3). E_{c1} is the secant modulus of elasticity of concrete from origin to peak compressive stress, E is the elastic modulus of concrete calculated as per ACI-318 known equation, ε_c is the concrete strain, $\varepsilon_{\mathrm{c1}}$ is the compressive strain at the peak stress f_{cm}.

$$\eta = \frac{\varepsilon_c}{\varepsilon_{\mathrm{c1}}} \tag{2}$$

$$k = \frac{E}{E_{\mathrm{c1}}} \tag{3}$$

3.2.2.3 **Concrete behavior in tension**

The tension behavior of concrete is considered to be a linear elastic until concrete cracking is initiated at a tensile strength in flexural, f_r, expressed by equation (4) based on the ACI code. After cracking, the softening behavior begins.

$$f_r = 0.62\sqrt{f_c'} \quad (4)$$

Among the available models for tension softening relationship, this study used bilinear tension behavior based on Model Code 2010 model for stress-crack opening relation (Figure 3-3) after converting the cracking opening axis to strain values by dividing to a characteristic length, l_c, assumed equal to element size as in (Ou & Nguyen 2014). The fracture energy G_f calculated by the following expression

$$G_F = 73(f_t)^{0.18} \quad (5)$$

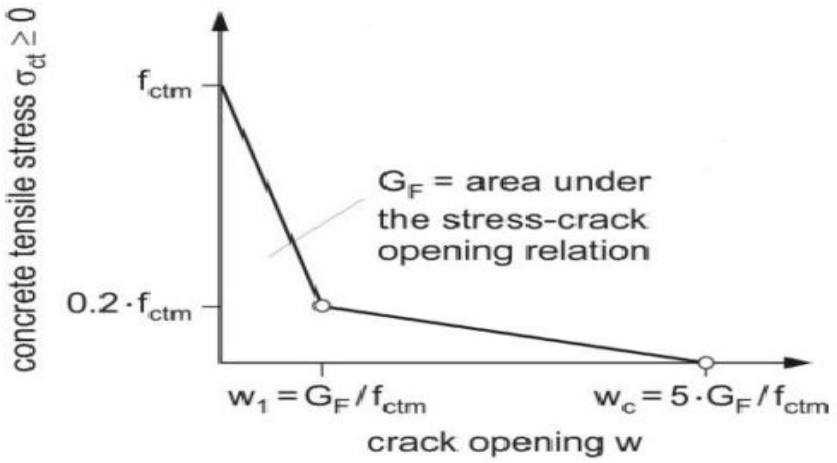

Figure 3-3: Stress vs. crack opening for uniaxial tension (according to fib Bulletin 42) (FIB 2010)

3.2.2.4 **Compression and tension damage parameters**

The last things to calculate for CDP model are the compression and tension damage parameters (d_c and d_t). The equation used to determine these parameters are based on (Birtel & Mark 2006) as shown in equations (6) and (7). Where b_c and b_t are values between 0 and 1 that result in maximum values of d_c and d_t close to 0.4 and 0.8 respectively. More details regarding these damage parameters and CDP in general are available in material section of ABAQUS analysis user's manual (Simulia 2013)

$$d_c = 1 - \frac{\sigma_c E^{-1}}{\varepsilon_c^{\mathrm{pl}}(1/b_c - 1) + \sigma_c E^{-1}} \quad (6)$$

$$d_t = 1 - \frac{\sigma_t E^{-1}}{\varepsilon_t^{\mathrm{pl}}(1/b_t - 1) + \sigma_t E^{-1}} \quad (7)$$

3.2.3 **Steel behavior model**

An elasto-plastic behavior with hardening was considered in this study. In ABAQUS, this behavior is first defined by the elastic behavior using the modulus of elasticity (E_s = 200000 N/mm^2) and the Poisson's ratio (ν = 0.3), then, the plastic behavior is defined by inputting tabular data of true stress vs. plastic strain. If the stress-strain curve for the un-corroded steel bar is not available from the experimental test, the curve can be estimated according to the steel stress-strain model of Mander (1983). As ABAQUS requires inputting true stress-strain values, converting from nominal stress-strain was done using the following two equations.

$$\sigma_{\mathrm{true}} = \sigma(1 + \varepsilon) \quad (8)$$

$$\varepsilon_{\mathrm{true}} = \ln(1 + \varepsilon) \quad (9)$$

3.3 Bond Modeling

Unlike FE for un-corroded beams, perfect bond assumption is not applicable for beams that have corroded reinforcements. Therefore, this study aims to get benefit from surface interaction techniques available in ABAQUS to simulate bond for both corroded and un-corroded beams.

Since the study of Eligehausen et al. (1983), who proposed a segmental bond-slip behavior model (shear stress in the interface surface vs. bar slip) after conducting tests exploring the effects of different parameters, most of the researchers in this area have concentrated on extra improvement to his bond-slip model (Wu & Zhao 2013). This model of Eligehausen et al. (1983) constitutes the basis of the bond-slip model given in (FIB 2010), see Figure 3-13 (a).

Three main options were used in the literature to simulate the concrete/steel bond in modeling beams by finite element analysis (FEA):

(1) The first option is the use of interface or spring element to transfers the stress between steel and concrete. One advantage of this element is that it can be used with 2D modeling in which steel rebars simulated by two-node truss elements and the nonlinearity of spring element is represented by entering the load vs. displacement relationship. However, this method consumes more time and effort and therefore impractical for modelling large 3D structures. Most researchers used this method in a different ways. The 1-D interface element, named translator in ABAQUS, was used by Li et al. (2014) to developed FE model for studying the behavior of concrete seawalls affected by corrosion. The element, that represents the bond, has two nodes connecting concrete and rebars elements. Researchers such as Thomas & Ramaswamy (2006) and Xiaoming & Hongqiang (2012) also used spring interface elements for bond modeling. Some other researchers used 4-noded interface element to represent the bond by using ABAQUS (Val & Chernin 2009; Murcia-Delso & Shing 2015) or using DIANA software as in (Kallias & Rafiq 2010).

(2) The second option is to make changes to concrete or steel element properties to simulate the effect of bond. In (Ziari & Kianoush 2014), material properties of small concrete region, called Bond Zone, in contact with the reinforcing bar were modified to represent better bond interaction. The fracture energy and the tensile strength were decreased in this zone. In the study of Dehestani & Mousavi (2015), equivalent strain of bond-slip effect was added to the strain of the steel bar to account for bond interaction.

(3) The third option is the bond as an interaction between two 3D surfaces. This method can be used in different approaches in ABAQUS for 3D model of both concrete and steel. Amleh and Ghosh (2006) used this method for finite element pullout tests for corroded and un-corroded case. Mechanical contact property was used in ABAQUS to describe the tangential and normal behavior between the contacting surfaces of concrete and steel.

In this study, different methods for bond modeling using surfaced based interaction (option 3) were used as explained below.Two main approaches can be used in ABAQUS for this surface interaction. The first approach is *Surface-based mechanical contact* and the second is *Surface-based cohesive behavior* which is a mechanical model based on traction-separation behavior. This cohesive behavior allows the bond between two surfaces to be

expressed as a linear elastic relationship between traction (**t**) and separation (**δ)**. In this study, both approaches, the contact and cohesive behavior, were investigated to simulate the bond in un-corroded RC beam. Then, method that gives good validation results was used later for corroded beams.

3.3.1 **Approach one: Surface-based Mechanical Contact**

In this approach, the behavior of the contact (Contact property) is defined in two directions: normal and tangential to the contacting surfaces. Pure Master-Slave contact system is used in ABAQUS in which nodes of the *Slave* surface cannot penetrate the other surface (the *Master*). In the case of reinforced concrete, the slave surface is the rebar and the master surface is the concrete (Amleh & Ghosh 2006). Mechanical contact approach can be further classified to many methods according to different properties that have to be inputted for normal or tangential direction such as friction and the pressure.

3.3.1.1 **Normal behavior of surface-based contact**

The normal behavior of the contact property can be defined by pressure-overclosure relationships. The behavior, called "hard" contact, is the default pressure-overclosure contact method in ABAQUS. In this behavior, the contact constraint, in direction normal to the contacting surfaces, is applied only when the separating distance between the two surfaces, called clearance, becomes zero. Contact pressure between the surfaces can go high with no upper limit. On other words, the behavior does not permit the transfer of tensile stress in normal direction across the interface when the surfaces are separated (Figure 3-4).

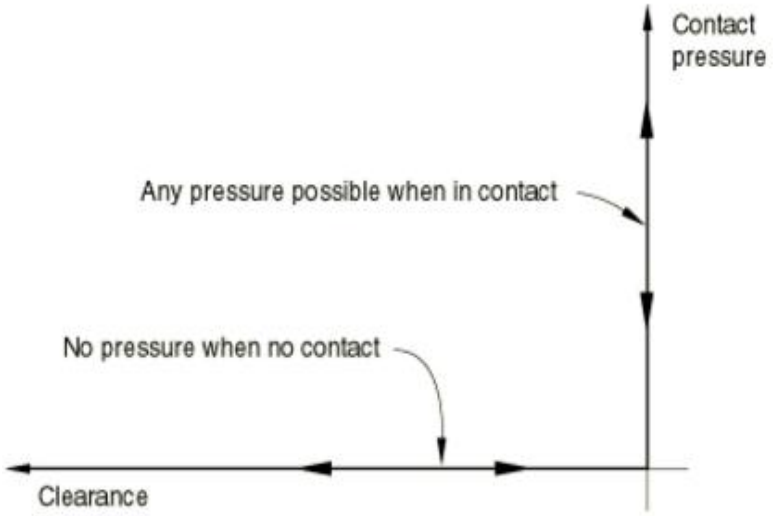

Figure 3-4: Contact pressure-clearance relationship for "hard" contact (Simulia 2013)

Other available types for pressure-overclosure behavior include using a linear law, a tabular piecewise-linear law, or an exponential law. Linear pressure-overclosure can be defined by specifying the contact stiffness in ($N/mm^2/mm$). The optimal type to model corrosion was found to be the exponential law (Amleh & Ghosh 2006), which is shown in Figure 3-5. This relationship takes into consideration the increase in pressure when the surfaces get closer, and allows the pressure to vanish if the surfaces are no longer in contact. Using the results from pull out tests presented in (Amleh & Ghosh 2006), the pressure at zero clearance (P_0) for un-corroded case was related to the concrete cover thickness (C) by equation (10), where P_0 is expressed in MPa and C is expressed in mm.

$$P_0 = 0.128C + 1.5 \quad (10)$$

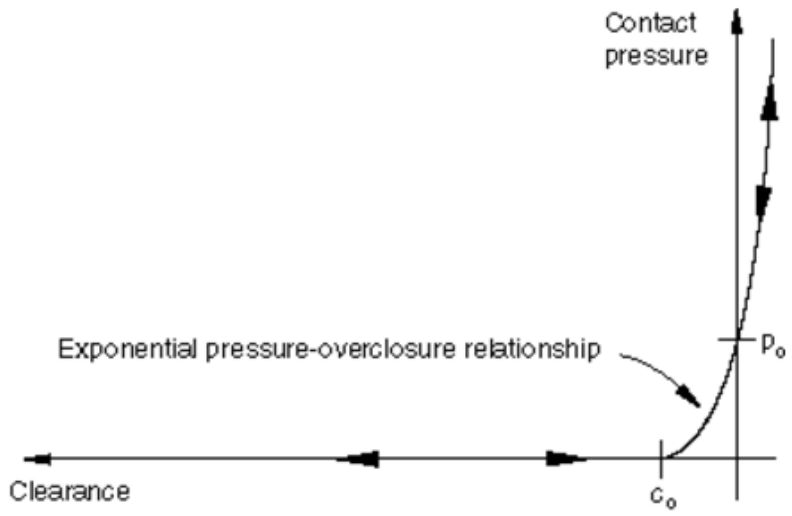

Figure 3-5: "Softened" exponential pressure-overclosure relationship (Simulia 2013)

3.3.1.2 **Tangential behavior of surface-based contact**

Across the interface, shear stress is transmitted between the contacting surfaces as well as the normal stresses. Therefore, frictional forces that resist the relative slipping of the surfaces should be considered. One common and basic model used in ABAQUS is the Coulomb friction. It describes the frictional behavior by a coefficient of friction, **μ**, in all directions (isotropic friction), which is usually a value less than one for most cases. For ideal friction, no tangential motion between the surfaces will occur unless the traction (shear stress) reaches a critical value, which affected by the normal contact pressure based on the following equation (Simulia 2013):

$$\tau_{\text{crit}} = \mu P \tag{11}$$

Because of the difficulty of simulating ideal friction, ABAQUS makes use of a penalty friction formulation in most situations, with a permitted slight relative slips (elastic slip) during surfaces sticking as illustrated via the dashed line in Figure 3-6. The slope of this line (penalty stiffness) is automatically chosen by ABAQUS to make the slip value very small portion of the length of the characteristic element (Simulia 2013).

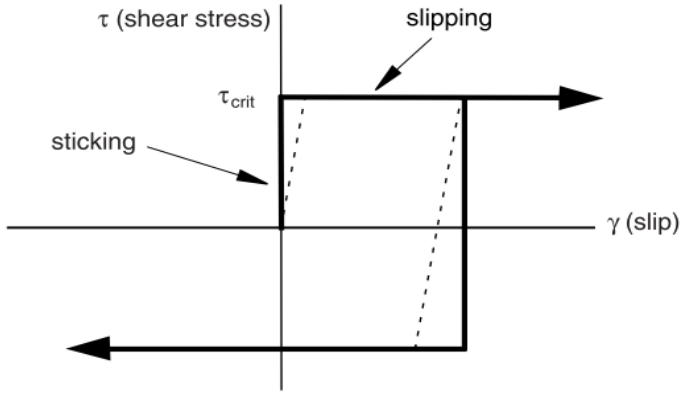

Figure 3-6: Penalty friction formulation behavior (Simulia 2013)

It is well known by experimental data that there are two coefficients of friction, the first acts against initial slipping called "static" friction coefficient, and the second, normally smaller than static coefficient, is active during the slipping and called the "kinetic" friction coefficient (Simulia 2013). The transference between these two coefficient values can be done in ABAQUS using exponential decay relationship in which the friction coefficient declines exponentially based on the following formula

$$\mu = \mu_k + (\mu_s - \mu_k)e^{-d_c\dot{\gamma}_{\text{eq}}} \tag{12}$$

Where μ_k is the kinetic friction coefficient, μ_s is the static friction coefficient, d_c is a user-defined decay coefficient, and $\dot{\gamma}_{\text{eq}}$ is the slip rate.

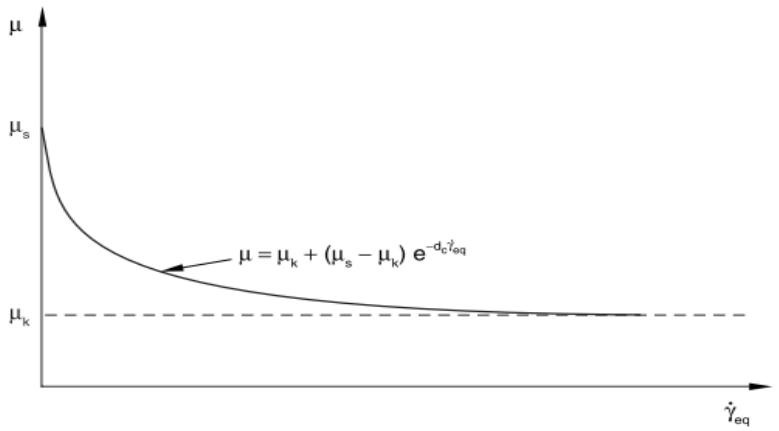

Figure 3-7: Exponential decay friction model (Simulia 2013)

3.3.2 **Approach two: Surface-based Cohesive Behavior**

In ABAQUS, this method is a mechanical model based on traction-separation behavior that allows the bond between two surfaces to be expressed as a linear elastic relationship between traction (**t**) (bond stress) and separation (**δ)** (slip). Some researchers used this method but in 2D modeling of pull-out tests such as (Wenkenbach 2011) who studied the tension stiffening in RC members with large diameter rebars. Henriques et al. (2013) used surface-based cohesive behavior in 3D modeling of beam but without considering bond loss.

Typically, ABAQUS has two methods for simulating the bonded interface behavior using traction-separation behavior. The first is cohesive elements, and the second is surface-based cohesive behavior. In the study, the thickness of the interface is negligible. Consequently, surface-based cohesive method is used due to its convenience and effectiveness. This traction-separation model consists of two parts in ABAQUS; first part is a linear elastic behavior, and the other part, which starts after the elastic part by specifying the initiation and evolution of bond damage. An elastic constitutive matrix represents the elastic behavior, which relates the shear and normal stresses to the shear and normal separations across the interface (Simulia 2013). The constitutive relation for elastic part is either uncoupled or coupled, as shown in (13) and (14) , respectively.

$$t = \begin{pmatrix} t_n \\ t_s \\ t_t \end{pmatrix} = \begin{pmatrix} K_{\mathrm{nn}} & 0 & 0 \\ 0 & K_{\mathrm{ss}} & 0 \\ 0 & 0 & K_{\mathrm{tt}} \end{pmatrix} \begin{pmatrix} \delta_n \\ \delta_s \\ \delta_t \end{pmatrix} = \mathrm{K}\delta \tag{13}$$

$$t = \begin{pmatrix} t_n \\ t_s \\ t_t \end{pmatrix} = \begin{pmatrix} K_{nn} & K_{ns} & K_{nt} \\ K_{ns} & K_{ss} & K_{st} \\ K_{nt} & K_{st} & K_{tt} \end{pmatrix} \begin{pmatrix} \delta_n \\ \delta_s \\ \delta_t \end{pmatrix} = K\delta \tag{14}$$

In this research, since the uncoupled behavior is used as suggested by many researchers, only the terms K_{nn}, K_{ss}, and K_{tt}, have to be defined. The unit of the constants in the K matrix is [Force/Length^2/ Length] that is representing the bond stiffness. The challenge behind this elastic model is to estimate the K matrix with values that reflect the steel-concrete bond.

Second part of this cohesive behavior is the initiation and evolution of damage. Damage is the term given to the interface behavior when it stops acting elastically. After the initiation of damage, the evolution of damage can be defined to model the behavior of the bond after the loss of elasticity.

The bond-slip relationship of steel bar can be approximated in this method by using the bond damage criterion where the damage initiates when any one of the three normal stresses exceeds a maximum allowable value. This criterion can be represented as

$$Max\left\{\frac{<t_n>}{t_n^0}, \frac{t_s}{t_s^0}, \frac{t_t}{t_t^0}\right\} = 1 \qquad (15)$$

The normal stress, t_n, in Eq. (15) has been placed within Macaulay brackets. This is to avoid a compressive stress ($t_n < 0$) resulting in damage initiation. To make the maximum shear stress controlling the behavior, large value for maximum t_n should be used. Note that maximum bond strength (τ_{max}) is represented in ABAQUS by t_s and the t_t has no effect on behavior since there is almost no stress in transverse direction of the bar.

Damage evolution describes the way in which the interface stiffness degrades once the damage initiation condition is met. In ABAQUS, there are choices of a linear, exponential, or user defined response for this cohesive damage evolution. Linear response is defined by specifying the maximum effective separation (Max. δ_m) at which the bond is fully degraded. It is define by:

$$\delta_m = \sqrt{<\delta_n>^2 + {\delta_s}^2 + {\delta_t}^2} \qquad (16)$$

In this study, linear damage evolution was used by specifying δ_m = maximum slip in long tangential direction (max. δ_s) because slip values in other two directions are very small compared to it. This damage evolution was chosen because it simple and gives enough accuracy. This is supported by the small difference in results of four different cohesive damage models in ABAQUS as presented in (Wenkenbach 2011). Figure 3-8 shows the full bond behavior characteristic that can be used as an approximation of bond-slip curve.

The damage initiation starts at point A and damage evolution is describing the behavior from point A to point B.

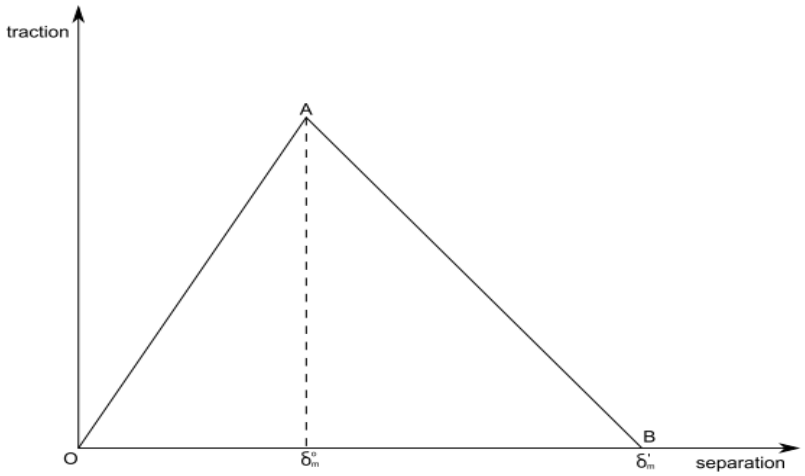

Figure 3-8: Traction-separation characteristic with linear damage evolution

3.4 Results of bond modelling approaches using control beam

3.4.1 Un-corroded beam used for bond model validation

One of the un-corroded beam specimens tested by Lachemi et al. (2014) was chosen for result validation of the of different bond modelling methods. In their study, Lachemi et al. (2014) experimentally examined shear behavior of corroded beams made of self-consolidating concrete (SCC) and same number of control beams specimens made by normal concrete (NC) that have equal strength (f_c' =45.5 MPa and f_t =5.2 MPa). The beams were subjected to four levels of corrosion, 5%, 10%, 15%, and 20% of mass loss in both stirrups and bottom bars. Dimensions of the tested beams are 150mm x 220mm x 1400mm and shear span ratio of a/d = 2.5, (see Figure 3-9). All beam specimens tested in (Lachemi et al. 2014), including the un-corroded specimen (NC-B2) used in this chapter for bond modeling, have small shear span length (440 mm) over which the reinforcement needs to be developed with no end hooks. Therefore, they are critical for bond strength.

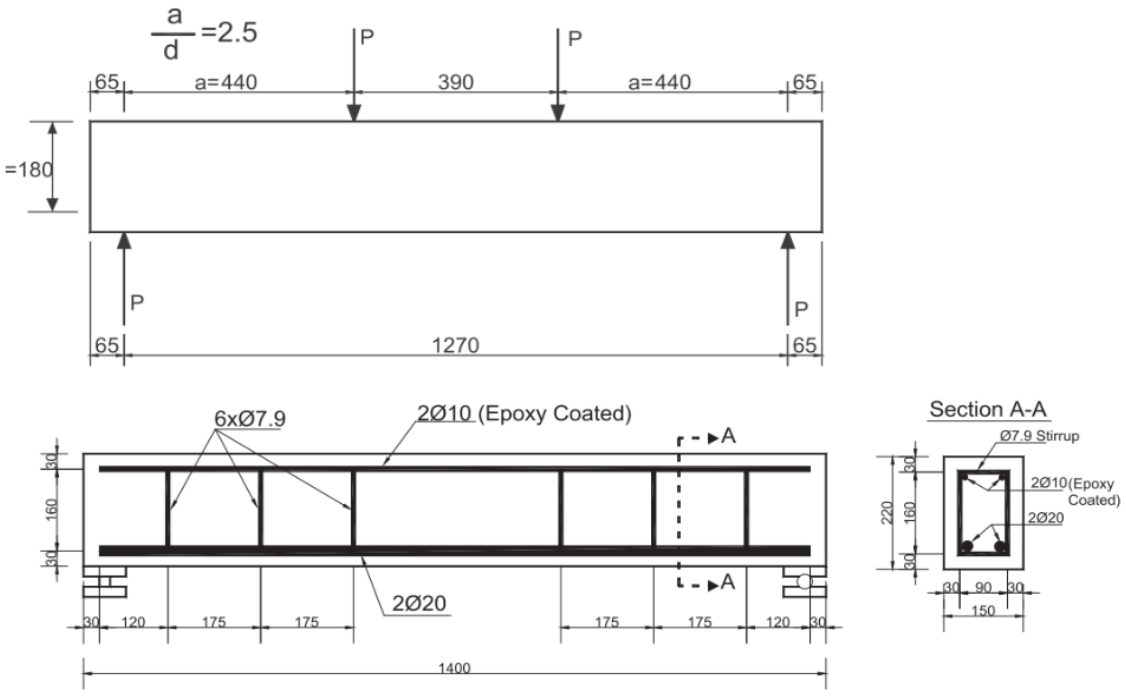

Figure 3-9 : Beam used for validation of bond modelling methods (Lachemi et al. 2014) (dimensions in mm)

3.4.2 **Perfect Bond Case**

Prior to investigating bond modelling by surface interaction methods, FE model for the un-corroded beam NC-B2 was constructed using simple perfect bond in which steel and concrete elements are tied by their connecting interface nodes. After validation of this perfect bond case with the experimental result, several FE models of the same beam were developed by changing the bond modeling method to find out the most accurate one.

Good agreement can be observed between the load vs. deflection curves of the experimental beam (NC-B2) and FE in Figure 3-10. It is well known that for beams with no corroded steel bars, the assumption of perfect bond is enough for simulation. However, this validation was conducted first to illustrate that material models and other aspect of the proposed FE model are accepted and the only remaining task is finding out the bond modeling method that can first simulate the un-corroded beam model accurately and then the corroded beam case.

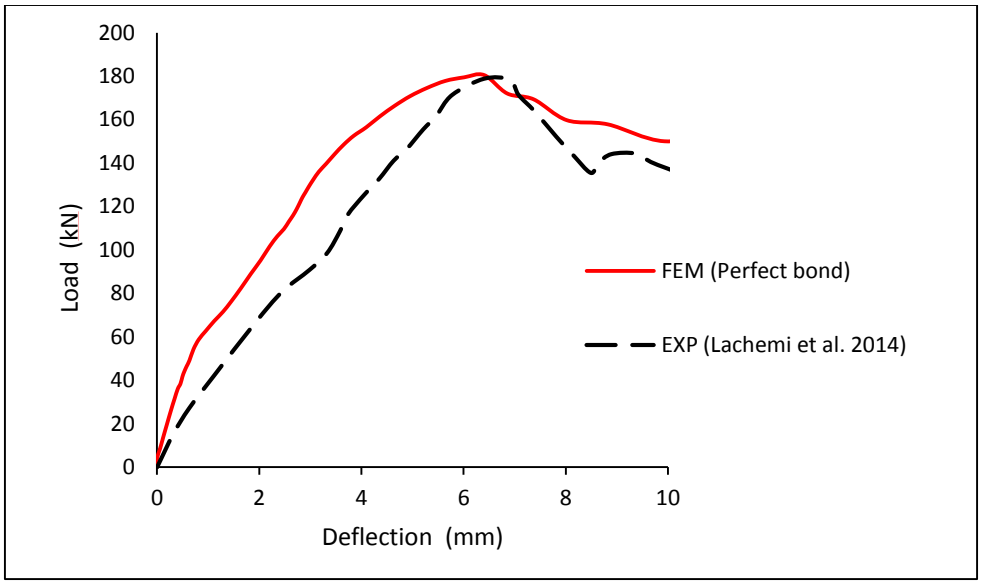

Figure 3-10: Load-Deflection curve validation for Perfect Bond Method for the selected beam (NC-B2)

3.4.3 **Results of Surface-based Mechanical Contact**

As mentioned earlier, this approach can be further classified to many methods according to different properties that have to be inputted for normal or tangential direction such as friction and the pressure. In this study, three different methods using the principle of surface-based mechanical contact were examined as the following:

1) **Method-1**: Contact property in which the tangential behavior is defined by a penalty friction formulation, using constant friction coefficient = 1.0 and no shear limit was used in this study for this method (see Figure 3-6), as initial FE modeling showed no effect. The normal behavior is defined by using a "hard" contact relationship (see Figure 3-4).

2) **Method-2**: Contact property in which the normal behavior is linear pressure-overclosure defined by contact stiffness = 1000 N/mm^2/mm, as suggested by (German & Pamin 2015). The tangential behavior is the same as method-1(i.e. penalty friction with coefficient = 1.0).

3) **Method**-3: Contact property with tangential behavior defined by exponential decay friction model (Figure 3-7) and normal behavior defined by softened contact with an

exponential pressure overclosure relationship (Figure 3-5). The parameters used for this third method was according to (Amleh & Ghosh 2006).

To investigate the above three options, same FE model of beam NC-B2 was modified by replacing the perfect bond method. Results of first two contact properties in Figure 3-11 show much lower load capacity. Therefore, these two methods failed to simulate the bond behavior of un-corroded RC beams. This indicates that friction alone in tangential behavior in these methods was not enough to develop good constraint especially if there is no additional applied pressure on steel bars to make the friction more effective. (Hard and linear stiffness behaviors do not apply any confined pressure unless it results from the respond of the beam to the applied loading).

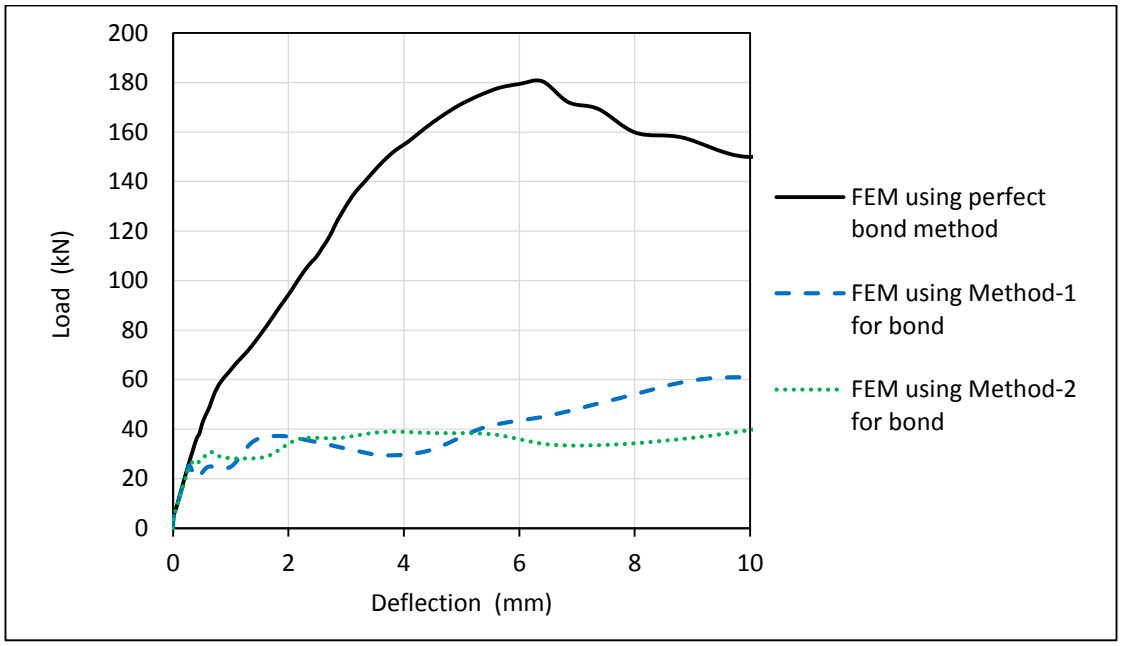

Figure 3-11: Results of bond modeling by Methods 1 and 2 of the approach one (surface-based contact) for NC-B2 beam

In Method-3, the values of the parameters in Eq. (12) for the tangential behavior were obtained for the un-corroded case from (Amleh & Ghosh 2006) ($\mu s = 1$, $\mu k = 0.4$, $dc = 0.45$) and γeq is calculated at each loading increment automatically by ABAQUS. In the normal behavior, pressure was used according to the equation (10), which was equal to 5.3 MPa, but the resulting capacity was very small compared to perfect bond case

(Figure 3-12). Therefore, other normal pressure values were used to capture the behavior of un-corroded RC beam. As shown in Figure 3-12 , even with the value of 15 MPa of Po, the capacity of the RC beam remained significantly lower than the actual capacity of beam. This is because of using larger values of Po resulted in early failure of the concrete prior to development the full strength of beam.

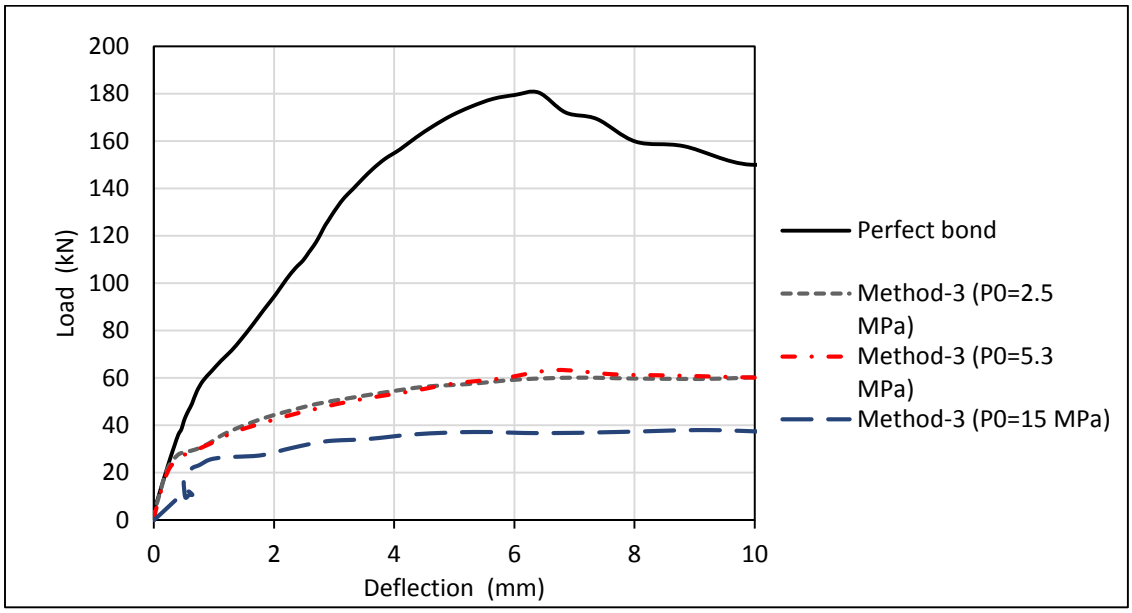

Figure 3-12: Results of bond modelling by Method-3 of the approach one (surface-based contact) with different P0 values for NC-B2 beam

In summary, none of three different methods of surface contact was able to simulate the interaction between the steel bars and the surrounding concrete. Although, Method-3 was used successfully by (Amleh & Ghosh 2006) to simulate pullout tests but not for the behavior of beams and it was done using different analysis method (ABAQUS Standards).

3.4.4 **Results of Surface-Based Cohesive Behavior Approach**

In order to model the concrete-reinforcement bond in ABAQUS by using Surface-based cohesive approach, parameters that define the cohesive interaction should be defined carefully to reflect the actual behavior of the bond-slip relation between concrete and steel rebars. There are various models available in the literature for bond-slip behavior for corroded and un-corroded RC members. Many researchers used, with some modifications, the model proposed by Eligehausen et al. (1983) and prescribed by the Model Code 2010

(FIB 2010) such as Henriques et al. (2013), Ou & Nguyen (2014), Hanjari et al. (2011), and Elbusaefi (2014). Figure 3-13 (a) and (b) show bond–slip model based on the Model Code 2010 and the approximation (in all three dimensions) of bond model that is used in ABAQUS, respectively (Henriques et al. 2013).

As mentioned earlier, in order to represent the bond-slip behavior using this method, tangential long direction (K_{ss}, t_s δ_s), which is the same direction of the bond-slip relationship (Figure 3-13 (a)), should be the critical direction of this cohesive behavior. Values of $\tau_{\max}$, S_1, and S_3 are needed to specify the bond initiation and evolution parameters and the bond stiffness values can be calculated using the expressions (17) and (18).

$$k_{\mathrm{ss}} = k_{\mathrm{tt}} = \frac{\tau_{\max}}{S_1} \tag{17}$$

$$k_{\mathrm{nn}} = 100k_{\mathrm{tt}} = 100k_{\mathrm{ss}} \tag{18}$$

The value of K_{nn} was considered as an infinite stiffness according to assumption by Gan (2000).

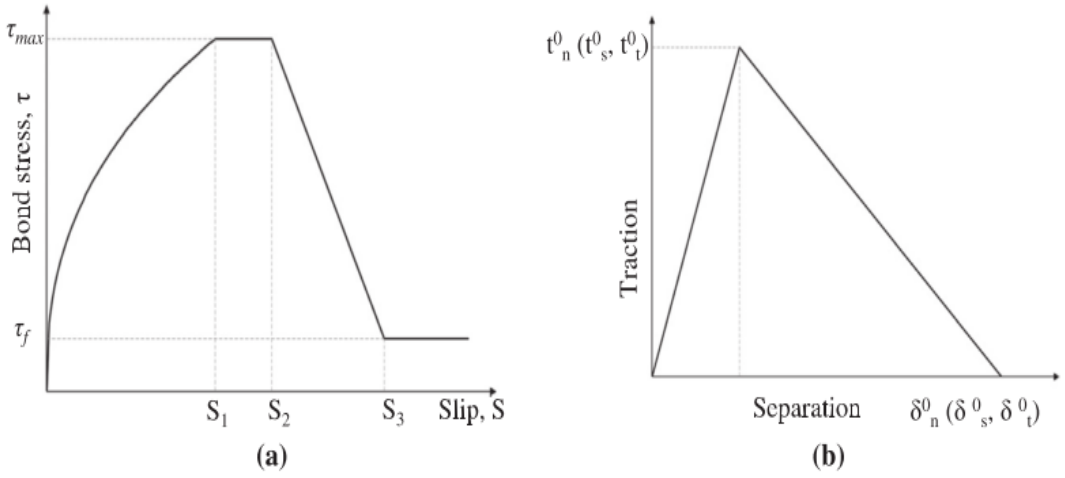

Figure 3-13: (a) Bond–slip model in Model Code 2010; (b) traction–separation behavior in ABAQUS (Henriques et al. 2013)

Maaddawy et al. (2005) used equation (19) to estimate of the bond strength $\tau_{\max}$ of un-corroded and corroded rebars in concrete (in MPa). It consists of two terms, the first is the contribution from concrete, and the second is the contribution from stirrups. This equation was chosen in this study because it includes the effect of various parameters on the bond strength and it is valid for both corroded and un-corroded case. Note that R is the reduction factor for bond loss and it is equal to 1.0 for un-corroded case.

$$\tau_{\max} = R(0.55 + 0.24\frac{c_c}{d_b})\sqrt{f_c'} + 0.191\frac{A_t f_{\mathrm{yt}}}{S_s d_b} \quad (19)$$

Where: c_c is smaller of concrete clear cover and one-half clear spacing between rebars, d_b is diameter of the rebar, S_s is spacing of the stirrup, A_t is the total area of stirrup within the S_s that crosses splitting planes, f_{yt} is yield stress of the stirrup.

Value of slip at maximum bond stress, S_1, is needed to compute stiffness values in Eq. (17). So a model for slip values used by Kallias & Rafiq (2010) was also used in this study. S_1 is equal to S_{max} expressed on Eq. (20) and maximum slip (S_2) = 0.35 C_0 , where C_0 = rib spacing = half of the bar diameter (assumed). The used bond-slip relation is shown in Figure 3-14 with dashed line indicates the approximation used in ABAQUS (note that u_{max} is the τ_{max}).

$$S_{\max} = 0.15C_0 e^{\frac{10}{3}\ln\left(\frac{\tau_{\max}}{\tau_1}\right)} + S_0 \ln\left(\frac{\tau_1}{t_{\max}}\right) \quad (20)$$

where $\tau_1 = 2.57\sqrt{f_c'}$, and S_0 = 0.4 mm for confined concrete.

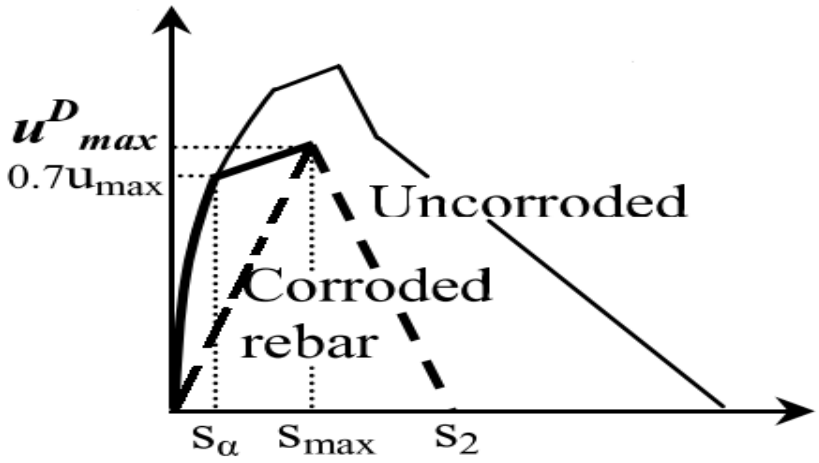

Figure 3-14: Bond-slip of Kallias & Rafiq (2010) and its approximation used in this study

Figure 3-15 shows load-deflection curve using the above equations compared with perfect bond case and experimental results of beam NC-B2. The result showed excellent agreement between the prefect bond case and cohesive bond model; moreover, FE curve using this bond method is closer to the experimental curve than the perfect bond case. After this successful validation for the un-corroded case, same bond modelling method will be used for corroded beams.

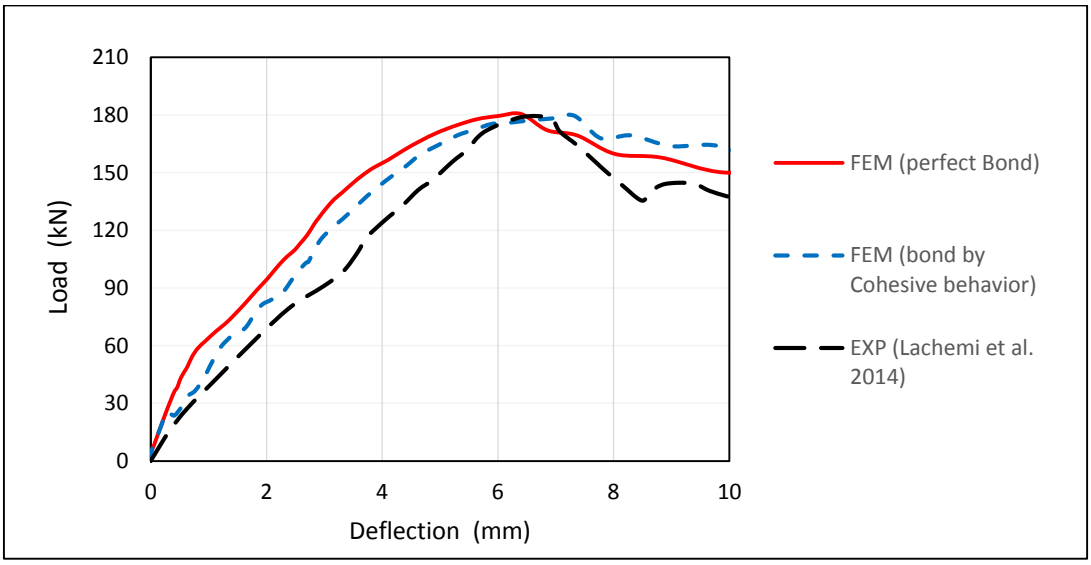

Figure 3-15: Results of bond modeling using approach two for bond (based cohesive behavior) with both perfect bond and experimental curves

3.5 FE modeling of corroded beam

To model the corroded beam, first FE model is constructed assuming no corrosion with bond modeled using approach two as elaborated earlier, then the model is upgraded to include all corrosion damages by implementing to ABAQUS the appropriate reduction empirical models available in the literature for corrosion-induced damages. These reductions were applied in this study as the following:

3.5.1 Reduction in Strength of Concrete in Cover Region

Corrosion in steel bars cause cracking of concrete cover near the corroded bar and this cracking will affect the behavior of the beam especially of this cracking in the compression region. the most common model to include this effect was presented in (Coronelli & Gambarova 2004). It was used in (Finozzi et al. 2014; Ou & Nguyen 2014b; Kallias & Rafiq 2010; Hanjari et al. 2011; Biondini & Vergani 2014).

Coronelli and Gambarova (2004) reported that the rust of the corrosion process would result into volume expansion that produces splitting stresses in the concrete and may cause the surrounding concrete cover to crack. In regions with high levels of confinement, the concrete cracks and the un-cracked parts in between the cracks contributes to the stiffness and load carrying capacity. It was proposed to use the following equations to reduce concrete strength of cracked concrete due to corrosion in compression zone (Figure 3-16):

$$f_{cc,cracked} = \frac{f_c'}{1 + K\frac{\varepsilon_1}{\varepsilon_o}} \tag{21}$$

where f_c' is the compressive strength of virgin concrete; K is a coefficient linked to bar diameter and roughness (K = 0.1 for ribbed bars with moderate diameter (Capé 1999)). ε_o is strain value at the highest compressive strength f_c'; ε_1 is the average tensile strain in the cracked concrete normal to the direction of the applied compression and can be calculated as:

$$\varepsilon_1 = \frac{(b_f - b_o)}{b_o} \tag{22}$$

where: b_o is the undamaged member section width and b_f is the member width increased by corrosion cracking. The increase in beam width (b_f - b_o), can be approximated as:

$$(b_f - b_o) = n_{bar} w_{cr} \tag{23}$$

w_{cr} can be estimated by using the crack width proposed by (Molina et al. 1993):

$$\sum w_{cr} = 2\pi(v_{r/s} - 1)P_r T \tag{24}$$

where n_{bar} is the number of reinforcement bars in the compression zone, w_{cr} is the crack width for a given corrosion penetration $P_r T$, T = time corrosion period. $v_{r/s}$ is the ratio of volumetric expansion of the oxides with respect to the virgin material and it varies from 1.7 for FeO and 6.15 for Fe (OH)33H_2O (Liu & Weyers 1998). However, the value of $v_{r/s}$ = 2.0 was commonly used in previous FE studied of corroded concrete and was chosen for this study.

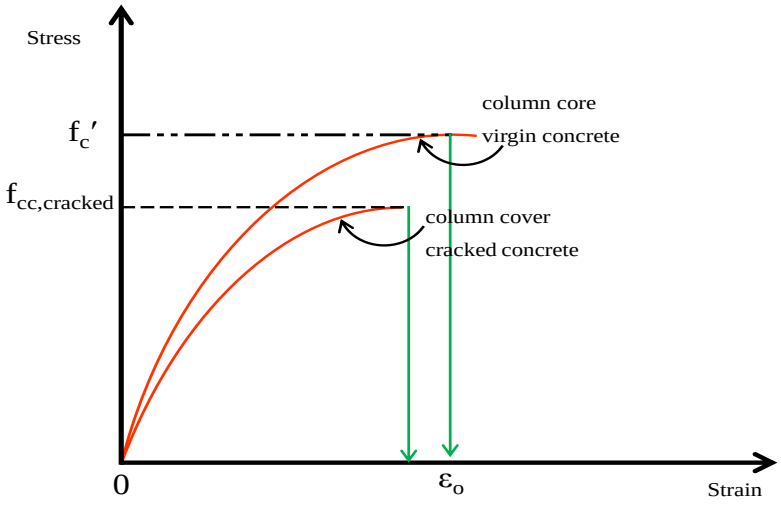

Figure 3-16: Reduced concrete strength in compression zone due to corrosion (Al-Osta-2013).

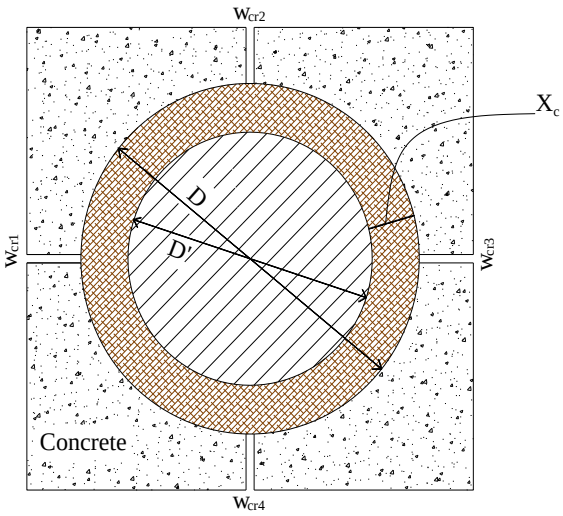

Figure 3-17: Corrosion product around the bar and the width of corrosion crack (Al-Osta-2013).

Eq. (24) can be derived from Figure 3-17 as follows (Al-Osta 2013).

The volume of steel rust/ unit length =

$$\frac{\pi}{4}(D^2 - (D - 2X_c)^2) = \pi D X_c \tag{25}$$

Equating increase in volume due to rust = $(v_{r/s} - 1)\,\pi D X_c$ and the increase in volume due to crack

$$\frac{\pi}{4}\left(D + \frac{\sum w_{cri}}{\pi}\right)^2 - \frac{\pi}{4}D^2 = \frac{D\sum w_{cri}}{2\pi} \tag{26}$$

The total width of cracks becomes

$$\sum w_{cri} = 2\pi(v_{r/s} - 1)X_c \tag{27}$$

Where: D is the original diameter of rebar; D′ is the diameter of corroded rebar; Xc is penetration depth and is equal to P_rT; Pr is metal loss rate or penetration rate; T is time corrosion period; $v_{r/s}$ is the volume ratio between rust and steel and $\sum w_{cri}$ is the total corrosion crack width

For columns and beam-columns with square or circular cross-section, ε_1 can be calculated as an average based on the perimeter as:

$$\varepsilon_1 = \frac{(P_e - P_o)}{P_o} = \frac{((4b_0 + n_{bar}\sum w_i) - 4b_0)}{4b_0} = \frac{n_{bar}\sum w_{cri}}{4b_0} \qquad (28)$$

Where: P_o is the undamaged member section perimeter and P_e is the member perimeter increased by corrosion cracking.

To illustrate the effect of corrosion on the compressive strength, the concrete strength ratio in compression zone versus metal loss X_p is plotted in Figure 3-18 using Eq. (21). It is observed that the concrete strength ratio in compression zone decreases with increasing the mass loss (Xp) due to corrosion.

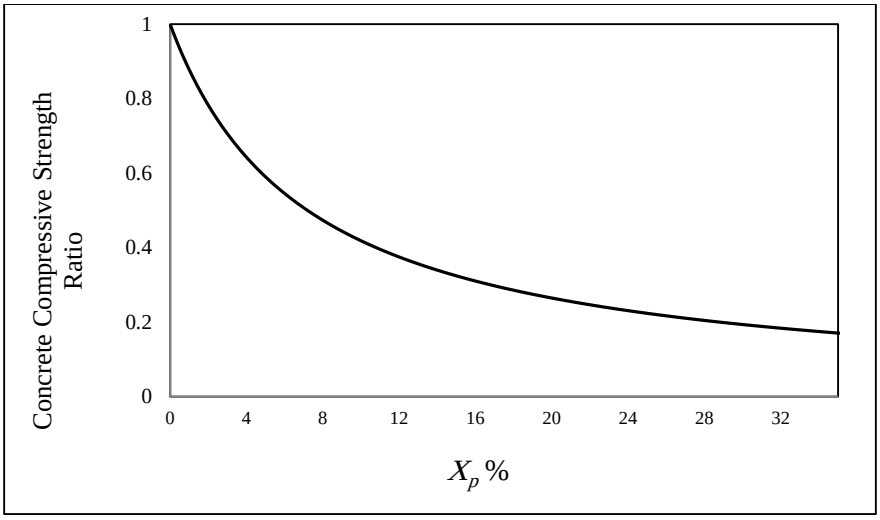

Figure 3-18: Corrosion effect on compressive strength of concrete (Al-Osta-2013).

In this study, the above reduction model was used for concrete cover zones in both top and bottom of the beam and the reduction in the tensile strength of the concrete was determined based on the same reduction factor in compressive strength (Hanjari et al. 2011):

$$f_{t,cracked} = \frac{f_{cc,cracked}}{f_{c'}} f_t \qquad (29)$$

3.5.2 **Reduction in Steel bar Properties**

It is well known that corrosion result in a reduction in the rebar's cross-sectional area, but this reduction in not uniform along the steel bar. In addition, the amount of average reduction in the cross-sectional area is same as of the amount of mass loss (X_p) in the same bar. Therefore, the average reduced cross-sectional area after corrosion can be expressed by (30). Where A_s is the residual area, and A_{so} is the original area of the rebar before corrosion.

$$A_s = \left(1 - 0.01X_p\right)A_{s0} \tag{30}$$

From the literature review: as the corrosion increase, residual yield (F_{yc}) and ultimate (F_{uc}) forces for reinforcement decrease more rapidly than the average area (As), therefore, there is a reduction in yield stress (f_y) in addition to the decrease in the area (Du et al. 2005). This decrease is due to pitting corrosion (non-uniformity in reduction), which causes stress concentration at pitting locations (Ou & Nguyen 2014). This is explained by expression (31). Note that if we have perfectly uniform corrosion both side of (31) should be equal because corrosion does not change the material properties of the remaining steel.

$$f_y = \frac{F_{yc}}{A_s}(\text{with corrosion}) \;<\; f_y = \frac{F_{y0}}{A_{s0}}(\text{no corrosion}) \tag{31}$$

Similarly, the irregular decreases around cross section and along bar length result in larger stress and strain values at pitting locations than in other locations. Therefore, the corroded bar failed at total average strain that is smaller than the ultimate strain of the un-corroded bar (Ou & Nguyen 2014). On other words, in addition to reduction in area and strengths, considerable reduction occurs in ductility (represented by ultimate strain value).

There are two methods to consider the pitting corrosion effects. First method is directly by using reduced area based on maximum pit depth, the other method is by using reduction in the yield strength in addition to average reduced area (As). The two reductions in area and yield strength can be combined by calculating the residual yield strength based on original un-corroded bar area (i.e. $f_{yc} = \frac{F_{yc}}{A_{s0}}$).

The maximum depth of the corrosion pit, *P(T)*, at the bar cross section can be estimated based on Stewart (2009) model as:

$$P(T) = 0.0116 \times I_{corr} \times Y \times T \tag{32}$$

Where: I_{corr} is the corrosion current density (normally expressed in ($\mu A/cm^2$); T is time since corrosion initiation in years; and $P(T)$ is in mm.

Gonzalez et al. (1995) suggested the maximum pitting factor Y from 4 to 8 for reinforced concrete samples open to natural environments.

Val & Melchers (1997) estimated the following equations to predict the area of the pit (A_{pit}) for the pit configuration shown in Figure 3-19.

$$A_{pit}(T) = \begin{cases} A_1 + A_2 & P(T) \le \dfrac{D}{\sqrt{2}} \\ \dfrac{\pi D^2}{4} - A_1 + A_2 & \dfrac{D}{\sqrt{2}} < P(T) \le D \\ \dfrac{\pi D^2}{4} & P(T) > D \end{cases} \tag{33}$$

Where:

$$b_p = 2P(T)\sqrt{1 - \left(\frac{P(T)}{D}\right)^2} \tag{34}$$

$$A_1 = 0.5\left[\theta_1 \left(\frac{D}{2}\right)^2 - b_p \left|\frac{D}{2} - \frac{P(T)^2}{D}\right|\right] \tag{35}$$

$$A_2 = 0.5\left[\theta_2 P(T)^2 - b_p \frac{P(T)^2}{D}\right] \tag{36}$$

$$\theta_1 = 2\, arcsin\frac{b_p}{D}; \quad \theta_2 = 2\, arcsin\left(\frac{b_p}{2P(T)}\right) \tag{37}$$

D is the original diameter of the un-corroded reinforcing bar so that, the cross sectional area of an un-corroded reinforcing bar is $\frac{\pi D^2}{4}$.

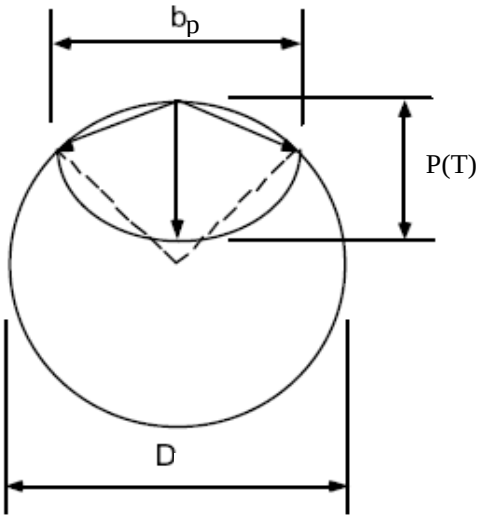

Figure 3-19: Pit configuration (Val & Melchers 1997).

Cairns et al. (2005) presented the following equations to change the steel properties based on the level of corrosion:

$$f_{\mathrm{yc}} = (1 - \alpha_y . Q_{\mathrm{corr}}) f_{\mathrm{y0}} \quad (38)$$

$$f_{\mathrm{uc}} = (1 - \alpha_u . Q_{\mathrm{corr}}) f_{\mathrm{u0}} \quad (39)$$

$$\varepsilon_u = (1 - \alpha_1 . Q_{\mathrm{corr}}) \varepsilon_0 \quad (40)$$

Where f_{yc} , f_{uc} are the yield and ultimate stress based on the original cross section (i.e. $f_{yc} = \frac{F_{\mathrm{yc}}}{A_{so}}$) , and $\varepsilon_u$is the ultimate strain, f_{y0}, f_{u0} and ε_0 represent the initial values of yield strength, ultimate strength and ultimate elongation, respectively, Q_{corr} is the average section loss expressed as percentage of original section (which is the same as mass loss percent X_p), and α_y, α_u and α_1 are empirical parameters. From Table 3-2, values for α_y and α_u range between 0 and 0.015, while values for α_1 have been reported to be within 0 and 0.039 (Cairns et al. 2005). Most research stated that accelerated corrosion produces more uniform section loss than service conditions corrosion, carbonation-induced corrosion is more uniform than chloride-induced, the major change in mechanical characteristics of corroded is in ductility and if values of α excess 0.01, it represents the effects of non-uniform corrosion attack.

Table 3-2: Empirical coefficients for strength and ductility reduction of reinforcement (Cairns et al. 2005)

Authors		Exposure	Q_{corr}, %	α_y	α_u	α_1
Palsson and Mirza[4]	Concrete	Service, chlorides	0 to 80*	0.0	0.0	NS
Castel, Francois, and Airliguie[7]	Concrete	Chlorides, 0.0 mA/cm^2	0 to 20	0.0	NS	0.035
Du[8]	Bare	Accelerated, 0.5 to 2.0 mA/cm^2	0 to 25	0.014	0.014	0.029
	Concrete	Accelerated, 1.0 mA/cm^2	0 to 18	0.015	0.015	0.039
Maslehuddin et al.[9]	Bare	Service, marine	0 to 1	0	0	0
Allam et al.[10]	Bare	Service Arabian coast	0 to 1	0	0	0
Morinaga[11]	Concrete	Service, chlorides	0 to 25	0.017	0.018	0.06
Zhang, Lu, and Li[12]	Concrete	Service, carbonation	0 to 67	0.01	0.01	0
Andrade et al.[13]	Bare	Accelerated, 1.0 mA/cm^2	0 to 11	0.015	0.013	0.017
Clark and Saifullah[14]	Concrete	Accelerated, 0.5 mA/cm^2	0 to 28	0.013, 0.012	0.017, 0.014	NS
Lee, Tomosawa, and Noguchi[15]	Concrete	Accelerated, 13.0 mA/cm^2	0 to 25	0.012	NS	NS
Present study	Concrete	Accelerated, 0.01 to 0.05 mA/cm^2	0 to 3	0.012	0.011	0.03

*Based on minimum, not average, residual section.
Note: NS = not supplied.

Al-Osta (2013) conducted a literature review and experimental tests for the reduction of yield strength and modulus of elasticity. Figure 3-20 shows the reduction, R, for some researchers. It is noted that three studies has very similar reductions including (Al-Osta 2013).

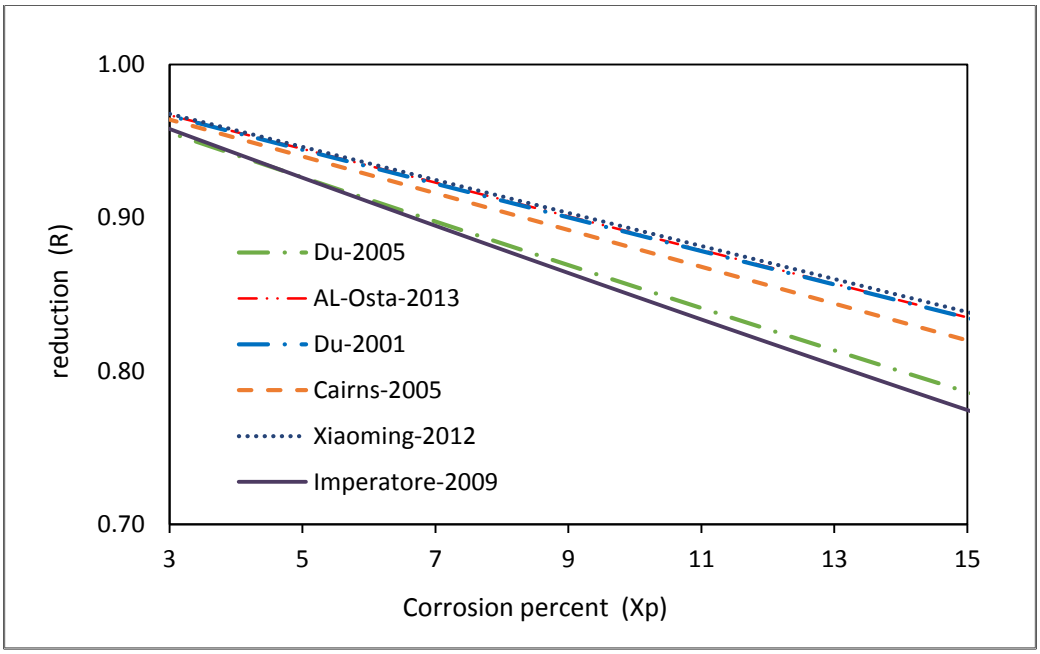

Figure 3-20: Reduction ratio for yield strength based on original area as a function of corrosion degree

In the FE model of this study, the used reduction values R was based on original area of the rebar as developed by (Al-Osta 2013) (equations (41) and (42)). This method of reduction enables the same 3D rebar element to be used for different degrees of corrosion. Moreover, corrosion reduction of strength of corroded steel was applied to both yield and ultimate strengths. Equation (43) with $\alpha_1 = 0.03$ used in this research to consider ultimate strain reduction (Du et al. 2005).

$$f_{yc} = Rf_y = (1 - 0.011X_p)f_y \quad (41)$$

$$E_{sc} = RE_s = (1 - 0.007X_p)E_s \quad (42)$$

$$\varepsilon_{uC} = (1 - \alpha_1 X_p)\varepsilon_{u0} \quad (43)$$

3.5.3 **Reduction of Bond Strength**

The proposed bond modeling method, surface-based cohesive method, depends on values of τ_{max}, S_1, and K_{ss}. In ABAQUS, reduction is done by reducing the max bond strength (τ_{max}) which is the value of t_s for cohesive interaction. To reduce the bond strength, τ_{max},

values less than 1.0 for R should be used in Eq. (19) according to following expression (Maaddawy et al. 2005).

$$R = \left(A_1 + A_2 X_p\right) \tag{44}$$

The advantage of using this reduction is that it depends on both mass loss (X_p) and variables A_1 and A_2 taken from Table 3-3 depending on the corrosion current density level used for accelerated corrosion process.

Table 3-3: A1 and A2 for computation of bond reduction factor (Maaddawy et al. 2005)

Current density, μA/cm²	**A_1**	**A_2**
40	1.003	-0.037
90	1.104	-0.024
50	1.152	-0.021
250	1.163	-0.011
500	0.953	-0.014
1000	0.861	-0.014
2000	0.677	-0.009
4000	0.551	-0.01

Maximum slip (S_1) and bond stiffness values then should be modified according to Equations (17), (18), and (20) but using the new reduced bond strength.

3.5.4 **Summary of the proposed FE model**

The following flow chart (Figure 3-21) shows the steps for constructing the proposed finite element model in ABAQUS.

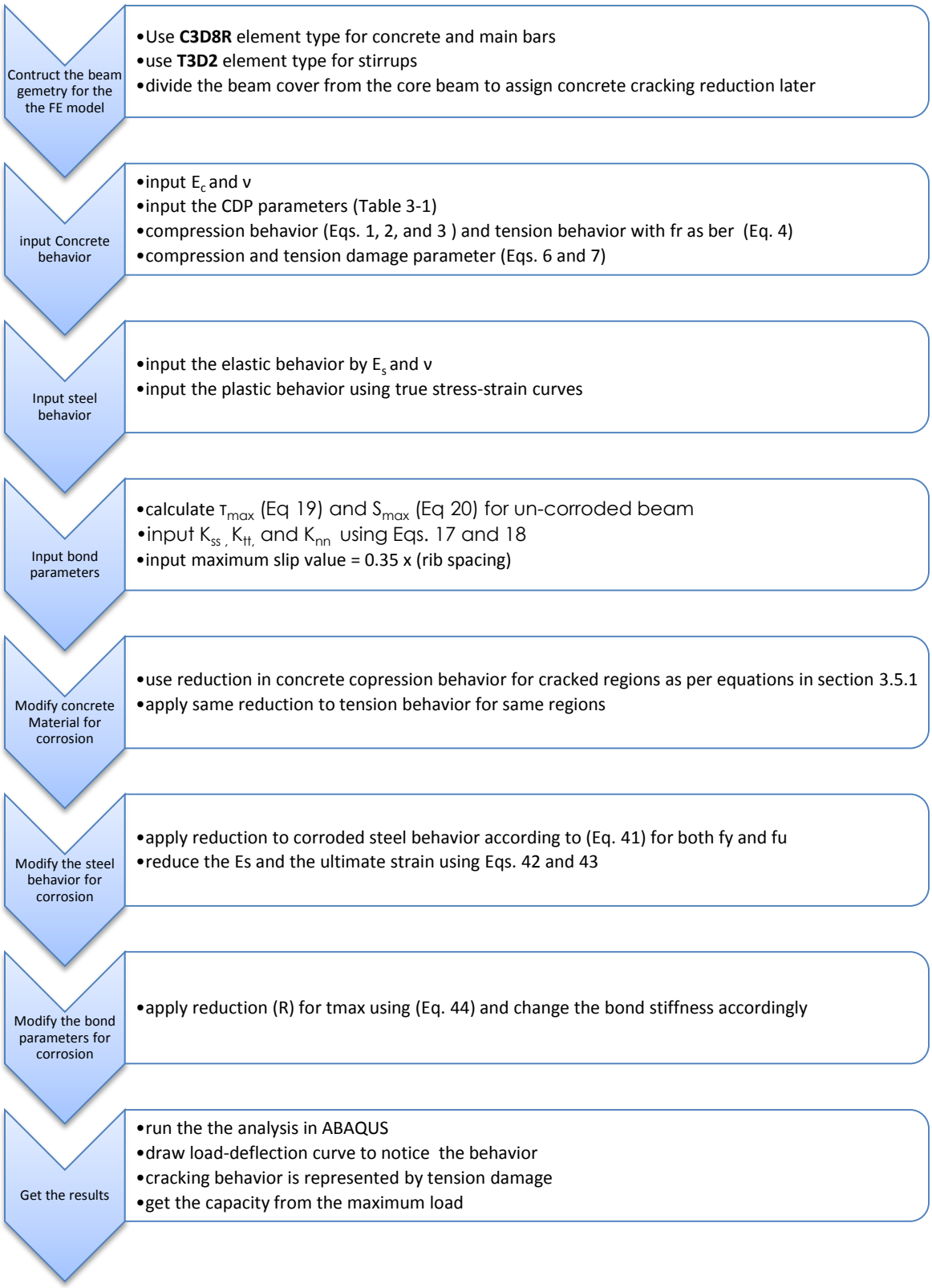

Figure 3-21: Flow chart for conducting the FE modelling of corroded beam

CHAPTER 4

VALIDATION OF THE FINITE ELEMENT MODEL

This chapter presents the validation of the FE model elaborated in chapter 3 for beams failed in flexural, shear, and bond. First, validation was done for flexural beam with mesh sensitivity analysis. Then the proposed FE model was validated against beams failed in shear and bond.

4.1 Validation of Flexural Beams

The most common experimentally tested corroded beams are the beams tested by (Rodriguez et al. 1996) as a part of a big research project on investigating the service life of deteriorated concrete structures. this study and many other FE studies selected these beams for validation such as (Ou & Nguyen 2014; Kallias & Imran Rafiq 2010; Coronelli & Gambarova 2004). Dimensions and details for corroded and un-corroded beams (type 11) used for validation in this study is shown in Figure 4-1. Beam specimens with their corrosion mass losses and the properties of steel used in the experiments are shown in Table 4-1 and Table 4-2 respectively.

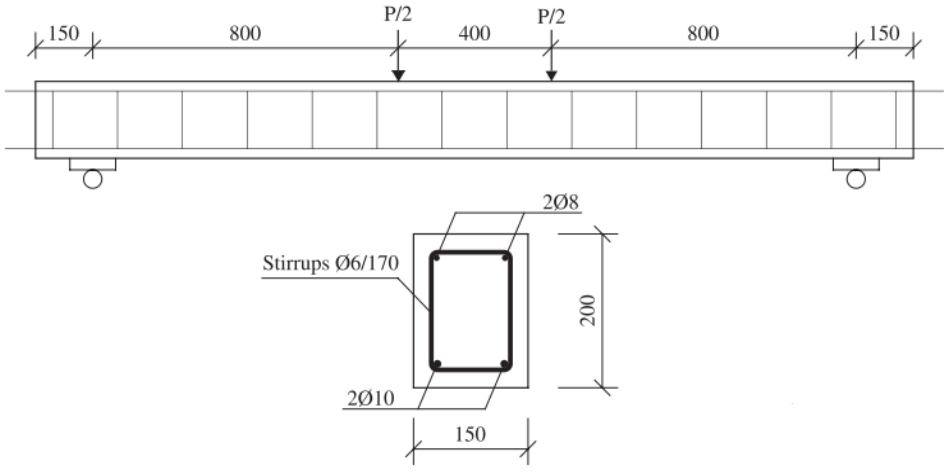

Figure 4-1: Type 11 of beams tested in (Rodriguez et al. 1996) (dimensions are in mm)

Table 4-1: Properties of Type 11 beams tested in (Rodriguez et al. 1996) and used for FE model validation

Beam Specimens	**Corrosion mass loss (X_p) %**			**f_c' (MPa)**
	Tension bars	**Compression bars**	**Stirrups**	
B111	(0.0) control beam (un-corroded)			50
B113	18.64	26.04	30	34
B115	13.9	12.58	23.15	34

Table 4-2 : Strength of the reinforcement bars used in type 11 beams (Rodriguez et al. 1996)

Bar diameter	**Yield strength (MPa)**	**Ultimate strength (MPa)**
6mm (stirrups)	626	760
8mm (top bars)	615	673
10mm (bottom bars)	575	655

Validation started by constructing and validation a FE model for the un-corroded beam (B111), afterwards, the corrosion damages were applied to steel, concrete cover, and bond as described in section 3.5 using corrosion degrees (Xp) given in Table 4-1 for the two corroded beams (B113 and B115).

Very good agreement, in terms of load-deflection curves, is observed in Figure 4-2 between FE and experimental results for both the control and the corroded beams (B111 and B113). Almost exact load capacity is obtained for B111 in the FE model, and just 3.4% difference between FE and EXP. Capacities for B113.

Regarding FE curve of un-corroded beam, B111, Linear rise is observed in load until a value of 15 kN fallowed by a rapid drop. During this linear stage, deflection values of FE curve are the same as values obtained by linear deflection formula of simply supported beam. Load value drop is explained by first cracking of concrete when it reaches its modulus of rapture, f_r, and the beam section is no longer elastic. This cracking in concrete releases energy and causes decrease in load reaction value. However, the decrease is not sharp in B113 because the bottom cover is already week in tension by corrosion cracks.

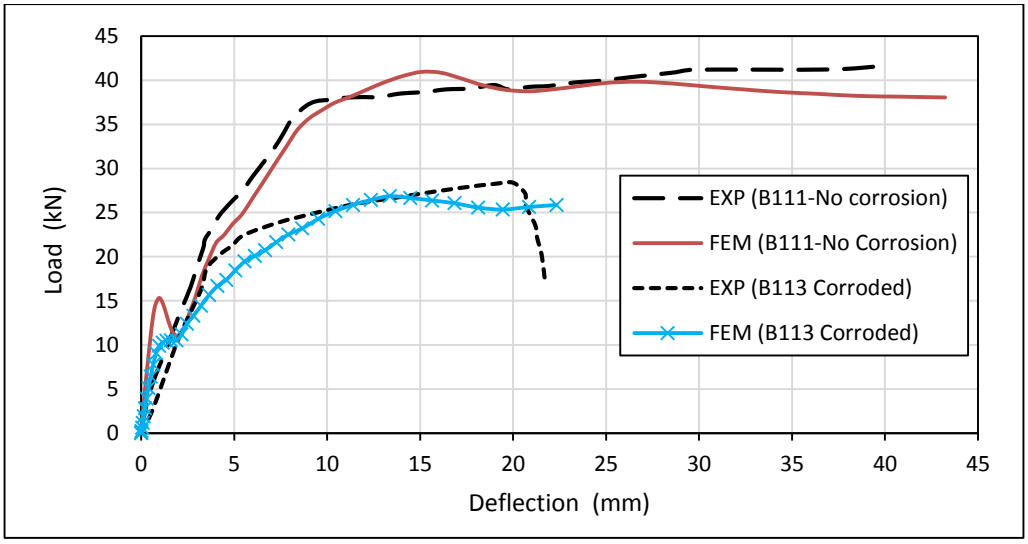

Figure 4-2: Validation of FE models of B111 and B113 with the experimental data

The stiffness of the both beams in Figure 4-2 is reduced first by concrete cracking and then by yielding of the steel bars. Furthermore, overall decrease in deflection is observed in FE results for the corroded beam compared with the control beam. Additional successful validation was done using the corroded beam B115 as shown in Figure 4-3 below.

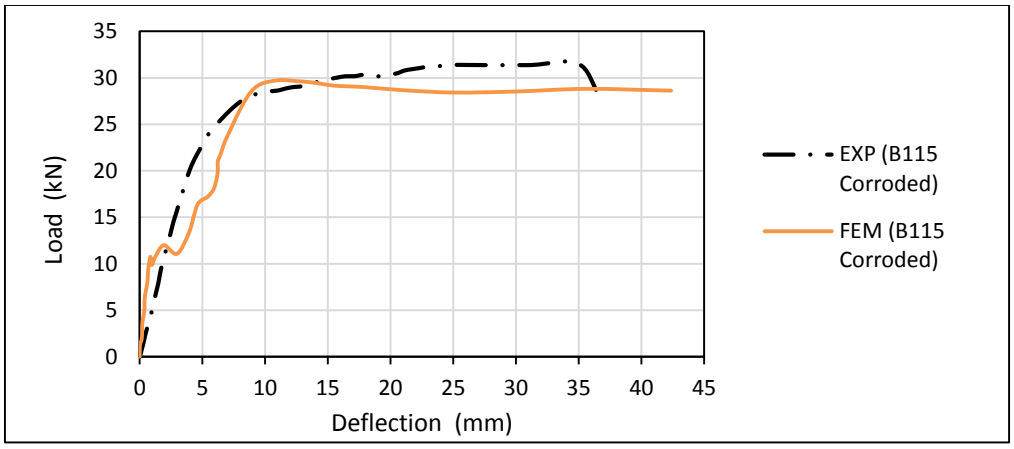

Figure 4-3: Validation of FE model of corroded beam B115 with the experimental data

Because steel bars has reached yield points in both corroded beams (B113 and B115), as noted in ABAQUS results, bond loss has small effect on the load capacity (this will be confirmed later in section 5.2). However, difference in crack pattern and width can be observed between B111 and B113 and it is correspond to bond loss. (See Figure 4-4 (a) and (b)).

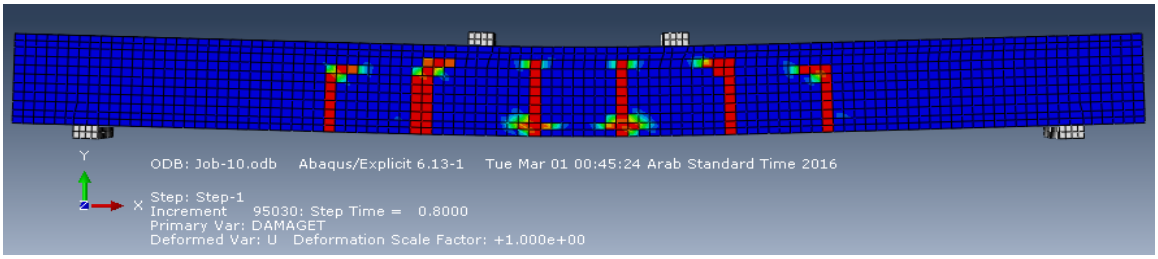

(a) Un-corroded beam (B111)

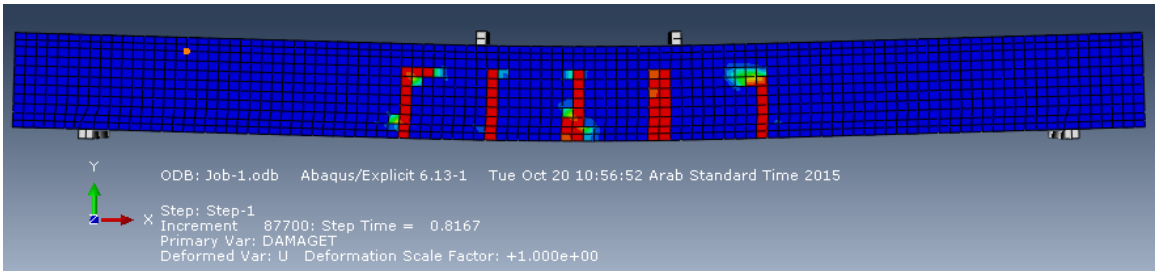

(b) Corroded beam (B113)

Figure 4-4: Indication of crack pattern (using tension damage, dt, in ABAQUS) at the stage when beam deflection is 25mm

In addition to the above validation, one corroded beam tested by (Du et al. 2007), denoted by T282, was chosen for further validation. Corrosion (11.1% mass loss) was applied was applied to bottom bars within 600mm of the span as illustrated below in Figure 4-5. The beam was made of concrete of 44.5 MPa strength, and the properties of steel used in the experiment are shown in Table 4-3.

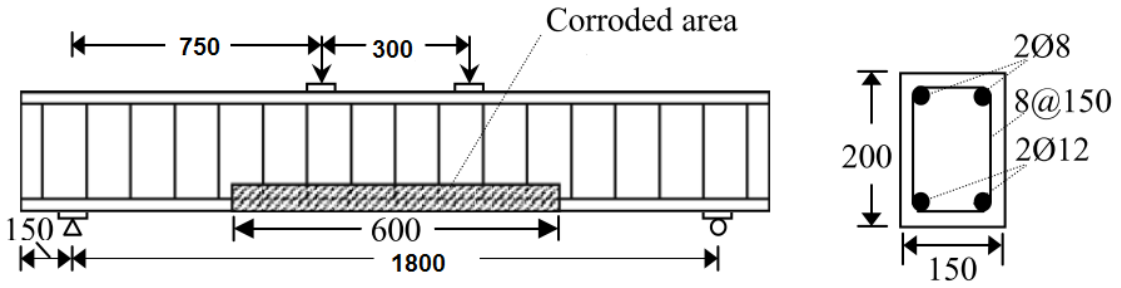

Figure 4-5: Dimensions (in mm) and reinforcement details for the corroded beam T282 tested by (Du et al. 2007)

Table 4-3: The properties of steel bars used in beam T282 (Du et al. 2007)

Steel Properties	**Bar diameter**	
	8mm	**12mm**
Yield strength (f_y), MPa	526	489
Ultimate Strength (f_u), MPa	619	595
Elasticity (E_s), N/mm2	203000	202000
Hardening Strain (ε_{sh})	0.022	0.02
Ultimate strain (ε_u)	0.082	0.132

In the FE model of this beam, the corrosion damage reductions were applied only to corroded bottom region. Excellent agreement, in terms of both behavior and ultimate load capacity, is shown in Figure 4-6 between the FE and the experimental results. This proves that the FE model presented in this study is also valid for beams with corrosion in specific zones.

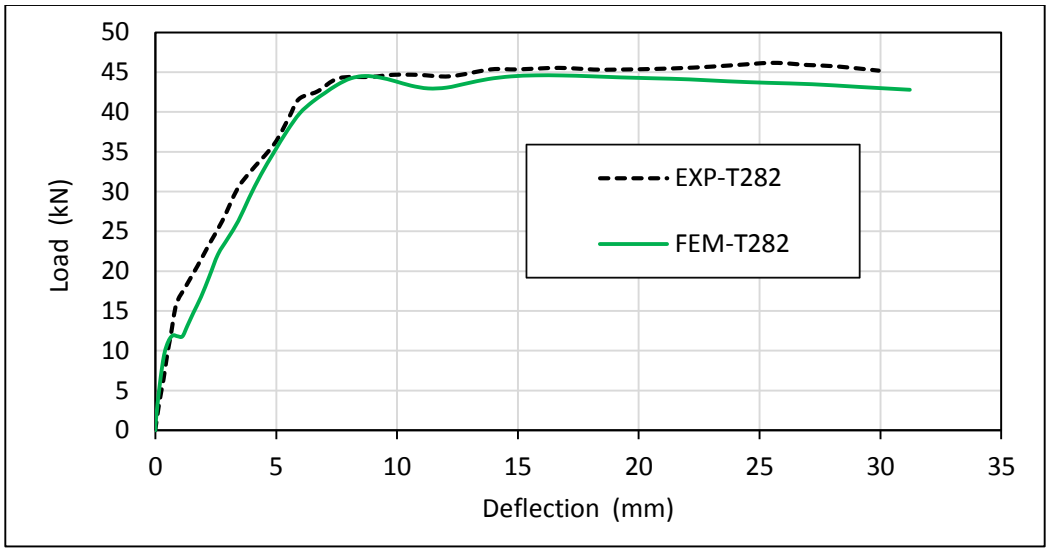

Figure 4-6: Validation of FE model of corroded beam T282 (Du et al. 2007) with the experimental result

4.2 Mesh Sensitivity Analysis

Some FE models for the corroded beam B113 (used above for the validation) were done with different mesh sizes to examine the effect of mesh size in the results. First, both meshes of concrete beam part and bottom steel bars part in ABAQUS changed by the same three different sizes (side lengths of the element cubes are 10, 22, 40 mm). The results in Figure 4-7 indicate that reducing mesh size did not improve the results.

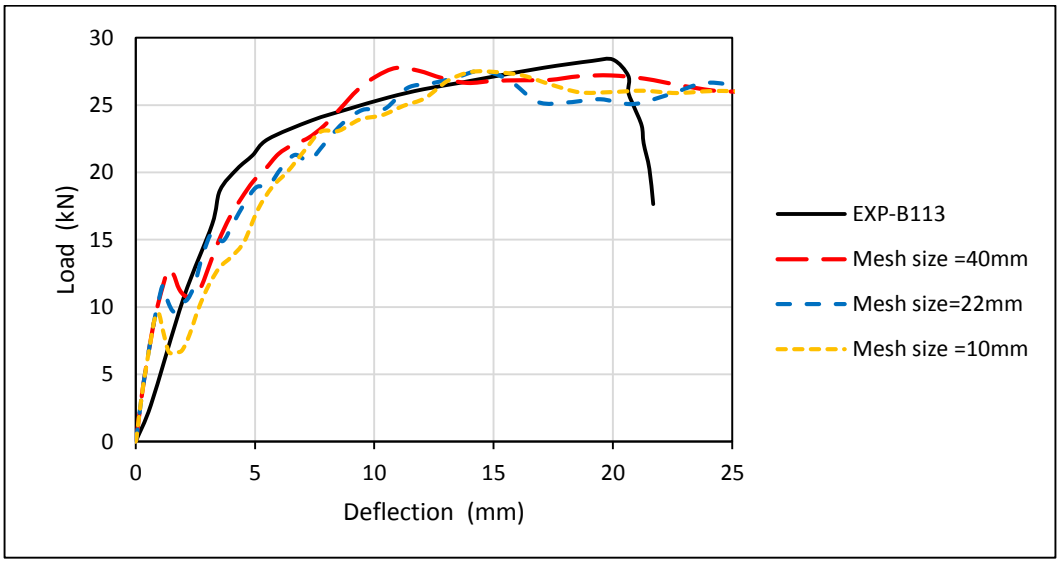

Figure 4-7: The effect of mesh size in FE model of beam B113

Then, other FE models for the same beam but with different in mesh sizes between concrete and bottom steel parts. Their results in Figure 4-8 suggest that using equal mesh sizes for concrete and steel bars gives better results.

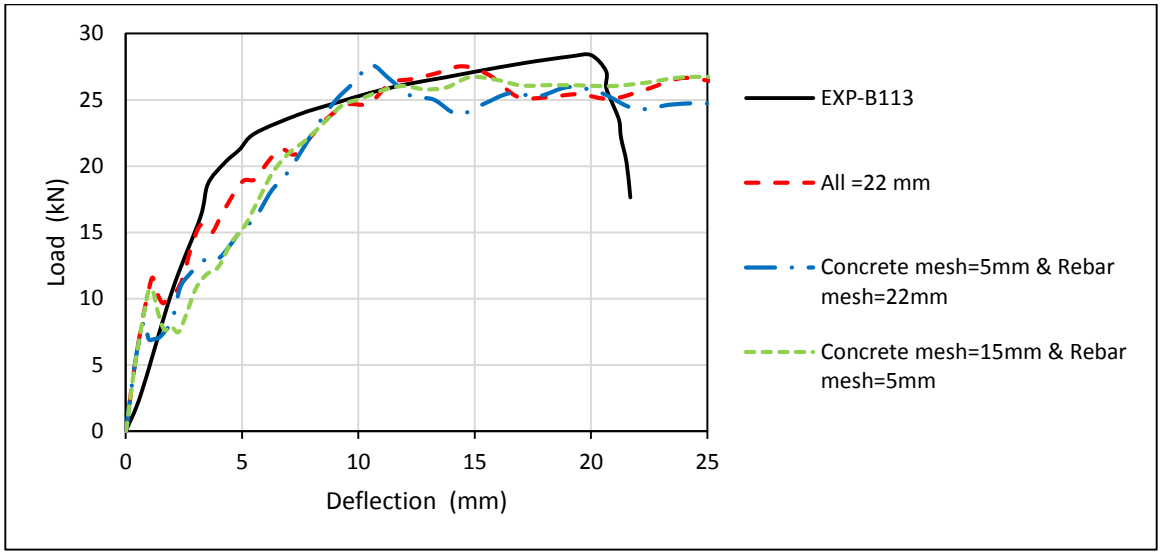

Figure 4-8: Effect of making different mesh sizes for steel and concrete parts

In summary, it can be concluded that using of small mesh size (10 mm) did not improve the results and it is better to use bar and beam mesh size close to each other. Therefore, the use of 20mm mesh size for steel and concrete, which is the case for the above validation models, is good enough for the coming FE models.

4.3 Validation of Shear-critical beams

The proposed FE model was further validated against short beams, which were designed to fail in shear. One of the shear-critical beams of Lachemi et al. (2014) has been used previously for validation of bond modeling in Section 3.4, which is the un-corroded beam (NC-B2). Other corroded beams that have same dimensions and reinforcement (see Figure 3-9), are used here to validate the FE model.

Corroded beam (denoted as NC-B7) with 10.61% mass loss in both stirrups and bottom tension bars used for validation as shown in Figure 4-9. The corrosion damages were applied as described in Section 3.5 but this time all cover zones were subjected to reduction in concrete compressive and tension strengths because the concrete at side cover has effect

on shear capacity unlike previous flexural beams of Rodriguez et al. (1996). Good matching, in terms of both failure load (less than 5% difference) and beam stiffness, is clearly shown in Figure 4-9. In addition, shear failure was also confirmed in the ABAQUS FE model by cracking pattern indicated using tension damage (Figure 4-10).

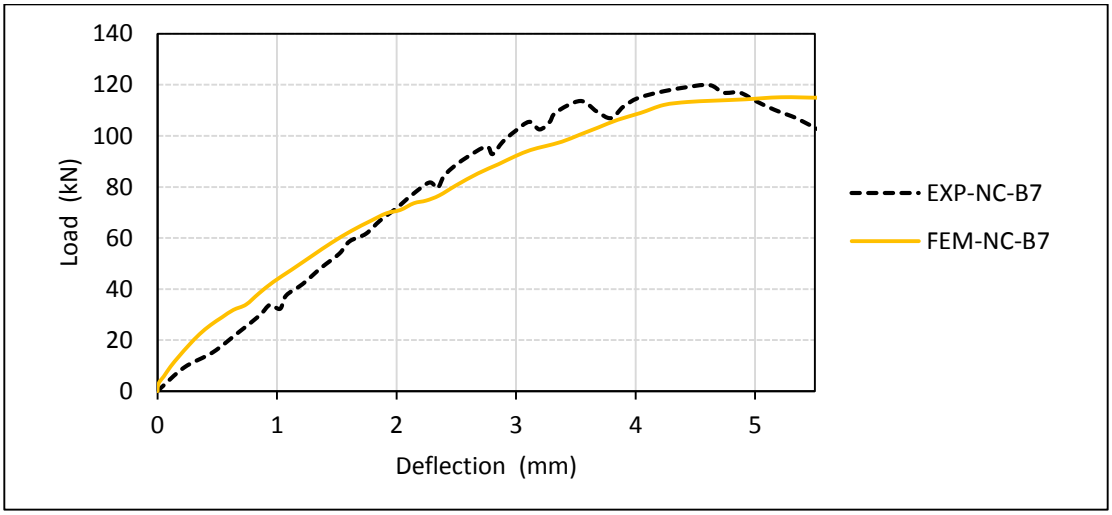

Figure 4-9: Validation of the FE model for corroded shear-critical beam, NC-B7 tested by Lachemi et al. (2014)

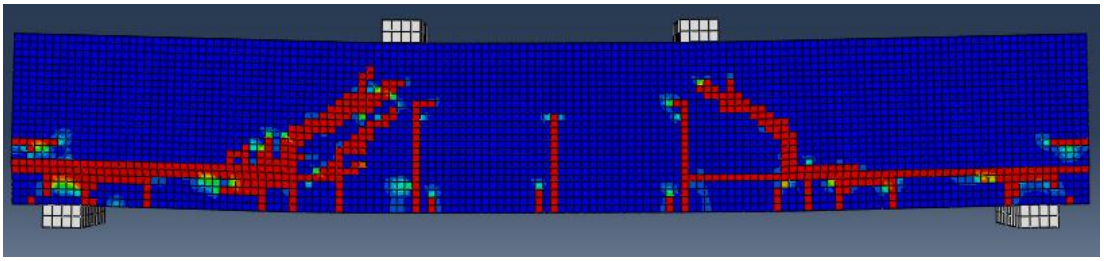

Figure 4-10: Cracking pattern as tension damage (dt) in ABAQUS for FE model of NC-B7 beam

4.4 Validation for Beams Failed because of Bond Loss

Some beams tested by (Lachemi et al. 2014) undergoes failure resulted from bond loss. Beam specimen (denoted as NC-B4) corroded by 14.62% failed by shear cracks but it has high and non-uniform separation between bottom bars and concrete. This beam used for FE validation in similar way as beam NC-B7, however, τ_{max} value in FE model was adjusted to match the experimental curve because of high non-uniformity of bond loss in the experimental beam. Figure 4-11 shows good validation results for this beam.

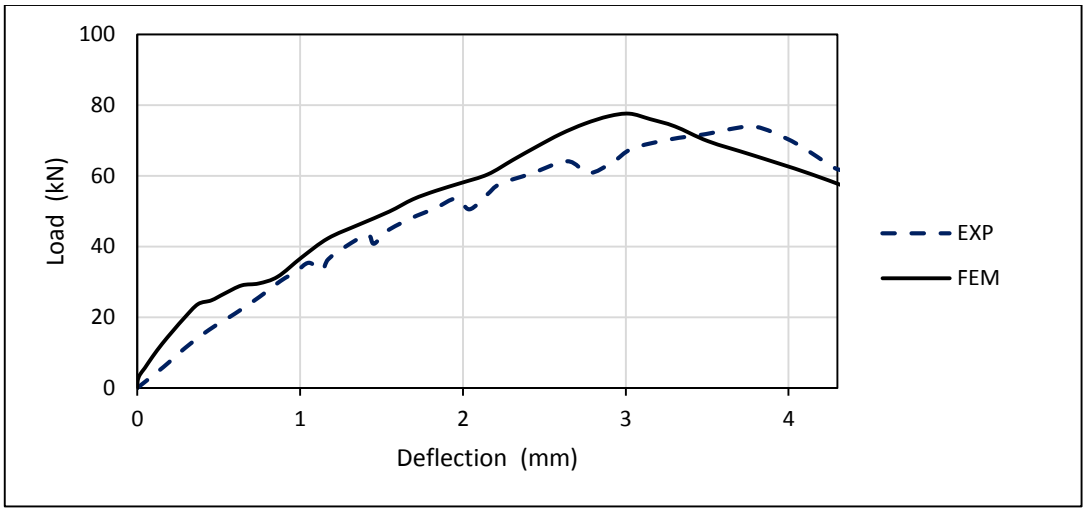

Figure 4-11: Validation of FE model for corroded shear-critical beam (NC-B4)

Three other beams, all corroded by around 20% mass loss, encountered bonding failure in the experiment. The proposed FE model succeeded to estimate their ultimate load capacities by changing only the maximum bond strength (τ_{max}) (see Figure 4-12). This illustrates that the proposed bond modeling method is capable to simulate the effect of different degrees in bond loss.

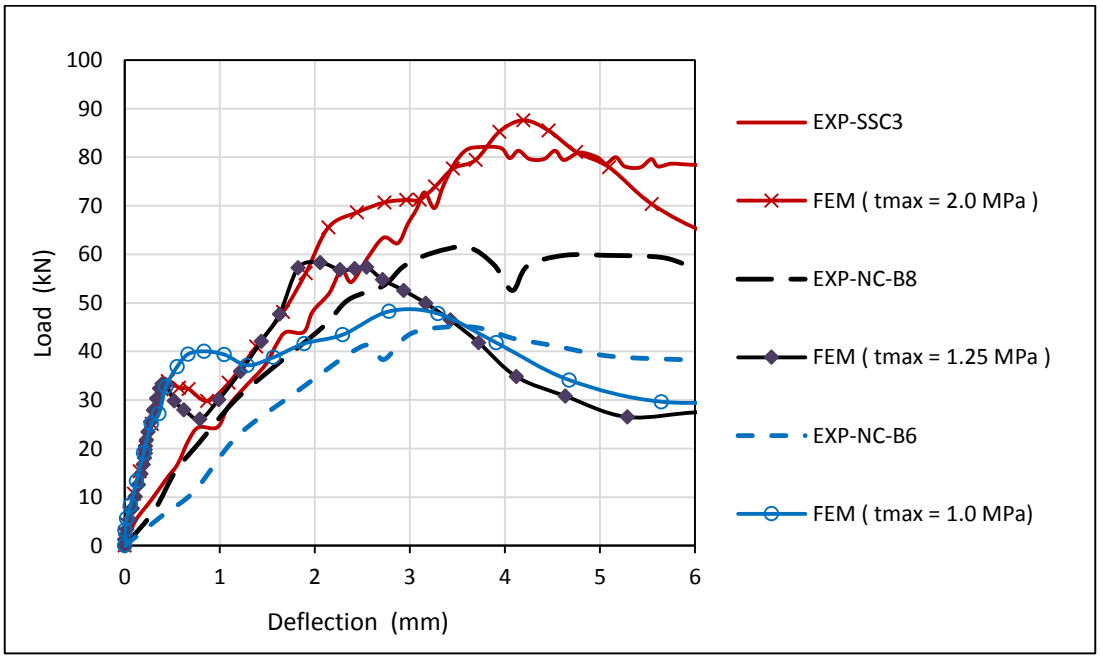

Figure 4-12: Validation of Bond-critical beams using values of bond strength

CHAPTER 5

PARAMETRIC STUDY

5.1 Introduction

This chapter presents the results of a parametric study, which investigate the effects of some parameters, mainly level and location of the corrosion, in the behavior response and capacity of the corroded beams. Beam B113, tested by Rodriguez et al. (1996) and used earlier for validation, is chosen for the parametric study. Refer to Figure 4-1 for the details of this beam.

In this chapter, cracked concrete zones were not assumed the whole cover as done previously in chapter 4 and by other researchers such as Coronelli & Gambarova (2004), Ou & Nguyen (2014), Kallias & Rafiq (2010). Instead, because concrete corrosion cracks depends on the arrangement of the rebars, concrete strength reductions were applied only to zones adjacent to the corroded rebar as recommended by Biondini & Vergani (2014) (see Figure 5-1). For this reason and to take the advantage of the 3D modeling, (i.e. studying the changes along the width of the beam), the cross section of the beam used for the parametric study was divided as shown in Figure 5-2. Note that each parts with cross hatch are considered cracked if their bars are corroded.

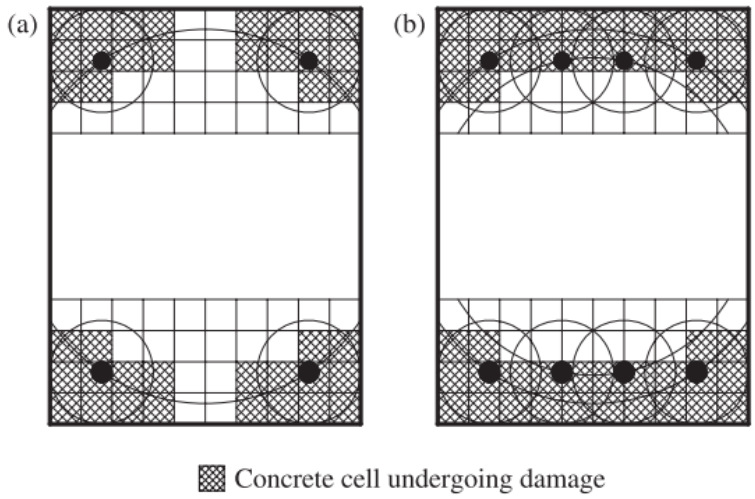

Figure 5-1: Damaged concrete zones: (a) wide bar spacing. (b) closely spaced bars (Biondini & Vergani 2014)

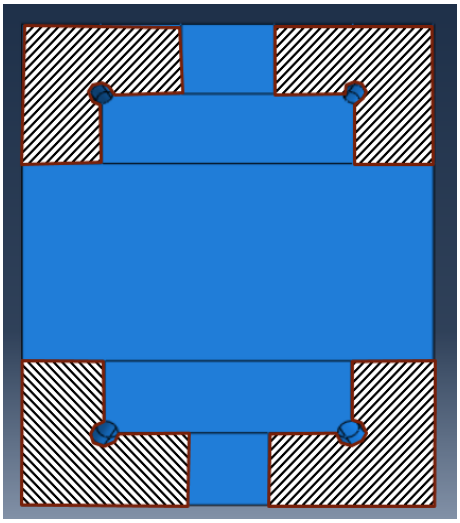

Figure 5-2: The divided cross-section for the parametric study beam

5.2 The Influence of Different Types of Corrosion Damages

To study the effect of the different damage parameters due to corrosion in the failure load of corroded RC beam B113, FE models were conducted for the same beam. In one of them, all detrimental effects resulting from corrosion were applied (loss of bond, reduction in compressive strength due to cracked concrete, and reduction in material properties of steel), which is the FE model of B113 shown in Figure 4-2, and the other case considered was similar to the pervious except that bond strength was not degraded. A comparison between

these models and experimental results of corroded beam B113 (Table 4-1) is demonstrated in Figure 5-3. It is indicated that bond loss is not critical for this particular beam because it has sufficient anchorage length at through its span length. Therefore, the effect of loss of bond in this beam is negligible.

Similarly, the effect of reduction in steel properties (area, yield strength, and ductility) due to corrosion on the behavior and failure load of corroded beam B113 was studied by isolating the influence of only these reductions. From the load-deflection curve in Figure 5-4, it can be concluded that most corrosion effects on failure load of corroded beam (B113) were from reduction in steel properties. Since the effect of loss of bond was noted to be minimal for this beam, the further reduction in load capacity on application of all detrimental effects may be attributed to cracking of concrete in the compression zone.

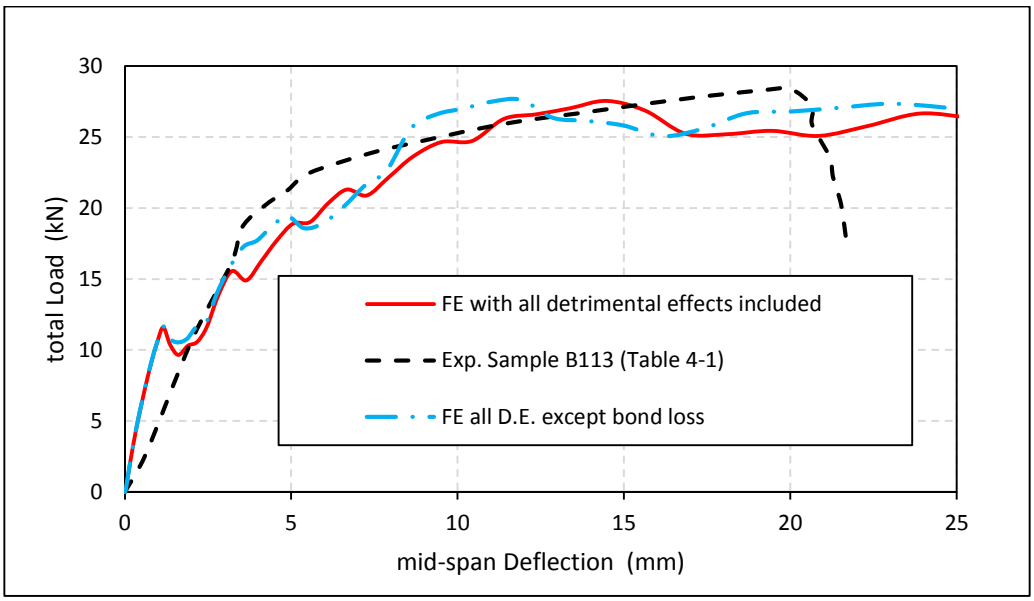

Figure 5-3: Effect of bond loss in corroded beam B113

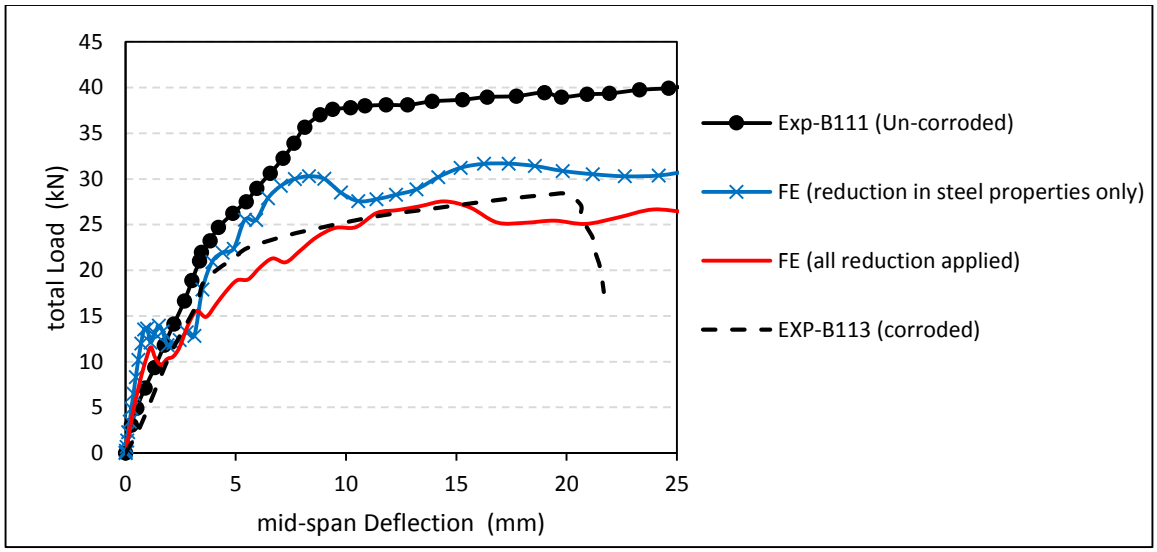

Figure 5-4: Effect of reductions in steel properties of corroded beam B-113 (Table 4)

5.3 Effect of the Degree of Corrosion

In order to observe the consequences of increasing the corrosion level, several FE models with five different corrosion levels (10% to 50% mass loss) were constructed for the same beam (B113). These corrosion degrees were applied either to the top bars alone or in other cases to bottom bars. Table 5-1 shows the residual properties, after applying corrosion reductions to the concrete cover, steel, and bond, calculated for different corrosion levels using equations presented in Chapter 3. Prior to applying corrosion effects, reference FE model (A-0) for the un-corroded beam was constructed which is the same as the FE model of beam no. B111 (see Table 4-1) but with concrete compressive strength (fc') =34 MPa instead of 50 MPa.

Table 5-1: Residual strengths of steel and concrete cover region around the corroded bar according to the degree of corrosion

Degree of corrosion (mass loss %)	Residual strengths (MPa) of the Bottom zone				Residual strengths (MPa) of the top zone			
	fy steel	fc (cover concrete)	ft (cover concrete)	τ_{max}	fy steel	fc (cover concrete)	ft (cover concrete)	τ_{max}
0	575	34	3.62	8.69	615	34	3.62	10.1
10	511.8	17.57	1.87	7.58	547.4	19.45	2.07	8.89
20	448.5	11.63	1.24	5.76	479.7	13.39	1.42	6.85
30	385.3	8.55	0.91	3.94	412.1	10.06	1.07	4.81
40	322	6.66	0.71	2.12	344.4	7.93	0.84	2.77
50	258.8	5.37	0.57	0.08	276.8	6.45	0.69	0.72

5.3.1 **Corrosion in Compression Rebar**

Five FE models (denoted as AT-10, AT-20, AT-30, AT-40, and AT-50) were created to investigate the impact of corrosion in top compression steel bars. They were created by modifying the material properties of A-0 beam according to corrosion degree from Table 5-1. Results of Load vs. deflection in Figure 5-5 indicate that no major change happened in the behavior and load capacity even with as high as 40% corrosion mass loss. Small decrease in ultimate load, around 8%, and in stiffness is noted for beam AT-50 with 50% corrosion.

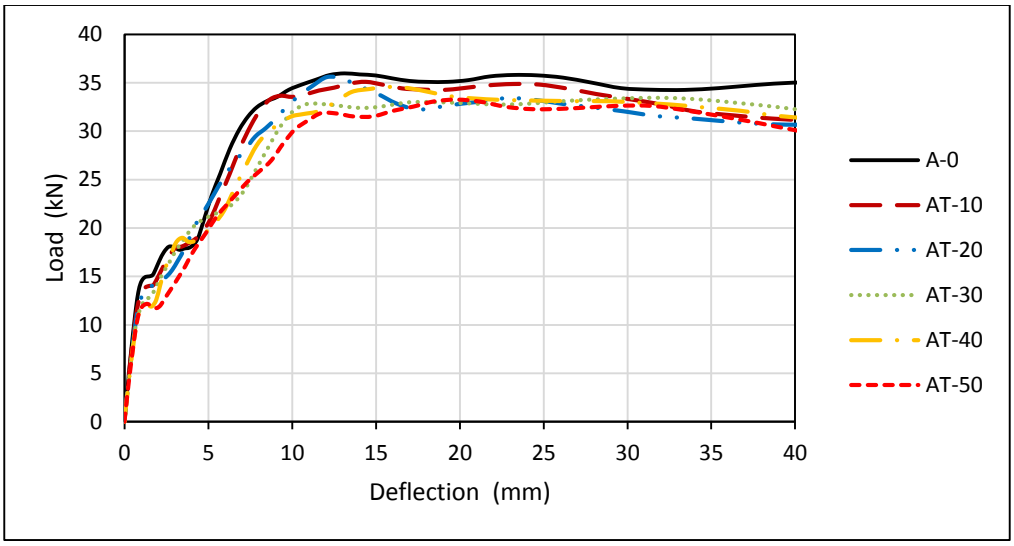

Figure 5-5: Results, in load-deflection curves, for FE models with corrosions on top bars only

These results are expected because of the fact that this beam is under-reinforced with bottom reinforcement steel ratio = 0.35 ρ_{max}. Therefore, steel bars in compression region have no effect on the flexural capacity of this beam. The slight reduction in load capacity is only due to reduction of compressive strength for the cracked concrete in compressive zones.

5.3.2 **Corrosion in Tension Rebars**

Since the flexural strength of beams highly depends on yield strength of tension reinforcement, other five FE models (AB-10… to AB-50) were done by applying corrosion in bottom tension reinforcement only. The graph below (Figure 5-6) gives the load-deflection results for these models and shows a uniform drop in the load capacity according to the corrosion degree. However, for AB-50, it is noted that this beam undergoes bond failure, in other words, failed as a beam without any reinforcement because of complete loss of bond (τ_{max} = 0.08 MPa, see Table 5-1). This failure is shown clearly in crack pattern, indicated by tension damage, dt, in Figure 5-7.

As for the model with just a little smaller corrosion degree (40%), AB-40 model, the capacity is very good compared with the capacity of AB-50. This is because its bond strength (τ_{max} = 2.12 MPa, see Table 5-1) was large enough to prevent bond failure, and

therefore, the beam used all residual yield strength of the bottom bars (fy = 322 MPa, see Table 5-1). The theoretical load capacity of AB-40 beam, when calculated based on moment capacity of the section using fy = 322, was 20.8 kN, which is close to FE result (22.4 kN). This is also the case with the remaining beams (AB-10, AB-20, and AB-30). Notice that, as explained earlier in chapter 3, the residual fy for corroded bars represents reduction of both bar area and yield strength.

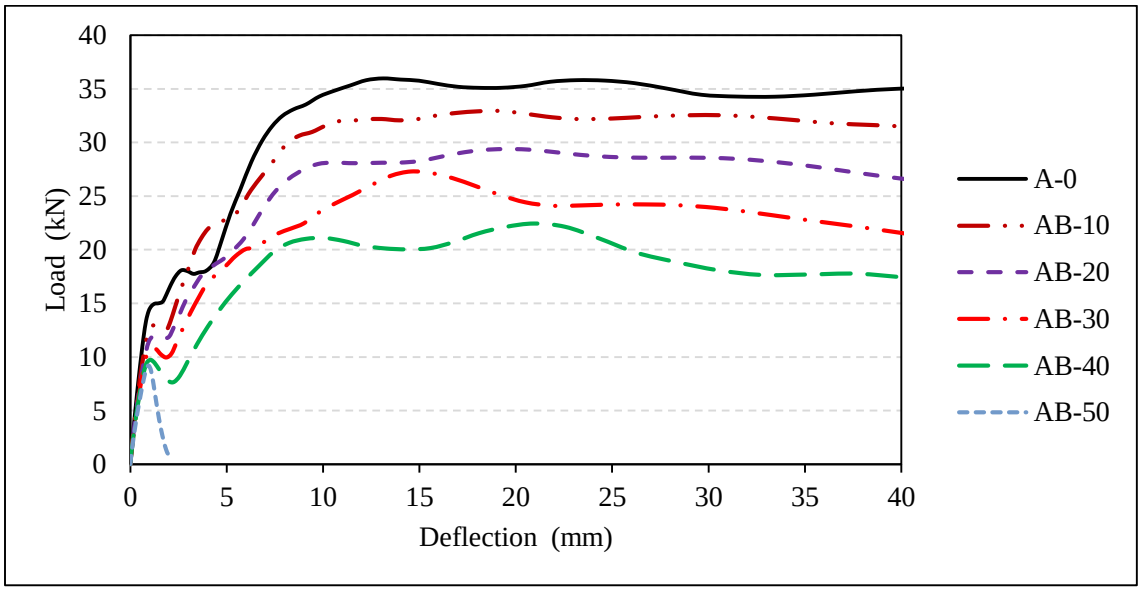

Figure 5-6: Results, in load-deflection curves, for FE models with corrosions on bottom bars only

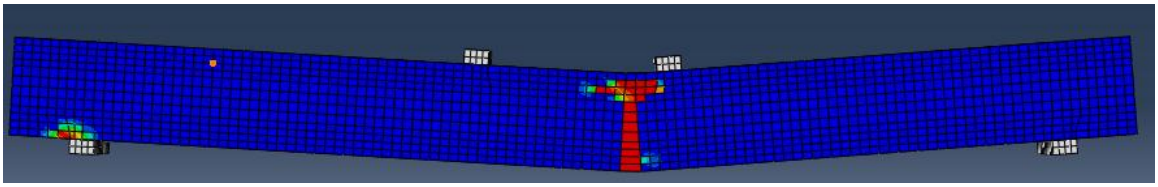

Figure 5-7 : Crack pattern indication for beam corroded by 50% at bottom bars (AB-50)

It is concluded form Figure 5-6 that load capacity of these corroded beams depends mainly on the residual bar area of tension reinforcement provided that enough bond strength is available to develop full yield stress.

Although bond loss in AB-40 beam (τ_{max} was reduced from 8.69 to 2.12 MPa) does not influence the residual load capacity, its effect is clear on making flexural cracks wider and fewer in numbers as noted in Figure 5-8 and Figure 5-9.

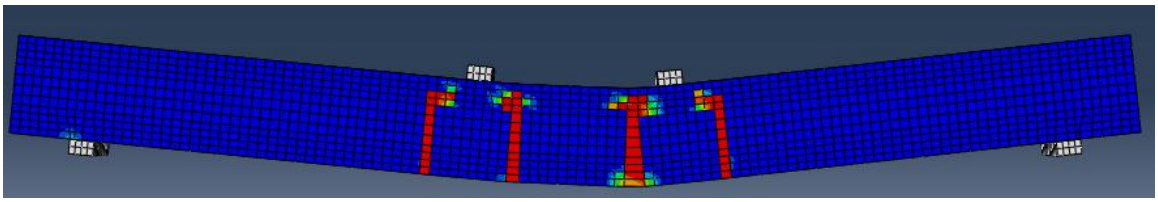

Figure 5-8: Crack pattern indication for beam corroded by 40% at bottom bars (AB-40)

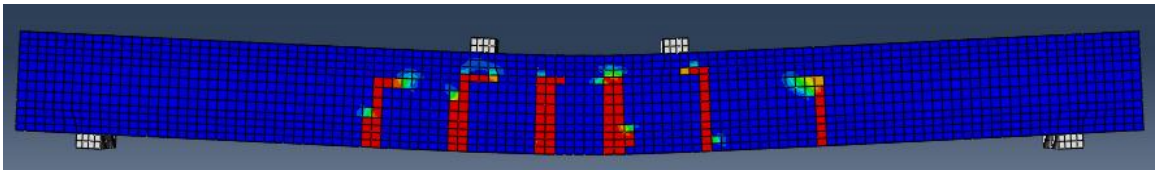

Figure 5-9: Indication for crack pattern for un-corroded beam (A-0)

5.3.3 **Corrosion in Stirrups**

Regarding the influence of corroded stirrups (6mm diameter), it was noted that the stirrups undergoes small stresses in all beam FE model of Figure 5-5 and Figure 5-6, although reduction of steel properties was applied also to the stirrups by same corrosion level of the long bars. This is shown below in Figure 5-10 for AB-40 beam (max. stress = 273 but the residual fy = 350 MPa). Because of that, no reduction in concrete strength was applied to concrete on the side covers as well as top and bottom parts of the cover (see Figure 5-2). However, two additional FE models were constructed for 40% corrosion to see the effect of applying reduction in fc' at sides of the beam only and in other case where only core concrete is considered un-cracked. Figure 5-11 proves that no significant effect for this reduction in concrete.

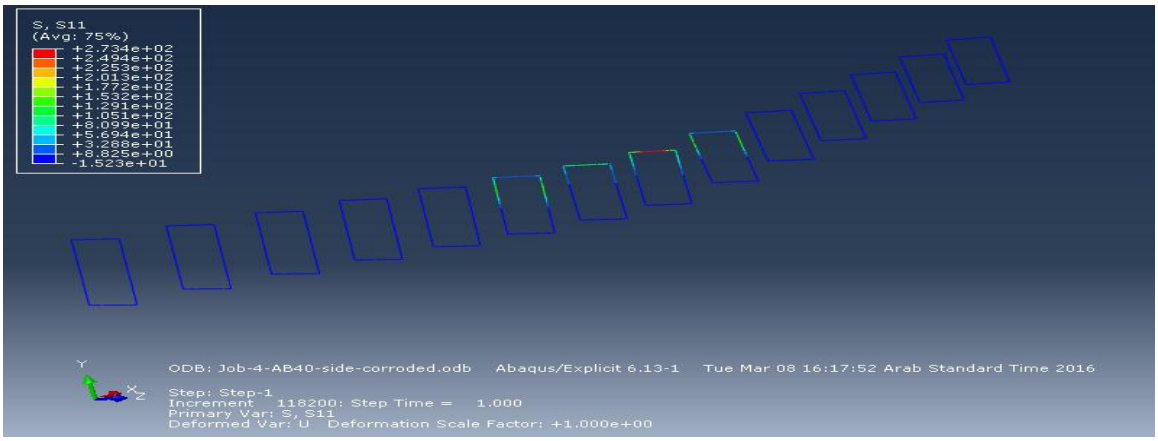

Figure 5-10: Von-mises stress values in stirrups at failure for AB-40

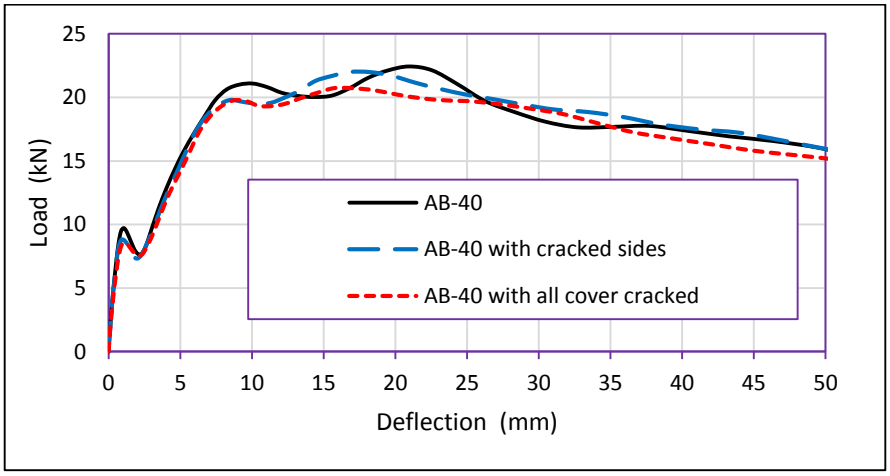

Figure 5-11: Effect of including reduction in fc' at sides and middle top and bottom cover parts

5.4 Effect of Changing the Location of Corrosion

In the previous section, the corrosion exists in the rebars along the whole length of the beam and for either both top or both bottom bars. This section discusses the effect of applying corrosion in specific portions along the longitudinal steel bars and along the width of the beam. In this regard, the beam was divided in the longitudinal direction, in addition to section divisions of Figure 5-2, to five portions as shown in Figure 5-12 (one middle part of 1000mm length, two side parts having 500mm long, and two small end parts with 150mm long). Recall that the total span is 2000mm.

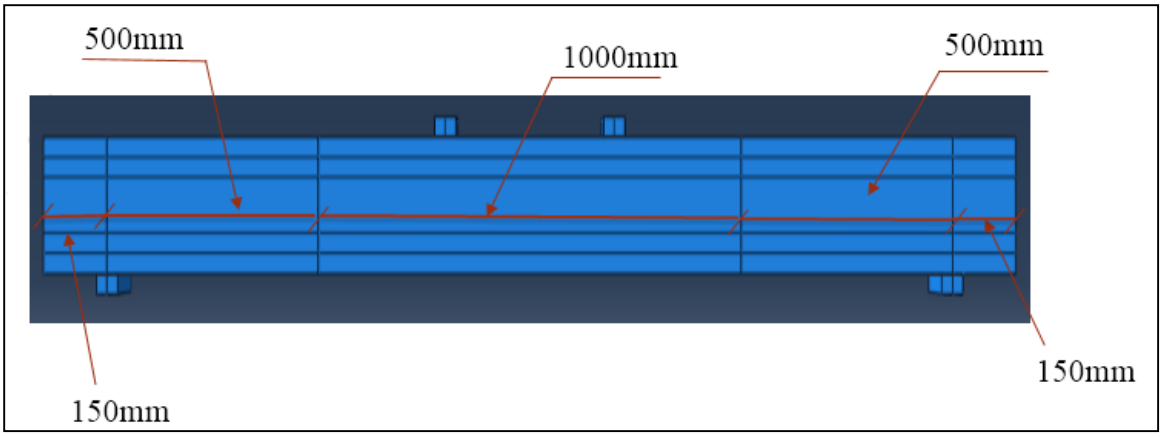

Figure 5-12: Divided beam in the longitudinal direction for the parametric study

Since corrosion in bottom bars is the critical for this beam, two levels of bottom corrosion (40% and 50%) were chosen for investigating the effect of changing the location of corrosion along the length and across the section of the beam. Sample of the FE models used for this purpose are shown in the following table:

Table 5-2: Some FE models details used for studying effect of corrosion location

Beam notation	Corrosion degree %	Location of applied corrosion	
		cross-section	longitudinal direction
AB-40	40%	both bottom bars	along the full length
AB-50	50%	both bottom bars	along the full length
AB-40-1	40%	one bottom bar	along the full length
MB-40	40%	both bottom bars	middle part only
TSB-40	40%	both bottom bars	in both 500mm sides
OSB-40	40%	both bottom bars	in only one 500 mm side
TSB-40-1	40%	one bottom bar	in both 500 mm sides
ASB-50	50%	both bottom bars	in both sides and ends (only the middle part is not corroded)
M&S-B-50	50%	both bottom bars	in middle part and both sides (only the 150 mm ends are not corroded)

5.4.1 Change in the Longitudinal Direction

First, three FE models were conducted for 40% corrosion applied to both bottom bars but in different longitudinal portions (they are MB-40, OSB-40, and TSB-40). It is observed

in Figure 5-13 that applying the 40% corrosion in the two sides did not decrease the load capacity compared to the un-corroded beam. This is explained by the fact that there is enough bond along beam sides (2.1 MPa as mentioned earlier) and the middle part has the full yield strength (575 MPa). On the other hand, dramatic drop on load capacity occured when applying the corrosion to middle part only as in MB-40 and its result is almost the same as applying the corrosion in the whole length.

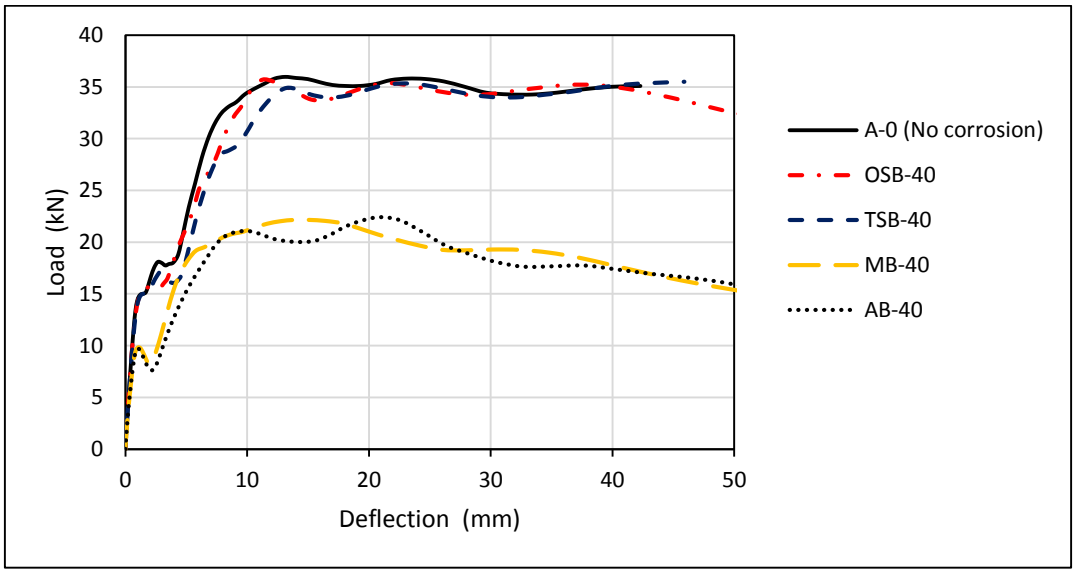

Figure 5-13: Effect of changing the 40% corrosion along beam's longitudinal direction

Then, similarly, 50% mass loss of corrosion was applied in different locations along the beam in the three additional FE models (TSB-50, ASB-50, and MB-50). By noticing the results in Figure 5-14, two observations can be seen. The first one is that ASB-50 beam, which has un-corroded middle part, failed because of bond loss like AB-50 beam but after a little higher load. This increase resulted from higher concrete tension strength in the un-corroded middle part. Note that tension bars undergoes no bond stress in region of constant moment (between the load plates in this beam) but the steel yield strength, fy, needs the anchorage length starting from outside the load points.

Second observation is that beam TSB-50 , which has corrosion in both 500mm sides and un-corroded 150mm ends, did not undergoes bond failure and has much higher load capacity than ASB-50 and this increase was only a result of good bond strength at the

150mm end zones. Therefore, the yield strength in the un-corroded middle part was utilized.

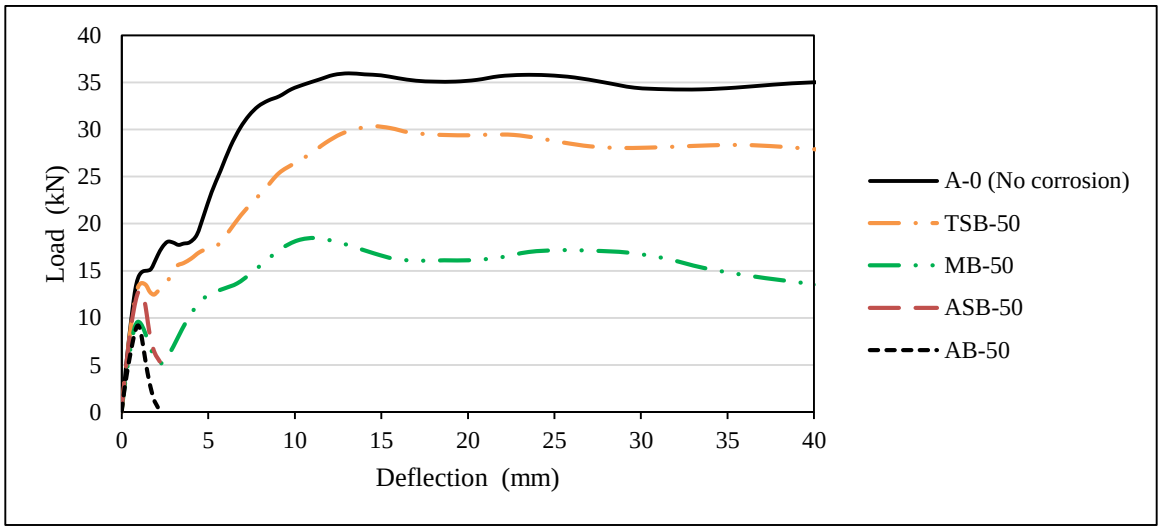

Figure 5-14: Effect of changing the 50% corrosion along beam's longitudinal direction

To examine more the effect of steel-concrete bond in these 150mm ends, FE model denoted as **M&S-B-50** was done by applying corrosion in the full length except these ends. Resulting load-deflection curve of this model (see Figure 5-15 below) shows considerably higher capacity than AB-50 and more important better failure mode (ductile flexural instead of brittle bonding failure).

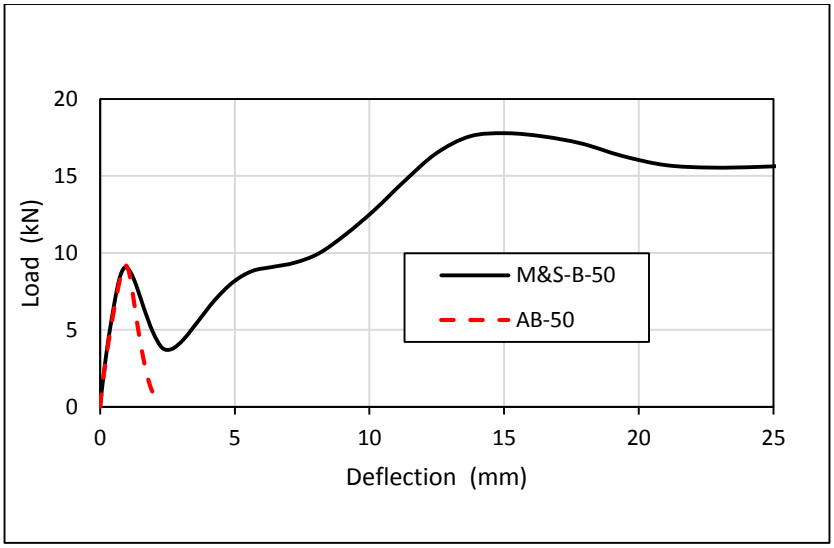

Figure 5-15: Effect of un-corroded end zone in the beam

In summary, Results showed that beam sides portions are the critical location for bond loss unlike the middle part, which is the zone where the yield strength is needed in the overall beam capacity. Furthermore, even the ends of the beam were found to have significant positive effect to save the beam from bond loss failure if they are un-corroded. It was also found that if the corroded zones have enough bond strength (as the case of 40% in this beam), the critical zone will be only the middle part because it is the region of high tension stress coming from bending moment.

5.4.2 **Change along the Width of the Beam**

As discussed earlier, one important advantage of using 3D FE modeling is the ability to investigate the effect of corrosion if it is not uniform along beam section. It was observed in section 5.3.1 that corrosion in top compression rebars has almost no effect in this beam. Therefore, for beam B113 used in this parametric study, situation in which only one bottom reinforcing bar is corroded was studied in this section.

First, FE model for 40% corrosion along one bottom bar only (denoted as AB-40-1) was done and compared with the AB-40 shown earlier. The result as shown in Figure 5-16 indicates that AB40-1 has 17% reduction in load capacity in reference to un-corroded beam A-0, whereas, AB40 model has around 37% reduction.

In addition, it is observed that the load capacities of models AB-20 (two corroded bar with 20%) and AB-40-1 are the same (30 kN). This is because they have the same residual tension force resulted from the same overall mass loss.

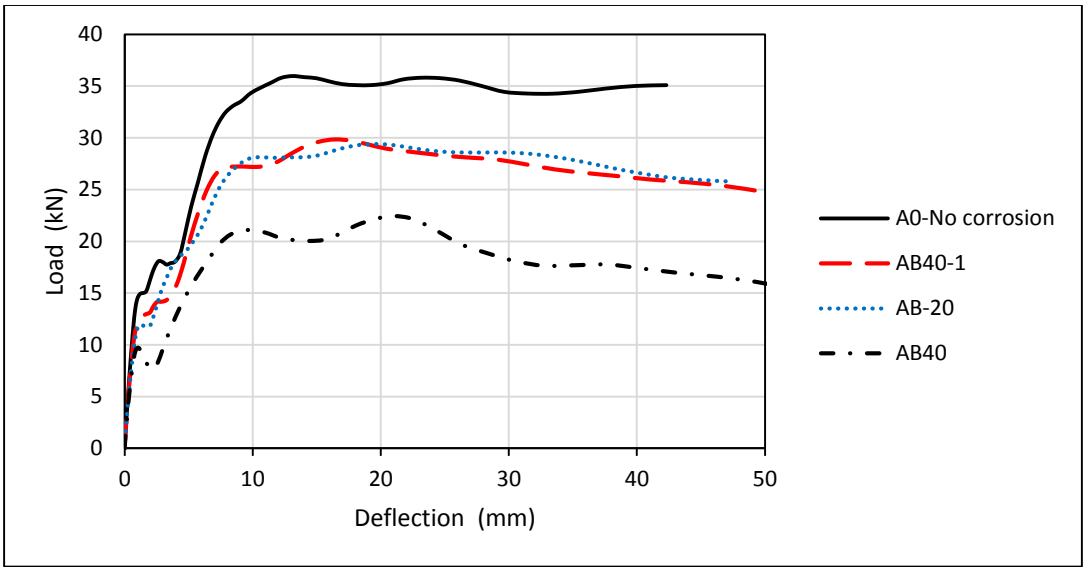

Figure 5-16: Effect of applying 40% degree corrosion in one bottom bar only

Similarly, AB-50-1 FE model having one bottom steel bar corroded by 50% was compared with AB-50. Their results shown in Figure 5-17 below indicate that higher load capacity was achieved in AB-50-1 because of the un-corroded bar.

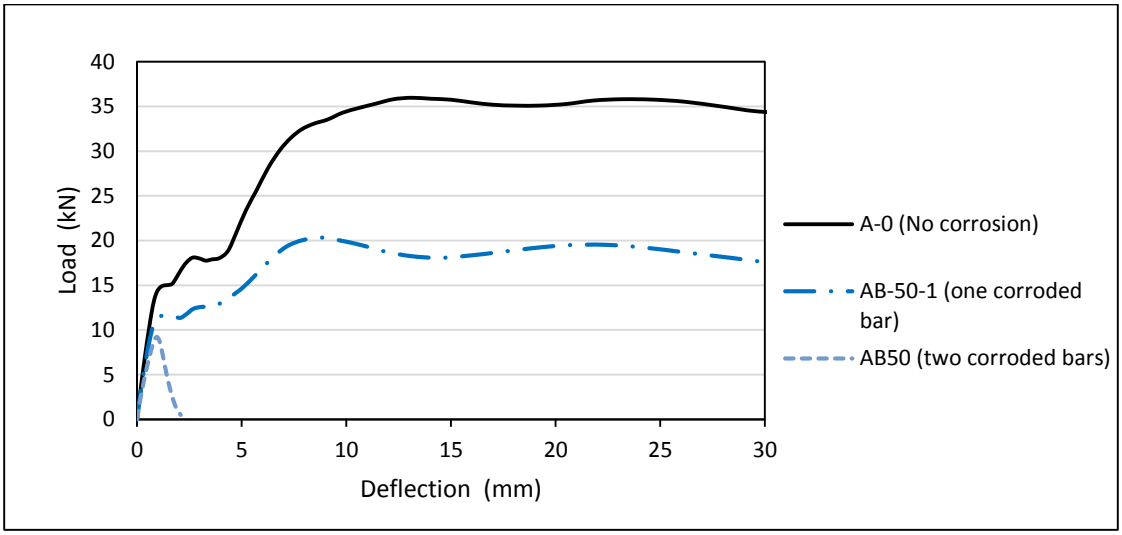

Figure 5-17: Effect of applying 50% degree corrosion in one bottom bar only

Because of un-symmetry along beam width, small lateral slip was observed (2mm in AB-40-1 and 7mm in AB-50-1) toward the side of corroded bar as shown in the two figures below.

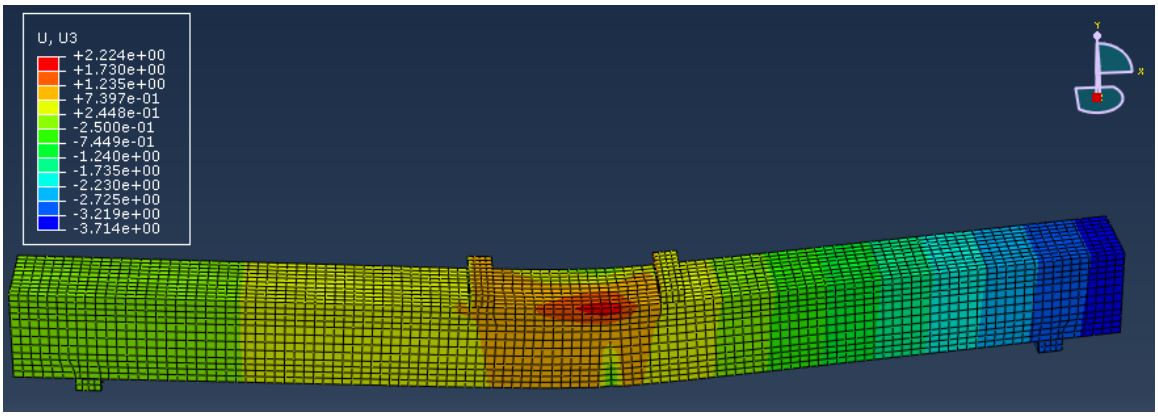

Figure 5-18: Lateral slip (2.22 mm) toward corroded bar in FE model no. AB-40-1

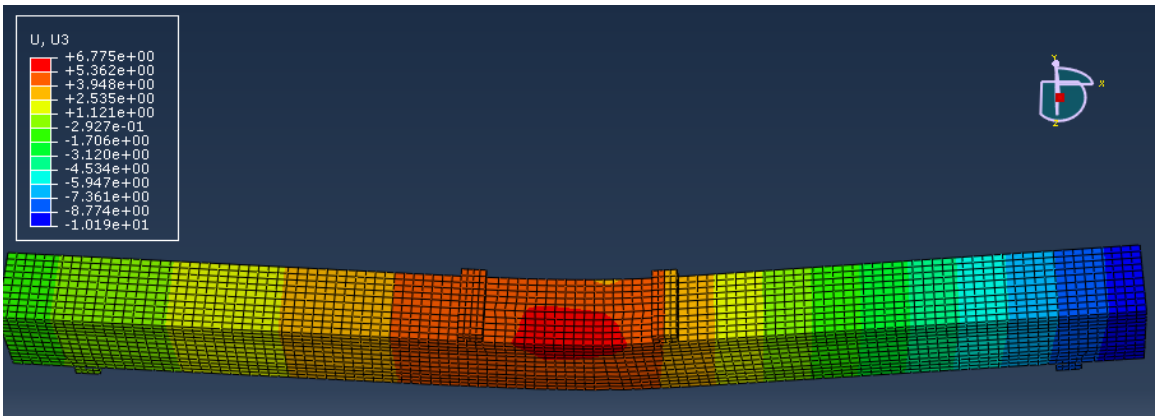

Figure 5-19: Lateral slip (6.78 mm) toward corroded bar in FE model no. AB-50-1

CHAPTER 6

CONCLUSIONS AND RECOMMENDATIONS

6.1 Conclusions

A 3D finite element (FE) simulation was introduced for modeling the corroded and un-corroded reinforced concrete beams. This nonlinear FE modeling used the Explicit Dynamic analysis technique in ABAQUS and Concrete Damaged Plasticity model (CDP) for concrete behavior. First for un-corroded beams, different surface interaction techniques were investigated to simulate the bond between the 3D elements of steel bars and the surrounding concrete: perfect bond, mechanical contact using different methods, and cohesive behavior. Validation with experimental data from other researchers, in flexural-critical and shear-critical beams, illustrated that the proposed FE model using surface-based cohesive behavior method for bond shows very good results for both corroded and un-corroded beam cases.

After validation, a parametric study was conducted for investigating the effects of (1) different corrosion levels in top or bottom reinforcements, and (2) changing the corroded zones along beam's width and longitudinal directions.

Main conclusions from FE validation results are summarized as follows:

- Constructing FE model with 3D surface interaction in ABAQUS to simulate the steel-concrete bond is very easy and quick for 3D modeling comparing to any other methods because it does not involve any additional interface part or elements to represent the bond.

- The best way among these surface-based methods is the surface-based cohesive interaction if appropriate values for bond stiffness, damage initiation, and damage evolution were used.

- Damage plasticity model for concrete in ABAQUS is found to be acceptable in modelling the behavior of RC beams subjected to corrosion.

- Good agreement was found, in terms of crack pattern and the load-deflection behavior, between the finite element model and the experimental results.

- The proposed FE model of corroded RC beams can be used to estimate the failure load as well as the failure modes (flexural, shear, or bond failure) with reasonable accuracy and can therefore serve as an acceptable numerical tool to investigate the effect of different parameters on the behavior of beams with corroded reinforcements.

From the results of the parametric study, other conclusions can be noted such as:

- Cracking of concrete in the compression side due to corrosion results in small reduction in capacity of corroded flexural beams that have low flexural reinforcement ratio.

- In flexural long corroded beam, the main source for loss of beam load capacity is the loss of steel yield strength in tension reinforcement, which represents the reduction in rebars' cross-sectional area and the effect of the non-uniformity of the corrosion together.

- Small reduction in bond strength does not affect the behavior of long beams that have enough embedded length or rebars that are well anchored at their ends; however, the crack pattern depends on bond strength.

- The most critical corrosion-induced damage is the complete loss of bond between reinforcement and the concrete as it causes sudden failure and the beam behaves as un-reinforced beam. In other words, substantial corrosion in zones of maximum bond stress is more critical than if it is in maximum moment zones.

- Corrosion level differences along beam width can cause lateral slip because of un-symmetric properties.

6.2 Suggestions for Future work

The following suggestions can be made for further research in this area:

- This work can be extended in a future research to capture the effect of dynamic loading on the corroded beam.
- Further study can be carried out on the effect of the use of CFRP to strengthen the corroded beam.
- Further study for the effect of corrosion in stirrups by using 3D element for stirrups, these stirrups should have enough anchorage length to be effective in shear capacity of the beam, and implementation of surface interaction for them to study bond loss.
- A parametric study can then be applied for shear-critical beams to investigate different parameters including corrosion in different zones in the beam width or along the stirrups, degree of corrosion, and stirrup spacing.
- A study can be conducted to develop FE models of Prestressed corroded beams.

References

Almassri, B., Al Mahmoud, F. & Francois, R., 2015. Behaviour of corroded reinforced concrete beams repaired with NSM CFRP rods, experimental and finite element study. Composites Part B: Engineering, 92, pp.477–488.

Almusallam, A. a., 2001. Effect of degree of corrosion on the properties of reinforcing steel bars. *Construction and Building Materials*, 15(8), pp.361–368.

Almusallam, A.A., Al-Gahtani, A.S. & Aziz, A.R., 1996. Effect of reinforcement corrosion on bond strength. *Construction and Building Materials*, 10(2), pp.123–129.

Al-Osta, M.A.M., 2013. *Reliability –based strength prediction model for corroded reinforced concrete columns and beam-columns.* PhD Thesis, King Fahd University of Petroleum and Minerals, Dhahran, Saudi Arabia.

Al-Sulaimani, G.J., Kaleemullah, M. & Basunbul, I.A., 1990. Influence of corrosion and cracking on bond behavior and strength of reinforced concrete members. *ACI Structural Journal*, 87(2), pp.220–231.

Amleh, L. & Ghosh, A., 2006. Modeling the effect of corrosion on bond strength at the steel-concrete interface with finite-element analysis. *Canadian Journal of Civil Engineering*, 33(6), pp.673–682.

Apostolopoulos, C. a., Demis, S. & Papadakis, V.G., 2013. Chloride-induced corrosion of steel reinforcement - Mechanical performance and pit depth analysis. *Construction and Building Materials*, 38, pp.139–146.

Apostolopoulos, C.A., Papadopoulos, M.P. & Pantelakis, S.G., 2006. Tensile behavior of corroded reinforcing steel bars BSt 500s. *Construction and Building Materials*, 20(9), pp.782–789.

Auyeung, Y., Balaguru, P. & Chung, L., 2000. Bond behavior of corroded reinforcement bars. *ACI Structural Journal*, 97(2), pp.214–220.

Ayop, S.S. & Cairns, J.J., 2013. Critical Study of Corrosion Damaged Concrete Structures. , 5(2), pp.43–50.

Azad, A., Ahmad, S. & Al-Gohi, B., 2010. Flexural strength of corroded reinforced concrete beams. *Magazine of Concrete Research*, 62(6), pp.405–414.

Azad, A.K., Ahmad, S. & Azher, S.A., 2007. Residual strength of corrosion-damaged reinforced concrete beams. *ACI materials journal*, 104(1).

Bernard, S., 2013. *Finite Element Modelling of Reinforced Concrete Beams with Corroded Shear Reinforcement*. MS Thesis, University of Ottawa.

Berto, L., Simioni, P. & Saetta, A., 2008. Numerical modelling of bond behaviour in RC structures affected by reinforcement corrosion. *Engineering Structures*, 30(5), pp.1375–1385.

Bhargava, K. et al., 2006. Model for cover cracking due to rebar corrosion in RC structures. *Engineering Structures*, 28(8), pp.1093–1109.

Bhargava, K. et al., 2007. Models for Corrosion-Induced Bond Strength Degradation in Reinforced Concrete. *ACI Materials Journal*, 104(6), pp.594–603.

Bhargava, K. et al., 2008. Suggested Empirical Models for Corrosion-Induced Bond Degradation in Reinforced Concrete. *Journal of structural engineering*, 134(2), pp.221–230.

Biondini, F. & Vergani, M., 2014. Deteriorating beam finite element for nonlinear analysis of concrete structures under corrosion. *Structure and Infrastructure Engineering*, 11(4), pp.519–532.

Birtel, V. & Mark, P., 2006. Parameterised Finite Element Modelling of RC Beam Shear Failure. In *2006 ABAQUS Users' Conference*. pp. 95–108.

Bossio, A. et al., 2015. Modeling of concrete cracking due to corrosion process of reinforcement bars. *Cement and Concrete Research*, 71, pp.78–92.

Cabrera, J. & Ghoddoussi, P., 1992. The effect of reinforcement corrosion on the strength of the steel/concrete bond. *Int. Conf., Bond in Concrete—from Res. to Pract*, 3, pp.10–11.

Cairns, J. et al., 2005. Mechanical properties of corrosion-damaged reinforcement. *ACI Materials Journal*102 ,-M29(102), pp.256–264.

Capé, M., 1999. *Residual service-life assessment of existing R/C structures*. MSc thesis, Chalmers University of Technology, Gothenburg, Sweden, and Milan University of Technology, Milan, Italy.

Castel, A., François, R. & Arliguie, G., 2000a. Mechanical behaviour of corroded reinforced concrete beams—Part 1: Experimental study of corroded beams. *Materials and Structures*, 33(9), pp.539–544.

Castel, A., François, R. & Arliguie, G., 2000b. Mechanical behaviour of corroded reinforced concrete beams—Part 2: Bond and notch effects. *Materials and Structures*, 33(9), pp.545–551.

Chan, S.H.C., 2012. *Bond and cracking of reinforced concrete*. PhD Thesis, Cardiff University.

Chen, H. & Nepal, J., 2015. Analytical Model for Residual Bond Strength of Corroded Reinforcement in Concrete Structures. *Journal of Engineering Mechanics*, pp.1–10.

Choi, Y.S. et al., 2014. Effect of corrosion method of the reinforcing bar on bond characteristics in reinforced concrete specimens. *Construction and Building Materials*, 54, pp.180–189.

Coronelli, D. & Gambarova, P., 2004. Structural assessment of corroded reinforced concrete beams: modeling guidelines. *Journal of structural engineering*, 130(8), pp.1214–1224.

Dang, V.H. & François, R., 2013. Influence of long-term corrosion in chloride environment on mechanical behaviour of RC beam. *Engineering Structures*, 48, pp.558–568.

Dang, V.H. & François, R., 2014. Prediction of ductility factor of corroded reinforced concrete beams exposed to long term aging in chloride environment. *Cement and Concrete Composites*, 53, pp.136–147.

Dehestani, M. & Mousavi, S.S., 2015. Modified steel bar model incorporating bond-slip effects for embedded element method. *Construction and Building Materials*, 81, pp.284–290.

Du, Clark, L.A. & Chan, A.H.C., 2005. Residual capacity of corroded reinforcing bars. *Magazine of Concrete Research*, 57(3), pp.135–147.

Du, Y., Clark, L. a & Chan, A.H.C., 2007. Impact of Reinforcement Corrosion on Ductile Behavior of Reinforced Concrete Beams. *ACI Structural Journal*, (104), pp.285–293.

Elbusaefi, A.A., 2014. *The effect of steel bar corrosion on the bond strength of concrete manufactured with cement replacement materials*. PhD Thesis, Cardiff University.

Eligehausen, R., Popov, E.P.E. & Bertero, V.V., 1983. Local bond stress-slip relationships of deformed bars under generalized excitations. *Rep. UCB/EERC-83/23 Earthquake Engineering Research Center, Univ.of California, Berkeley, CA*.

FIB, 2010. *Model Code 2010 - First complete draft, Volume 1*, fib Special Activity Group 5, New Model Code.

Finozzi, I.B.N. et al., 2014. Numerical modeling of the corrosion effects on reinforced concrete beams. In *11th World Congress on Computational Mechanics (WCCM XI)*. pp. 20–25.

François, R., Khan, I. & Dang, V.H., 2013. Impact of corrosion on mechanical properties of steel embedded in 27-year-old corroded reinforced concrete beams. *Materials and Structures*, 46(6), pp.899–910.

Gan, Y., 2000. *Bond stress and slip modeling in nonlinear finite element analysis of reinforced concrete structures*. MS thesis, University of Toronto.

German, M. & Pamin, J., 2015. FEM simulations of cracking in RC beams due to corrosion

progress. *Archives of Civil and Mechanical Engineering*, 15(4), pp.1160–1172.

Gonzalez, J.A. et al., 1995. Comparison of rates of general corrosion and maximum pitting penetration on concrete embedded steel reinforcement. *Cement and Concrete Research*, 25(2), pp.257–264.

Han, S.-J. et al., 2014. Degradation of flexural strength in reinforced concrete members caused by steel corrosion. *Construction and Building Materials*, 54, pp.572–583.

Hanjari, K.Z., Kettil, P. & Lundgren, K., 2011. Analysis of mechanical behavior of corroded reinforced concrete structures. *ACI Structural Journal*, 108(5), pp.532–541.

Henriques, J., Simões da Silva, L. & Valente, I.B., 2013. Numerical modeling of composite beam to reinforced concrete wall joints. Part I: Calibration of joint components. *Engineering Structures*, 52, pp.747–761.

Higgins, C. & Farrow III, W.C., 2006. Tests of Reinforced Concrete Beams with Corrosion- Damaged Stirrups. *ACI Structural Journal*, (103), pp.133–141.

Imam, A., 2012. *Shear strength of corroded reinforced concrete beams*. MS Thesis, King Fahd University of Petroleum and Minerals, Dhahran, Saudi Arabia.

Jnaid, F. & Aboutaha, R.S., 2014. Residual Flexural Strength of Reinforced Concrete Beams with Unbonded Reinforcement. *ACI Structural Journal*, 111(6), pp.1419–1430.

Kallias, A.N. & Rafiq, M.I., 2010. Finite element investigation of the structural response of corroded RC beams. *Engineering Structures*, 32(9), pp.2984–2994.

Lachemi, M. et al., 2014. The effect of corrosion on shear behavior of reinforced self-consolidating concrete beams. *Engineering Structures*, 79, pp.1–12.

Lee, H.-S. & Cho, Y., 2009. Evaluation of the mechanical properties of steel reinforcement embedded in concrete specimen as a function of the degree of reinforcement corrosion. *International journal of fracture*, 157(1-2), pp.81–88.

Lee, H.-S., Noguchi, T. & Tomosawa, F., 2002. Evaluation of the bond properties between concrete and reinforcement as a function of the degree of reinforcement corrosion. *Cement and Concrete Research*, 32(8), pp.1313–1318.

Lee, J. & Fenves, G., 1998. Plastic-damage model for cyclic loading of concrete structures. Journal of engineering mechanics, 124(8), pp.892–900.

Li, C.-Q., Yang, S.T. & Saafi, M., 2014. Numerical Simulation of Behavior of Reinforced Concrete Structures considering Corrosion Effects on Bonding. *Journal of Structural Engineering*, pp.1–10.

Liu, Y. & Weyers, R.E., 1998. Modeling the time-to-corrosion cracking in chloride contaminated reinforced concrete structures. *ACI Materials Journal*, 95(6).

Lubliner, J. et al., 1989. A plastic-damage model for concrete. *International Journal of Solids and Structures*, 25(3), pp.299–326.

Lundgren, K. et al., 2009. Analytical model for the bond-slip behaviour of corroded ribbed reinforcement. *Structure and Infrastructure Engineering*, 8(2), pp.157–169.

Maaddawy, E., Soudki, K. & Topper, T., 2005. Analytical Model to Predict Nonlinear Flexural Behavior of Corroded Reinforced Concrete Beams. *ACI Structural Journal*, 102(4), pp.550 – 559.

Malumbela, G., Alexander, M. & Moyo, P., 2010. Variation of steel loss and its effect on the ultimate flexural capacity of RC beams corroded and repaired under load. *Construction and Building Materials*, 24(6), pp.1051–1059.

Mander, J.B., 1983. *Seismic design of bridge piers*. PhD Thesis, University of Canterbury, New Zealand.

Mangat, P.S. & Elgarf, M.S., 1999. Bond characteristics of corroding reinforcement in concrete beams. *Materials and structures*, 32(March), pp.89–97.

Mangat, P.S. & Elgarf, M.S., 1999. Flexural strength of concrete beams with corroding reinforcement. *ACI Structural Journal*, 96(1), pp.149–158.

Mercan, B., 2011. *Modeling and behavior of prestressed concrete spandrel beams*. PhD Thesis, University of Minnesota.

Molina, F.J., Alonso, C. & Andrade, C., 1993. Cover cracking as a function of rebar corrosion: part 2—numerical model. *Materials and structures*, 26(9), pp.532–548.

Moreno, F.E., Escamilla, C.A. & Cánovas, M.F., 2007. Ductility of reinforcing steel with different degrees of corrosion and the "equivalent steel"criterion. *Materiales de Construcción*, 57(286), pp.5–18.

Murcia-Delso, J. & Shing, P.B., 2015. Bond-Slip Model for Detailed Finite-Element Analysis of Reinforced Concrete Structures. *Journal of Structural Engineering*, 141(4), pp.1–10.

Ogura, N., Bolander, J.E. & Ichinose, T., 2008. Analysis of bond splitting failure of deformed bars within structural concrete. *Engineering Structures*, 30(2), pp.428–435.

Ou, Y. & Nguyen, N.D., 2014. Plastic Hinge Length of Corroded Reinforced Concrete Beams. *ACI Structural Journal*, 111(5), pp.1049–1057.

Potisuk, T. et al., 2011. Finite Element Analysis of Reinforced Concrete Beams with Corrosion Subjected to Shear. *Advances in Civil Engineering*, 2011.

Richard, B. et al., 2010. A three-dimensional steel/concrete interface model including corrosion effects. *Engineering Fracture Mechanics*, 77(6), pp.951–973.

Rodriguez, J. et al., 1996. Assessing Structural Conditions of Concrete Structures with Corroded Reinforcement. In *Concrete Repair, Rehabilitation and Protection: proceedings of the international conference held at the University of Dundee, Scotland, UK*. pp. 65–78.

Rodriguez, J., Ortega, L.M. & Casal, J., 1997. Load carrying capacity of concrete structures with corroded reinforcement. *Construction and building materials*, 11(4), pp.239–248.

Sánchez, P.J. et al., 2010. Mesoscopic model to simulate the mechanical behavior of

reinforced concrete members affected by corrosion. *International Journal of Solids and Structures*, 47(5), pp.559–570.

Santos, J. & Henriques, A.A., 2015. New finite element to model bond–slip with steel strain effect for the analysis of reinforced concrete structures. *Engineering Structures*, 86, pp.72–83.

Shang, F. et al., 2011. Three-dimensional nonlinear bond model incorporating transverse action in corroded RC members. *Journal of Advanced Concrete Technology*, 9(1), pp.89–102.

Simulia, 2013. Abaqus User's Manual version 6.13. *Dassault Systèmes Simulia Corp.: Providence, RI, USA*.

Stewart, M.G., 2009. Mechanical behaviour of pitting corrosion of flexura and shear reinforcement and its effect on structural reliability of corroding RC beams. *Structural Safety*, 31(1), pp.19–30.

Suffern, C.A., 2008. *Shear Behaviour of Disturbed Regions in Reinforced Concrete Beams with Corrosion Damaged Shear Reinforcement*. MS Thesis, University of Waterloo.

Taha, N.A. & Morsy, M., 2015. Study of the behavior of corroded steel bar and convenient method of repairing. *HBRC Journal*.

Tang, F. et al., 2014. Three-dimensional corrosion pit measurement and statistical mechanical degradation analysis of deformed steel bars subjected to accelerated corrosion. *Construction and Building Materials*, 70, pp.104–117.

Toongoenthong, K. & Maekawa, K., 2004. Interaction of pre-induced damages along main reinforcement and diagonal shear in RC members. *Journal of Advanced Concrete Technology*, 2(3), pp.431–443.

Val, D. V, 2007. Deterioration of strength of RC beams due to corrosion and its influence on beam reliability. *Journal of Structural Engineering*, 133(9), pp.1297–1306.

Val, D. V & Chernin, L., 2009. Serviceability reliability of reinforced concrete beams with

corroded reinforcement. *Journal of structural engineering*, 135(8), pp.896–905.

Val, D. V & Melchers, R.E., 1997. Reliability of deteriorating RC slab bridges. *Journal of structural engineering*, 123(12), pp.1638–1644.

Wang, X.H. & Liu, X. La, 2008. Modeling the flexural carrying capacity of corroded RC beam. *Journal of Shanghai Jiaotong University (Science)*, 13 E(2), pp.129–135.

Wang, X.-H. & Liu, X.-L., 2010. Simplified Methodology for the Evaluation of the Residual Strength of Corroded Reinforced Concrete Beams. *Journal of Performance of Constructed Facilities*, 24(2), pp.108–119.

Wenkenbach, I., 2011. *Tension Stiffening in Reinforced Concrete Members with Large Diameter Reinforcement*. MS Thesis, Durham University.

Wu, Y. & Zhao, X., 2013. Unified bond stress-alip model for reinforced concrete. *Journal of Structural Engineering*, 139(11), pp.1951–1962.

Wurst, D., 2013. *Finite element analysis to simulate reinforced concrete corrosion in beams and bridge decks.* MS thesis, University of Delaware.

Xiaoming, Y. & Hongqiang, Z., 2012. Finite element investigation on load carrying capacity of corroded RC beam based on bond-slip. *Jordan Journal of Civil Engineering*, 6(1), pp.134–146.

Xu, S. et al., 2003. The shear behavior of corroded reinforced concrete beam. In *International conference on advances in concrete and structures*. RILEM Publications SARL, pp. 409–415.

Zhu, W. et al., 2013. Effect of corrosion of reinforcement on the mechanical behaviour of highly corroded RC beams. *Engineering Structures*, 56, pp.544–554.

Zhu, W. & François, R., 2014. Experimental investigation of the relationships between residual cross-section shapes and the ductility of corroded bars. *Construction and Building Materials*, 69, pp.335–345.

Ziari, A. & Kianoush, M.R., 2014. Finite-Element Parametric Study of Bond and Splitting Stresses in Reinforced Concrete Tie Members. *Journal of Structural Engineering*, 140(5), p.04013106 (10 pp.).

Vitae

Name : Hamdi Ahmed Al-Sakkaf

Nationality : Yemeni

Date of Birth : 7/10/1987

Email : hsakkaf@hotmail.com

Address : Mukalla, Hadramout, Yemen

Academic Background :

- **Master of Science in Civil Engineering (Structures)**

Jan. 2013 - May 2016, King Fahd University of Petroleum and Minerals (KFUPM), Dhahran, Saudi Arabia. GPA: 3.78/4.0.

- **Bachelor of Science in Civil Engineering /Structures Option.**

Sep. 2006 - Jun.2011, Jordan University of Science and Technology (JUST), Irbid, Jordan, Grade: Excellent (87.6%), Third of the class (274 Students).